ABSTRACT

Title of Document: REASSORTMENT AND GENE SELECTION OF INFLUENZA VIRUSES IN THE FERRET MODEL AND POTENTIAL PLATFORMS FOR IN VIVO REVERSE GENETICS

Matthew Gray Angel,
Doctor of Philosophy, 2014

Directed By: Dr. Daniel R. Perez,
Professor
Department of Veterinary Medicine

Influenza A virus is a highly infectious agent that cause seasonal epidemics affecting 5-15% of the world population with mild to severe illness and possibly death. While this pathogen represents a significant disease burden to the human population, it can also infect a wide range of animals including swine and land-based poultry, which are thought to serve as intermediate hosts between the human and natural wild aquatic bird reservoir. Here, two viruses, a swine-origin pandemic H1N1 and a seasonal human H3N2 are examined for segment fitness during co-infection of *in vivo* animal models. In three independent co-infections, reassortment between seasonal and pandemic viruses resulted in the selection of an H1N2 virus with a seasonal PB1 with an otherwise pandemic internal gene constellation. Selection for the seasonal PB1 and NA as well as the pandemic M segment was observed to occur rapidly during segment resolution. As pandemic M gene reassortant strains are being consistently

identified in the field, studies were performed to identify the genetic determinants in pandemic M gene selection. Research here shows that both the M1 capsid protein and M2 ion channel from the pandemic virus are sufficient to drive the selection of the entire M segment. As swine represent an important intermediate host for the adaptation of potentially pandemic viruses, including pandemic M gene reassortant strains, alternative DNA and recombinant baculovirus-based platforms are investigated for their ability to generate influenza viruses from porcine polymerase I promoters and serve as potential vaccine candidates. Research here shows that influenza A virus can be rescued *de novo* using the porcine polymerase I promoter in an eight plasmid system. Furthermore, a single bacmid can be constructed that rescues influenza virus or baculovirus encoding the influenza reverse genetic system in mammalian tissue culture or Sf9 cells, respectively. These represent a new generation of species-tailored vaccine platforms.

# REASSORTMENT AND GENE SELECTION OF INFLUENZA VIRUSES IN THE FERRET MODEL AND POTENTIAL PLATFORMS FOR IN VIVO REVERSE GENETICS

By

Matthew Gray Angel

Dissertation submitted to the Faculty of the Graduate School of the
University of Maryland, College Park, in partial fulfillment
of the requirements for the degree of
Doctorate of Philosophy
2014

Advisory Committee:
Daniel R. Perez, Chair
Georgiy A. Belov
James N. Culver
Kim Y. Green
Siba K. Samal

# Dedication

This dissertation is dedicated to my loving wife who brings imagination and creativity to every part of my life.

# Acknowledgements

First and foremost, I would like to thank my advisor, Dr. Daniel Perez. Without his guidance and support, none of this research would have been possible. Throughout my tenure in his lab, he has allowed me to shape my own research interests while challenging me to address pressing scientific questions. In addition to being an excellent mentor, Dr. Perez has provided me with the tools and environment necessary to complete my graduate research and has surrounded me with a group of the most exceptional people. I will always be grateful for the truly unique experiences that I've had while working in his lab.

I would also like to thank Drs. Green, Samal, Culver, and Belov for dedicating their time and support to my graduate advisory committee. I would like to extend my gratitude to Dr. Green in particular for her mentorship over the course of my entire graduate career.

My sincerest gratitude goes to my parents, William Angel and Beth Passmore, whose sacrifices ensured that my sister and I always had the best education possible and who always encouraged us to succeed.

Finally, I would like to thank my wife, Deborah Berman, for enduring every moment of this process with me. None of this work could have been done without her unwavering support, constant companionship, and eternal love. Thank you for always pushing me to be the best version of myself.

# Table of Contents

# List of Figures

# Abbreviations

AcNPV – Autographa californica nuclear polyhedrosis virus
BAC – Bacterial artificial chromosome
BSA – Bovine serum albumin
BGH – Bovine growth hormone
BV – Baculovirus
CRAC – Cholesterol recognition/interaction amino acid consensus
DC – Direct contact
DI – Directly inoculated (see also Inf)
ELISA – Enzyme-linked immunosorbent assay
FBS – Fetal bovine serum
ER – Endoplasmic reticulum
ERK – Extracellular signal-regulated kinase
EYFP – Enhanced yellow fluorescent protein
FISH – Fluorescent *in situ* hybridization
HA – Hemagglutinin
HDV – Hepatitis delta virus
HPAI – Highly pathogenic avian influenza
HEK – Human embryonic kidney
HEPES – 4-(2-hydroxyethyl)-1-piperazineethanesulfonic acid
HRP – Horse radish peroxidase
IAV – Influenza A virus
Inf – Infected
LAIV – Live attenuated influenza virus
M – Matrix segment
M1 – Matrix protein 1
M2 – Matrix protein 2
M98 – A/Memphis/14/1998 (H3N2)
MAPK – Mitogen-activated protein kinase
MDCK – Madin-Darby canine kidney cells
MEK – Mitogen-activated protein kinase kinase
MEM – Minimal essential medium
MES – 2-(N-morpholino)ethanesulfonic acid
MGB – Minor groove binding protein
MID – Multiplex identifier
MOI – Multiplicity of infection
mRNA – messenger RNA
mTerm – murine polymerase I termination sequence
NEP – Nuclear export protein
NS – Non-structural segment
NS1 – Non-structural protein 1
NS2 – Non-structural protein 2 (see NEP)
NA – Neuraminidase
NL602 – A/Netherlands/602/2004 (H1N1)
NLS – Nuclear localization signal

NP – Nucleoprotein
OD – Optical density
OPD – *o*-phenylenediamine
ORF – Open reading frame
pCMV – Cytomegalovirus RNA polymerase II promoter
PA – Polyacidic protein
PB2 – Polybasic protein 2
PB1 – Polybasic protein 1
PBS – Phosphate buffered saline
PBST – PBS with Tween 20
PCR – Polymerase chain reaction
PK(15) – Porcine Kidney (15) cells
Pol I – Polymerase I
Pol II – Polymerase II
Poly(A) – Polyadenylation signal
RBC – Red blood cell
RC – Respiratory droplet contact
RG – Reverse genetic
RL – Rapid library adaptor
RNA – Ribonucleic acid
RNP – Ribonucleoprotein
RS – Restriction site
RT – Reverse transcriptase
SA – Sialic acid
SNP – Single nucleotide polymorphism
S-OIV – Swine-origin influenza virus
TBI – Transfection-based inoculation
$TCID_{50}$ – Tissue culture infectious dose 50%
TEM – Transmission electron microscopy
TK – Thymidine kinase
TPCK – Tosyl phenylalanyl chloromethyl ketone
TR – Triple reassortant
TRIG – Triple reassortant internal gene
Ty/04 – A/turkey/OH/313053/2004 (H3N2)
UTR – Untranslated region
VLP – Virus-like particle
vRNA – Viral RNA
vRNP – Viral Ribonucleoprotein
WHO – World Health Organization
WSN – A/WSN/1933 (H1N1)
WT – Wild-type

# Chapter 1: Introduction

## *1.1 General introduction and genera*

Influenza A belongs to the Orthomyxoviridae family of viruses and is the causative agent of mild to severe respiratory illness affecting an estimated 5 million people every year (1). Together with influenza A, the family is divided into an additional five groups: influenza B and C, Thogotovirus, Isavirus, and the recently discovered Quaranjavirus (2). As group V viruses under the Baltimore classification system, the genome of all genera within this family is composed of single-stranded, negative-sense RNA (3). Additionally, their genomes are further divided into multiple segments, each encoding at least one protein product. Influenza A, influenza B, and Isavirus each contain eight segments (4, 5); influenza C contains seven segments while Thogotovirus and the newly described genus Quaranjavirus contain six (6). While segmentation of the viral genome introduces an additional level of complexity to the replication cycle, segment exchange provides a mechanism to increase both the genetic diversity and potentially the host range of these viruses.

Of the six genera within Orthomyxoviridae, five are known to cause disease in humans. Isavirus, the sole exception, primarily infects North Atlantic salmon and represents a significant burden to fish farms during epidemic outbreaks (7). Infection is associated with anemia due to viral infection of erythrocytes and endothelial membranes followed by death or immune deletion of these cells (8-10). The more recently classified Thogotovirus and Quaranjavirus genera are distinctive in that ticks may function as an intermediate vector. Human infection with these viruses may be

severe, resulting in febrile responses and encephalitis, but is rare compared to influenza A, B, and C viruses due to the vector mode of transmission, and is not known to cause epidemics or pandemics.

While group B and C influenza viruses are primarily human pathogens, influenza A virus (IAV) is known to infect a wide range of species. Based on serological assays, IAV can be further classified into subtypes denoted by the hemagglutinin (H or HA) and neuraminidase (N or NA) serogroups as HxNy. There are currently 17 known subtypes for HA and 10 for NA. With the exception of the recently discovered H17N10 in bats, wild aquatic waterfowl are believed to be the primary reservoir of all influenza HA and NA subtypes (11). Despite the wide range of available subtype combinations, only a select few have successfully crossed species barriers to establish lineages in humans. In recent history, these have been limited to H1N1, H2N2, and H3N2 viruses (12). Whether these subtypes are in some way intrinsically special or if other combinations could adapt given time is unknown. Current evidence suggests that the latter is possible.

Zoonotic infections with influenza subtypes not generally associated with seasonal epidemics are not uncommon. Of particular note are highly pathogenic avian influenza (HPAI) subtype H5 and H7 viruses. While human-to-human transmission has not been observed with these subtypes, sporadic infections of humans with these viruses lead to high morbidity and mortality. Currently, the WHO recognizes 637 confirmed cases of H5N1 with 378 associated deaths. While H7N7 has only resulted in one known death in the Netherlands, this virus and others within the H7 clade contain genetic markers of particular concern should sustained transmission be

achieved. In addition to H5 and H7 viruses, avian H9N2 viruses are known to cause infection not only in swine, but also in humans. The disease phenotype is much less severe compared to H5 and H7, but attention to pandemic preparedness is given due to its ability to replicate well in humans and a large number of intermediate host species.

While predicting the next influenza pandemic is nearly impossible, work has been done with many of these high-risk subtypes to determine the associated genetic markers of a pandemic virus. These gain-of-function studies allow scientists to compare what a pandemic virus might look like to what is currently circulating in nature. To this end, many groups have adapted high-risk, prototypical viruses to the ferret model to obtain an aerosol transmissibility phenotype in these animals (13-15). Generally regarded as the gold standard, the ferret has long been used as an animal model to study influenza virus infection, pathogenesis, and transmission and in many respects may recapitulate disease phenotypes observed in human cases (16, 17). While ferrets have been indispensable to modeling these aspects of influenza in humans, little has been done in this model to understand how genetic exchange between viruses affects these factors.

In addition to humans, IAV also represents an enormous burden to swine producers, resulting in decreased feed efficiency and decreased weigh gain from infected animals due to loss of appetite and lethargy. The infection in swine is often acute and subclinical, but disease signs such as coughing, fever, and labored breathing may be observed. While the primary method to control is biosecurity in the animal facilities, vaccination using commercially available products may also be

effective (18). Vaccine efforts, however, are complicated by the circulation of multiple, antigenically diverse subtypes. To better match strains circulating within individual facilities or regions, autogenous inactivated vaccines are often produced (19).

*1.2 Structure, genome organization, and gene products of influenza A virus*

The structure of IAV ranges from spherical particles that are approximately 80-100 nm in diameter to elongated filamentous particles that exceed 1 μm in length (20). Electron micrographs of section virions reveal a host cell-derived viral membrane studded in protein spikes corresponding to HA trimeric and NA tetrameric surface glycoproteins (for example, see (21)). Electron density under the viral envelope corresponds to matrix protein 1 (M1), which coats the inner leaflet (22). The core contains the genetic content of the virus, arranged in eight electrodense bundles composed of the viral polymerase and RNA and wrapped around nucleocapsid multimers, with minor amounts of a nuclear export protein (NEP) (21, 23, 24). While not visible by TEM, the viral membrane is penetrated by the M2 ion channel protein tetramer, which is composed of a small external domain, a larger internal domain, and a transmembrane domain (25, 26).

The genome of IAV is approximately 14 kb in length with individual segments ranging from 890bp to 2.3kb (4). Each segment contains two untranslated regions flanking at least a single coding sequence. The first 13 and last 12 nucleotides of the viral RNA (vRNA) are highly conserved with a single, segment specific polymorphism in the latter sequence (27-29). These untranslated regions are partially

complementary and form intrastrand base pairing (30). Once paired, the RNA is thought to form either a panhandle or corkscrew structure, which is recognized as a

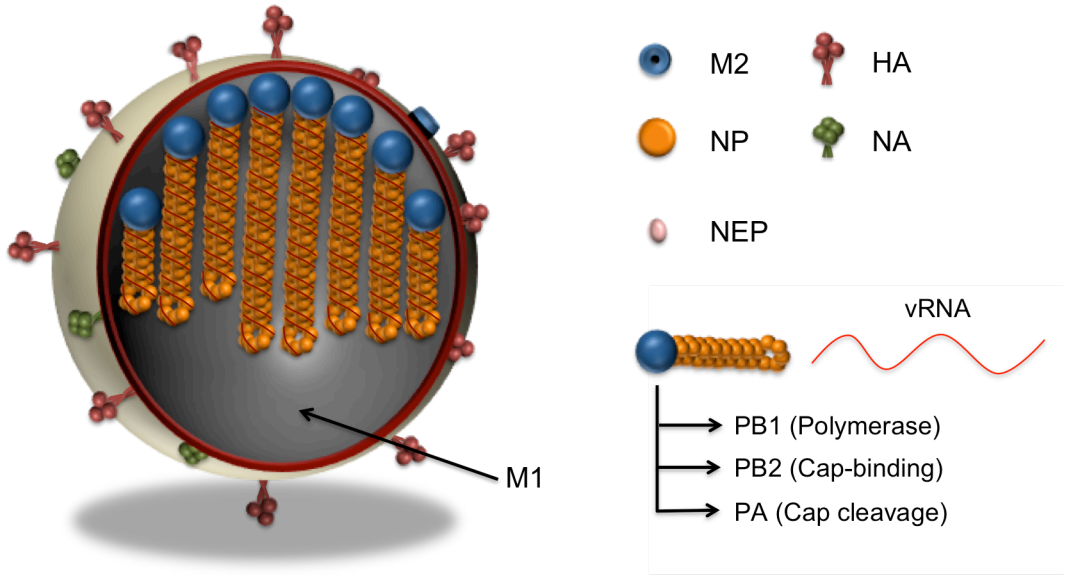


Figure 1.1: Schematic diagram of the influenza A virion. HA and NA major surface glycoproteins stud a host cell membrane derived envelope. Spanning the membrane is the M2 ion channel with a small external and a larger internal domain. Coating the inner leaflet of the envelope is the M1 matrix protein. Within the virion are eight RNA segments, which are coated in NP and bound by a heterotrimeric polymerase complex to make up the vRNP. NEP is bound to the vRNP to facilitate nuclear export (not shown).

promoter by the viral polymerase (30-33). Additionally, each vRNA segment is encapsulated in nucleoprotein trimers (NP), the primary transcript from segment 5, which binds the negatively charged vRNA phosphate backbone through basic amino acids in an RNA binding grove (34, 35). Binding of vRNA to NP induces oligmerization of NP to form a helical capsid that is bound by the viral polymerase. Together, the polymerase complex and the NP coated RNA is known as the viral ribonucleoprotein (vRNP), which is tightly associated with M1 in the viral particle (36, 37).

The three longest segments of IAV encode the viral polymerase proteins as their primary transcripts: Polybasic 2 (PB2), Polybasic 1 (PB1), and Polyacidic (PA). PB2 and PA bind PB1 through its C-terminus and N-terminus, respectively, to form a heterotrimer (38-43). Although all subunits are required, the polymerase activity required for replication and transcription is associated with the PB1 polymerase subunit (44, 45). Until recently, the roles of the PB2 and PB1 subunits were unclear. Influenza messenger RNAs (mRNA) are translated in a cap-dependent manner, yet the polymerase itself is unable to synthesize a cap structure for its transcripts. Instead, the viral polymerase associates closely with the c-terminal domain of host RNA polymerase II where cellular capping occurs. Capped host mRNAs are bound by the viral polymerase, cleaved into short primers, and used by the viral polymerase to prime transcription (46). As such, all viral transcripts have host-derived sequence on their 5' end. Cap-binding activity and nuclease activities had long been ascribed to PB2 and PB1, respectively, with PA playing an unknown function (47, 48). Supporting these ideas were studies showing that antibodies against PB2 could inhibit

transcription. Furthermore, antibodies directed against PA showed no inhibition of this process (49). Capped primer cross-linking also suggests that the nuclease domain resides within the PB1 subunit (47). However, these results were recently challenged by a pair of studies conclusively demonstrating that the endonuclease domain resides within the N-terminal region of the PA subunit. These new results were based on structural homology and biochemical activity, reconciling previous results by showing a close proximity of cross-linked residues in PB1 to the active site of PA (50, 51).

The HA surface glycoprotein is encoded by segment four, and functions for both receptor binding and membrane fusion. It is synthesized as a type I transmembrane homotrimer with a short cytoplasmic tail. The bulk of the protein is in the extracellular domain, and has two predominant features—a long stalk domain and a globular head. HA requires maturation by proteolytic cleavage to be fusion competent (52, 53). This occurs most frequently at a monobasic cleavage site composed of a single arginine or, more rarely, at a lysine, separating HA1 and HA2 fragments that are held together by a single disulfide bond. Maturation most often occurs in the lung and intestinal extracellular spaces by tissue specific trypsin-like proteases (54, 55). However, this tropism can be expanded by the acquisition of multiple basic residues within the cleavage site, allowing maturation of the hemagglutinin to occur within the Golgi network by the ubiquitous furin protease (56). In chickens and other domestic poultry, the polybasic cleavage site allows the virus to spread systemically to sites other than intestine and lung tissues, including the brain, liver, kidneys, spleen, and heart. Moreover, infection with these viruses may

result in the rapid death of the animal in a time frame ranging from hours to days. This single genetic variation in the cleavage site can alter the pathogenic phenotype of a virus, transforming low pathogenic viruses into highly pathogenic viruses (57).

Segment 6 encodes the NA surface glycoprotein, a lipid raft associated type II transmembrane homotetramer. Enzymatically, NA functions to destroy viral receptors by cleaving sialic and neuraminic acids from the host cell surface and the surrounding environment (58-60). The protein is composed of a large extracellular domain with a globular head and a long stalk (61). The cytoplasmic domain is short and composed of about 29 amino acids (62). Like HA, the cytoplasmic tail interacts with M1 to enhance the membrane association of the capsid protein with the budding platform (63).

While M1 capsid is the primary transcript from segment 7, nuclear replication allows the virus to expand its coding capacity in this segment by utilizing the spliceosome to produce an additional transcript. M2 is a 97 amino acid integral membrane protein with a small and highly conserved 24 amino acid ectodomain, a 19 amino acid transmembrane domain, and a larger, 54 amino acid endodomain that forms an amphipathic helix running parallel to the viral membrane (26, 64, 65). The protein forms a homotetramer in the membrane that is known to have ion channel activity, and serves primarily to conduct protons from the luminal compartment of the endosome to the interior of the virus (66).

Segment 8 of IAV is also known to produce two protein products. The first is non-structural protein 1 (NS1), which is produced from an unspliced transcript starting from the initial start codon. About 10% of the primary transcript undergoes

splicing and produces the nuclear export protein (NEP) (67). NEP is known to bind both the vRNP and the nuclear export receptor, Crm1, the functional consequences of which will be discussed later (68).

NS1 is the most abundant, the most studied, and perhaps the most functionally diverse of all non-structural proteins produced by IAV (69, 70). The primary function of NS1 is to act as an antagonist to the innate immune system, specifically the interferon α and β (IFN-α/β) antiviral response (71-73). The protein is small a homodimer, being composed of only about 230 to 237 amino acids depending on strain, and can be divided into an RNA-binding domain, an effector domain, and a disordered tail. NS1 mainly localizes to the nuclei of infected cells, although it may also be found in the cytoplasm (74). Studies have shown the NS1 can indirectly inhibit the activation of NFκB, IRF-3, and c-Jun/ATF-2 transcription factors of IFN-β (75, 76).

Although the ten protein products discussed so far are required for efficient replication of all IAVs, some strains express one or two additional proteins. The first is expressed from an additional typically 87 amino acid open +1 reading frame (ORF) found in segment 2, termed PB1-Frame 2 (PB1-F2) (77). Truncations and extensions of the ORF are common in other strains. Discovered as part of a CD8+ T-cell epitope screen, initial characterization within the A/Puerto Rico/8/1934 (H1N1) suggested that the protein localized to the mitochondrial membrane and induced apoptosis in monocytes (77). Little difference was observed in the growth kinetics of a variety of other cell types in the presence or absence of this ORF. The *in vivo* relevance of this protein, however, has been the subject of intense debate. Effects have been found to

be largely strain and host specific, suggesting that the observed phenotypes associated with PB1-F2 may rely on polygenetic markers (78, 79).

In addition to PB1-F2, a second protein product has been recently identified in segment 3. Termed PA-X, it was putatively identified bioinformatically and encodes the N-terminal endonuclease domain of PA fused to an additional -1 ORF that is accessed by ribosomal frameshifting (80). While little is currently known regarding the function of this protein, mice infected with PA-X deletions or truncations in the reconstructed A/Brevig Mission/1/1918 (H1N1) background showed an increase in disease, suggesting that PA-X modulates the pathogenicity of this virus *in vivo*.

*1.3 Life cycle and genomic replication, gene transcription*

The life cycle of IAV begins with HA recognition of terminal sialylated glycans on the surface of host cells. Sialic acid conjugates to galactose exist as two stereoisoforms, alpha-2,3 and alpha-2,6 linked. Alpha-2,3 linked sialic acids (α2,3 SA) are highly enriched in the intestine of wild ducks, and viruses of these animals display a high binding preference to this conformation (81, 82). By contrast, influenza viruses of humans generally recognize carbohydrates terminating in the alpha-2,6 (α2,6 SA) conformation which are highly expressed in the upper airways.

Once HA has bound to sialic acid on the cellular surface, the virion is internalized into the early and eventually late endosome (83). A hydrophobic fusion peptide is released from HA and intercalates into the endosomal membrane to form a pre-fusion complex (84, 85). As the pH of the endosome decreases, a number of pH-dependent processes occur. The M2 ion channel acidifies the internal compartment of the virion, which initiates the dissociation of the vRNP complexes from the M1

capsid (86, 87). Additionally, HA undergoes a conformational change that fuses the viral and endosomal membranes together, exposing the internal compartment of the virion and the eight vRNPs to the cytoplasm (85).

Although the viral polymerase is responsible for mRNA transcription, the process relies heavily on host nuclear machinery. Caps for viral mRNAs are obtained directly from host RNA polymerase II, and the spliceosome is strictly required to process primary transcripts from segments 7 and 8 into mRNAs encoding M2 and NEP, respectively. As such, all eight vRNPs must translocate from the cytoplasm into the nucleus for RNA transcription to occur. Nuclear translocation of the vRNPs is an active process, relying on the host transport machinery to pass the complexes through the nuclear pore. Although each protein component of the vRNP contains at least one nuclear localization signal (NLS), the unconventional NLS located at the N-terminus of each NP in the vRNP complex was found to drive import into the nucleus through the nuclear pore (88-90). Import is facilitated by karyopherin α1 (importin α) that binds to the NLS on NP (89). Karyopherin β is then thought to bind the importin α subunit its cargo to a nucleoproin for Ran-GDP import into the nucleus (91-93).

Many isoforms of importin α exist and they vary widely in sequence identity. This variation not only is observed between isoforms, but also between species. As a result, different isoforms may not be functional equivalents between their paralogs or interspecies orthologs. A recent study investigated the ability of an avian virus and its mammalian-adapted counterpart to replicate in importin α silenced cells and knockout animals (94). Findings suggest that IAVs circulating in different hosts may be

adapted to utilize different isoforms of importin α, which may represent a significant barrier to virus exchange between reservoirs.

Once in the nucleus, the viral polymerase must make three different RNA species. Protein production is the first priority, and mRNA is transcribed from template vRNA using host-derived, $m^7G$ capped RNA primers as previously described. As mRNA transcription proceeds, the 3' end of the viral RNA is threaded through the active site to form a loop structure with the 5' end still bound to the polymerase. The loop closes during transcription until the polymerase can progress no farther on its template due to the steric hindrance of the RNA wrapped around the polymerase. Conserved at the 5' end of the viral RNA is a stretch of uracils upon which the polymerase is thought to repeatedly slip to incorporate a growing number of adenosines into the mRNA transcript. Viral derived mRNA is then either processed further by the spliceosome or exported out of the nucleus to be translated on the ribosome.

During this initial phase of replication, protein products for new virions must be sorted correctly. All components of the vRNP contain nuclear localization signals, and are concentrated in the nucleus after synthesis until later phases of the cycle. A growing field of evidence suggests that PB2 enters the nucleus alone, and that PB1 and PA must dimerize in the cytoplasm before the two proteins can enter the nucleus (95-97). Once in the nucleus, PB2 must bind the PB1-PA dimer to form the replication competent complex (42). Adaptation of viruses from an avian to a mammalian host has been shown to generate allelic variations in these proteins that modulate the interactions and inhibit nuclear trimerization of the polymerase complex

(98). These and other factors modulating viral protein-protein interactions may serve to inhibit genetic exchange between reservoirs (99, 100).

HA, NA and M2 are all translated on the endoplasmic reticulum for expression, and each contains apical targeting signals. HA begins to fold co-translationally in the ER and forms homotrimers rapidly thereafter (101). Prior to being transported to the Golgi complex, the signal peptide is trimmed from HA0 and select asparagine residues are glycosylated. Six disulfide bonds are formed between twelve conserved cysteine residues in the HA ectodomain, one of which covalently joins what will become HA1 and HA2 post-cleavage (102). Although cleavage of most human influenza viruses historically has been thought to occur extracellularly in the respiratory tissues, recent evidence suggests that these tissue specific proteases may cleave HA within the Golgi complex prior to HA expression on the cell surface (54). The HA protein and precursors are acid sensitive and must be protected from premature activation before the next infection cycle (103, 104). The pH of the Golgi, measured as low as 6.4 at a resting state, is neutralized by the concurrent expression of M2 (105, 106). While this has been shown to slow the transport of proteins through the secretory pathways, it also protects HA0 and HA from early pH-triggered activation.

After transport to the cell surface, HA and NA associate with detergent-resistant raft domains to form an assembly platform from which the virus will ultimately bud (107, 108). M2 is only found in these domains during the course of a viral infection and is excluded when expressed in cells alone, suggesting a role of other viral proteins in the recruitment of M2 to the lipid rafts (109). M1, like M2,

does not directly associate with the lipid raft but is thought to bind the cytoplasmic tails of HA, NA, and M2 (108, 110, 111). The remaining structural viral proteins are located in the nucleus and require export to the assembly site before budding can continue (112).

At late stages of the infection cycle, M1 and NEP bind the vRNP complex within the nucleus; both are essential for mediating export of the vRNP from the nucleus to the cytoplasm (68, 113). The vRNPs are bound by nuclear M1 through its C-terminal domain (114). In turn, NEP is thought to bind and obfuscate the NLS present on the N-terminal M1, thus preventing re-import of the vRNP-M-NEP complex (115). Finally, NEP binds to Crm1 cellular export complex through its N-terminal leucine-rich nuclear export signal for transport through the nuclear pore to the cytoplasm (116). Formation of the vRNP-M-NEP complex, however, is not sufficient to mediate nuclear export, as an external stimulus is required. Cells treated with inhibitors of the Raf/MEK/ERK MAPK signaling cascade retain vRNPs in their nuclei during viral replication (117). Furthermore, accumulation of HA in the cytoplasmic membrane has been shown to activate this cascade (118). This suggests that HA accumulation may trigger export of the vRNP from the nucleus to the cytoplasmic assembly platform for incorporation into budding virions.

In order to be infectious, new progeny must contain a copy of each of the eight vRNPs. While existing data supports the existence a selective mechanism for the packaging of all eight vRNPs over random incorporation, the precise mechanism by which packaging occurs is largely unknown. Thin-section electron tomography has shown the structure of vRNPs within the virion with each docked to the distal

terminus of the budding virus, possibly coming into contact with each other at this point (27). The location of these possible contacts suggests the interaction of sequences near the 5' and 3' termini of each RNA segment, and may correspond with regions previously identified as containing segment-specific packaging signals (28, 58, 64, 73, 80, 108). Using a similar technique, other research has identified possible RNA tethers between the vRNPs at other sites (76). Despite these inroads to understanding the mechanism of vRNP packaging, it remains largely unknown – and yet it is of immense consequence to viral diversity and public health.

The final phase of the infectious cycle is the budding and release of infectious particles from the apical membrane. While HA and NA are both able to initiate bud formation, M1 is thought to be the primary driving force behind the process (119). M1 is known to induce curvature to the membrane and can produce virus-like particles (VLP) in the absence of other viral proteins (120, 121). Despite this, VLP production is most efficient when HA, M1, and M2 are all present, and it is unknown if the mechanisms of budding in single or subset protein studies are analogous to the process *in vivo* (122).

Membrane scission and subsequent release of the virus particle from the host cell is thought to be mediated by M2. Studies have shown that M2 is not only capable of altering membrane curvature through a highly conserved amphipathic alpha helix in its cytoplasmic tale, but also that it accumulates at the neck of the budding virus and facilitates scission *in vitro* and *in vivo* (123). This is consistent with observations showing M2 localization around the extremities of the lipid assembly raft, presumably at the interface of the budding neck and the non-raft membrane (123).

Release of the budded virion is finally mediated by NA digestion of sialic acids from the membrane surface (59). This function is absolutely required as virus replication is severely attenuated in the absence of NA or in the presence of neuraminidase inhibitors (124, 125). Electron micrographs of NA deficient or inhibited viruses show the budded virions attached to one another due to HA recognition of sialic acids on the viral and cellular surface. The attenuated phenotype can be rescued by the removal of inhibitors or the addition of exogenous bacterial neuraminidase (125). Once released, the virus particle repeats this infection cycle by entering into a new, uninfected cell.

### *1.4 Control of influenza virus infections*

Influenza A virus is highly infectious among humans and swine. In both of these groups, the virus is thought to spread through direct contact, respiratory droplet transmission, and fomite transmission. While each mode may play an important role, their respective contributions to efficient transmission may vary between groups. Spread of the virus is most effectively limited where strict biosafety and biosecurity measures are observed. In humans, this means isolation of sick individuals and decontamination of hands and touched surfaces. In swine production facilities, biosecurity practices generally limit the people allowed to enter the operation, monitoring employees for flu-like symptoms and restricting them from work if symptoms exist, vaccinating employees against influenza, enforcing the use of personal protective equipment, and strict entry and exit procedures (126).

In humans and in swine production facilities, biosafety and biosecurity, respectively, remain the most effective means to prevent the spread of influenza virus.

Failing this, however, vaccination may help lessen the severity and reduce clinical signs and symptoms associated with infection. Influenza vaccines are most effective against the strains used in their formulations, and may provide partial protection against closely related viruses. Due to antigenic drift and shift, however, vaccine formulations must be re-evaluated annually to remain efficacious against current circulating strains.

There are currently three types of IAV vaccines approved for human use in the United States. Inactivated vaccine viruses represent the majority of those administered, followed by live-attenuated and protein subunit vaccines (127). The HA and NA surface antigens are determined by the WHO, who makes recommendations for candidate strains based on the current circulating subtypes and their cross-reactivity to prior vaccines (128). The WHO, however, is frequently required to update its recommendations due to antigenic divergence of the HA, which is driven by immunological pressure. Perhaps the best visual depiction of this process is observed by using antigenic cartography. This method maps the antigenic relatedness of similar strains within a lineage and places them on a 2D or 3D map surface with more related strains mapping more closely together. Using this technique, H3N2 viruses from the previous 30 years have been shown to cluster into groups, which generally correlated with vaccine efficacy during the seasonal epidemics of those periods (129).

Inactivated influenza vaccines are almost exclusively used in swine. These are designed to match the most common circulating strains and subtypes, and limited protection is commonly observed due to the antigenic and genetic diversity of

influenza viruses circulating in pig populations (130-132). Furthermore, continued use of these commercial vaccines will most likely result in immune pressure and antigenic divergence of circulating viruses, necessitating the reformulation of commercial vaccines. For these reason, many swine producers have turned to autogenous vaccines to better match strains circulating within their own herds. The use of autogenous influenza vaccines has grown rapidly in recent years due to the diversity of viruses circulating in United States pig populations (19). While they are not yet approved for use in swine, live-attenuated influenza vaccines (LAIV) have been shown to provide significant protection to homo- and heterosubtypic challenge in both human and swine models (132-136). While both autogenous and LAIV could fill an efficacy void left by commercial vaccines, their production still relies heavily on virus growth in eggs or tissue culture systems.

Antivirals may also be used as prophylaxis to control an infection and limit the severity of the symptoms, especially when no vaccine is available. For current circulating seasonal strains, the FDA has approved the use of two antiviral drugs in humans, oseltamivir and zanamivir. Both of these drugs act as selective neuraminidase inhibitors and limit viral growth by inhibiting detachment after membrane secession (137). Although viruses with resistant mutations exist, zanamivir is effective against the current seasonal H1N1 (post-2009), H3N2, and influenza B strains. Only the seasonal H3N2 and influenza B viruses are sensitive to oseltamivir, as resistant mutations have arisen within the seasonal H1N1 virus (138). Older drugs, such as M2 ion channel inhibitors amantadine and rimantadine, , are no longer

effective against circulating strains because overuse has rapidly selected for resistant mutations.

Many other vaccine and antiviral strategies are currently being investigated. Next generation vaccines aim at providing universal or broad-spectrum protection against many different HA subtypes. One example is influenza vaccines aimed at producing protective B-cell responses toward the structurally conserved hemagglutinin stalk domain (139-142). Other universal vaccine strategies target the small, external domain of the M2 ion channel, but these have not been shown to be very effective (143, 144).

# Chapter 2: Genomic reassortment: A literature review

## *2.1 Genomic reassortment*

Copy-choice RNA recombination is thought to be very rare in influenza A viruses and does not appear to contribute greatly to their genetic diversity. Due to their segmented genome, however, two viruses that have infected the same cell can theoretically generate 254 ($2^8$-2) progeny that are genetically distinct from either of the parental strains. This process, known as reassortment, can greatly increase the genetic diversity of these viruses and may even expand their host range. A direct consequence of the latter is the introduction of novel antigens, primarily HA and NA, into serologically naïve populations, resulting in an antigenic shift away from circulating immune epitopes and potentially precipitating the emergence of a pandemic virus.

The past century has seen the emergence of five pandemic influenza viruses, at least three of which have been the result of reassortment. The first pandemic virus, and perhaps the only one not thought to result from reassortment, was the H1N1 virus that started to circulate in the spring of 1918. Initially presenting as a mild respiratory disease in humans, subsequent waves later in the fall and during the spring of 1919 were significantly more virulent with a mortality rate estimated at 2.5% (145). During these two periods, an estimated 500 million people were infected with 50 to 100 million deaths attributed to this virus (146, 147). While the origins of this virus cannot be determined for certain, strong evidence suggests that this virus transmitted and adapted to humans from the avian reservoir (148-150). While not thought to be a

product of reassortment itself, the 1918 influenza virus established human and swine lineages that would be the foundation of all subsequent pandemics.

In 1957, a new pandemic virus was observed in humans that was found to be immunologically unrelated to previously circulating strains (151). Thought to have emerged from Southern China, this "Asian influenza" appears to have been a reassortant between an avian H2N2 virus and the previously circulating H1N1 (152). The avian strain is thought to have donated the H2 HA, the N2 NA, and the PB1 gene to the pandemic virus as well (153). Interestingly, the emergence of this new pandemic virus eradicated the epidemic H1N1 (12, 154). It is speculated that this may be due to cross-reactive antibodies against the group 1 conserved HA stalk, which served to lessen the severity of the pandemic infections while eradicating the epidemic strain (154).

Eleven years later, the H2N2 was replaced by the emergence of an H3N2 pandemic virus. First detected in Hong Kong, this new virus was found to be a reassortant between the current circulating H2N2 virus and an H3 virus from the avian reservoir. In addition to the H3 hemagglutinin segment, the pandemic virus also contained the avian PB1 segment (152, 153). As before, the emergence of the pandemic H3N2 coincided with the extinction of the epidemic strain (12, 154).

The forth pandemic of the last century was not the result of a reassortment event, but was most likely due to accidental release. Oligonucleotide mapping of the 1977 Russian H1N1 flu isolates revealed surprising similarities to isolates obtained in 1950 but not to later isolates, suggesting that this virus remained in stasis for 27 years (155). Curiously, the emergence of a new subtype did not result in the extinction of

the previously circulating strain as before. Instead, H3N2 and H1N1 viruses continued to co-circulate until the emergence of the next pandemic virus in 2009.

The natural history of the 2009 swine-origin pandemic virus (S-OIV) is complex, and is the result of multiple reassortant events. Despite being of an H1N1 subtype, little to no cross-reactivity had been observed with seasonal H1N1 viruses circulating since 1977 (156). H1N1 viruses became established in pig populations following the 1918 pandemic lineage and continued to circulate as "classical swine" viruses until the mid-1990s. In 1998, a triple reassortant (tr) event between csH1N1, human H3N2, and North American avian strains generated a trH3N2 virus. These viruses contained a triple reassortant internal gene (TRIG) cassette composed of avian PB2 and PA; human PB1; and swine NP, M, and NS genes that became prolific in swine. Further reassortment of the trH3N2 with csH1N1 generated trH1N1 and trH1N2 viruses, all with the conserved TRIG cassette. Finally, a subsequent reassortment event between a trH1N1 virus and a Eurasian swine H1N1 disrupted the TRIG cassette with donation of the NA and M from the Eurasian virus (157). This resulted in the 2009 pandemic virus.

Despite its importance, the mechanism by which influenza viruses reassort and select progeny constellations is poorly understood. At its core, however, the process is predicated on the ability of two viruses to infect not only the same host, but also the same cell. Once inside, both viruses must be able to replicate and package their genomes into new virions for reassortment to occur. A recent study using two phenotypically identical yet genotypically distinct viruses demonstrated that, in the absence of selective pressures, reassortment occurs readily *in vivo* and can approach

mathematically expected frequencies (158). As expected, the frequency of reassortment increased with dose and decreased if the co-infection was delayed.

Natural reassortment does not, however, occur under ideal conditions for both viruses. Reproductive capacity, tissue tropisms, infectious dose, and the time of co-infection may vary significantly, thus reducing the probability of reassortment (158). Segment incompatibilities between viruses may even prohibit the production of specific constellations (159). While these factors are difficult to study in a laboratory setting, determining which reassortant strains are highly favored and the phenotype of these strains in the context of disease is of immense importance to human health.

Co-infection of the same cell initially requires that both viruses recognize the sialic acid conformations expressed on the cellular membrane surface. While avian viruses recognize terminal sialic acids in an α-2,3 conformation and human viruses recognize those in an α-2,6 conformation, both conformations are expressed in varying proportions throughout many different tissue types in both avian species and in human airways (160, 161). Although it is these conditions under which viruses may move from the avian to the human reservoir, direct transmission between these reservoirs, as observed during the 1918 pandemic, is thought to rarely occur. Instead, exchange of viruses from the avian to the human reservoir is thought to most efficiently occur through intermediate hosts such as land-based poultry or swine. These hosts exhibit a strong overlap of both avian and human-like sialic acid receptors within their respiratory tracts, allowing viruses to adapt their sialic acid binding preferences to human-like receptors (162, 163).

*2.2 Genomic packaging*

Once co-infection has occurred, and assuming that all 16 segments are replicated within the nucleus of the infected cell, reassortment can then take place as segments are packaged into newly formed, budding virions. In order for a single virion to be infectious, it must contain each of the eight segments. While packaging is known to occur, the mechanism by which segments are incorporated into budding virions is unknown. Random and selective mechanisms have been proposed to account for vRNP incorporation.

The random model for vRNP incorporation suggests that a mechanism exists to bring each vRNP to the budding site, but that each is randomly incorporated into the virion. Evidence suggesting that segments may compete for incorporation serves to bolster this theory (164). Additionally, this may account for the low infectivity of influenza virus particles, in which the ratio of infectious to non-infectious particles has been measured at around 10% (165). While the probability of randomly incorporating eight distinct vRNPs into a virion is very low, the probability of forming infectious virus increases if additional segments are incorporated or if multiple defective yet complementary viruses bud and enter a new cell (166-168).

Evidence for a selective mechanism that can discriminate vRNPs from one another for incorporation into new virions has grown significantly over the past decade. The initial evidence for this mechanism was gleaned from observations in which viral RNAs are present at roughly equal molar amounts within purified virions despite a disparity of species within the infected cell (4, 169, 170). Additionally, it was observed that defective interfering RNAs, composed of UTR and small amounts

of coding sequence, diminished the incorporation of progenitor, full-length RNAs (171). The identification of DI RNA species supported the idea that RNA within the coding sequence contained information required for packaging. Experiments followed to identify the minimal coding sequence in each segment that was sufficient to package a foreign gene into virus particles (172-177). While the precise mechanism remains unclear, these studies elucidated a platform upon which influenza viruses could differentiate segments from one another and package them into virions in a selective manner.

Perhaps the best evidence for the selective incorporation theory has emerged in recent years using both thin-layer electron micrographs depicting the internal core of the virion and single-molecule fluorescent in situ hybridization (smFISH). First, by sectioning the budding surface, eight electron-dense regions were identified within the majority of particles, which are hypothesized to be the eight vRNPs (21). Given that the majority of particles in the study contained no more than eight segments, a non-selective mechanism does not account for the observed infectivity of influenza virus particles. This study does not, however, show that each vRNP is a separate segment. Comparing serial sections suggested that the internal core of the virion is composed of parallel rod-like structures, some of which are of different lengths, but the resolution was insufficient to show the precise lengths of each segment (21). When the internal core of the virion was observed with electron tomography or scanning transmission EM tomography, the length of each vRNP was measured with more accuracy to show that one of each segment is likely to reside in the virion, lending even further credence to a selective mechanism for vRNP incorporation (178,

179). The most conclusive evidence for this model was gathered by Chou *et al*. by immobilizing single viruses on a glass slide and the genetic content interrogated with RNA-hybridization probes to each segment. It was found that the majority of viruses contained a single copy of each segment, an observation that cannot be accounted for by a random incorporative mechanism (180).

While the growing body of evidence supports a selective model, the specific mechanism remains unknown. Direct RNA-RNA interactions may play a role in segment discrimination, but no structures and few sequences has been identified as playing a crucial role, apart from the relatively large packaging signals on each segment (181). Mutational analysis of the identified packaging signal regions suggests that specific residues, and not the entire region, may play a role in the incorporation of the mutated segment as well as other segments within the virion, indicating that there is cross talk between the segments (182-185).

The majority of work to identify packaging signals has been performed in model influenza viruses such as A/WSN/1933 (H1N1) or A/Puerto Rico/8/1934 (H1N1). Both of these strains are lab adapted, and may not be representative of environmental strains. The regions that comprise the identified packaging signals may be relatively conserved among circulating viruses, especially for many of the internal genes. This may not be the case, however, for the highly divergent viruses or the HA and NA surface genes, which are under strong immunological pressure, or within NS, in which multiple clades have diverged (181). Studies investigating the role of packaging signals in the context of reassortment are therefore limited, and it is unclear whether the mechanism is conserved among all influenza viruses. To answer

this question in part, a recent study identified two highly divergent viruses, one from a human H3N2 and the other from an avian H5N2, whose isolation dates were nearly a decade apart (186). It was found that the M segment for both viruses could drive incorporation of their cognate HA. Additionally, when chimeric HA proteins were constructed using identified HA packaging signals from the other virus, HA incorporation could be rescued with a mismatched M gene. The study went on to test the putative packaging signals found in the M gene and similarly observed that the incorporation of a mismatched HA could be rescued in the presence of a chimeric M segment. The authors speculated that selection of HA is driven by the packaging signals present in both HA and M, but it is impossible to attribute the selection primarily to RNA sequence when the protein sequence is divergent between the two viruses present in these regions. This study highlights a difficulty encountered by all reassortment studies, especially when considering RNA packaging: the balance between investigating relevant strains and using well studied models. While regions required for packaging have been studied for a select number of highly adapted strains, it is impossible to know if the underlying mechanism is conserved in other relevant models. Despite these difficulties, it is upon the platform of packaging in which genetic reassortment between to viruses occurs. Further understanding of this process may make it possible to predict the outcome of co-infection, and aid in preparedness prior to the emergence of a pandemic virus.

### *2.3 Laboratory methods to generate reassortant viruses*

Perhaps the most difficult barrier to studying reassortment under a lab setting is the number of genetically distinct progeny that are possible upon the mixing of two

viruses. Prior to the advent of influenza reverse genetics, reassortment, classically known as recombination, was achieved by co-infection and yielded a high frequency of reassortant viruses (187-189). Isolating specific genotypes could, however, be cumbersome. Live-attenuated and inactivated vaccine viruses are still made through classical reassortment by co-infection with a wild-type virus and a "master donor" strain, typically a cold-adapted A/Ann Arbor/6/60 (H2N2) virus or a high-yielding strain such as A/Puerto Rico/8/1934 (H1N1) (190). Selection of HA and NA genes from the non-donor strain can then be accomplished by supplementing growth media with sera directed against the donor strain (191). Further analysis is required to identify allelic frequencies of each segment population and the genetic constellation of individual viruses resulting from the co-infection.

Co-infection remains a useful tool for studying reassortment *in vitro* and *in vivo*, and has many advantages over other models. Co-infection with two viruses ensures that each set of eight genes is appropriately represented and introduced into infected cells. Entry into target cells, nuclear replication, and export for packaging occurs naturally since the vRNPs are already packaged in a virion, and replication only depends on the susceptibility of the target cell to the virus. The degree and temporal separation of co-infection can also be controlled to more closely mimic a natural co-infection. Studies have shown that reassortment depends heavily on both factors—decreasing with the disparity of virus inoculates and increasing with a larger interval between co-infection times (158).

An alternative approach has become available in recent years with the advent of reverse genetic systems for influenza viruses. Each of the eight genes can be

cloned out of the virus and into a reverse genetic vector. The virus can then be reconstituted by transfection of these eight plasmids into an appropriate cell line (68, 192-194). With each viral segment encoded in a separate plasmid, homogenous populations of custom reassortant strains can be generated and grown by mixing plasmids from different viruses without the need to purify and screen many colonies for the constellation of interest. Many studies have used reverse genetics to identify potentially significant reassortants, but the large number of possible combinations that exist between two viruses makes such an approach very difficult and time consuming if all 254 reassortant strains are to be generated. By constraining the parameters of the study, for example by considering only reassortants containing one HA, the number of viruses required to be produced for a study can be significantly decreased (195). While generating all possible combinations resulting from a reassortment event between two viruses may be the most straightforward method to isolate different constellations, this relies heavily on the efficiency of virus rescue from plasmids and growth in primarily MDCK cells. Furthermore, these studies generally identify high growth constellations *in vitro*, which may not be representative of viral fitness *in vivo*. Regardless of the drawbacks, these "brute force" methods have contributed greatly to pandemic preparedness by showing that reassortment alone may be insufficient to produce a pandemic-like virus in the absence of host adaptation (99, 195, 196).

Transfection-based inoculation (TBI) is a hybrid of the two approaches, in which reverse genetic plasmids encoding genes from multiple viruses are transfected into permissible cells. This method allows for the complex selection of reassortant

viruses to occur in a manner similar to co-infection but also permits stoichiometric control of each gene segment. Additionally, TBI has been applied to both *in vitro* and *in vivo* selection models for the purpose of identifying biologically relevant reassortants that could either increase the pathogenicity of circulating viruses or introduce viruses from the avian reservoir to humans (197, 198).

*2.4 Pandemic preparedness*

Given that reassortant viruses have caused the majority of pandemics in the past century, much attention has recently been given to pandemic preparedness and the identification of biologically significant reassortants prior to the emergence of those strains. Although the H1, H2, and H3 subtypes are the only ones known to cause human pandemics, other subtypes have been identified as having pandemic potential—most notably H5, H7, and H9 subtypes that have been able to cross species barriers and infect humans—but lack the ability for sustained transmission. It is also speculated that a new pandemic will most likely arise from a reassortment of a circulating strain with one of these potentially pandemic strains, as was the case with the 1957 and 1968 pandemics. For this reason, most studies involving co-infection focus on reassortment between these H5, H7, and H9 subtypes and current circulating strains.

Interest in the pandemic potential of HPAI H5N1 viruses, which are H9N2 reassortants themselves, has followed the 1997 outbreak in China that produced 18 reported infections and 6 fatalities (199, 200). The mortality associated with these viruses was not isolated to the outbreak; since 2003 alone, there have been 648 confirmed human cases from H5N1 with 384 deaths (201). Although the virus infects

humans and is capable of causing severe disease, respiratory droplet (aerosol) transmission from human to human contacts has not been observed. In order to identify whether reassortments between a HPAI H5N1 and a prototypical H3N2 were genetically compatible and could produce reassortants capable of efficient respiratory droplet transmission, studies were performed in which some or all possible H5N1 constellational combinations were generated by reverse genetics. Although transmission studies in ferrets failed to identify transmissible constellations with wild-type genes, it was found that there is a high degree of genetic compatibility between genes of the two subtypes (99, 195). Furthermore, many constellations exhibited highly virulent phenotypes in the mouse pathogenicity model, which further underscored the need to identify potentially pandemic mutations or reassortants from this subtype (195). Despite the effort invested to produce custom constellations, transmissible H5N1 reassortants were not identified. Additionally, testing the transmissibility of each constellation in *in vivo* transmission models, such as the ferret or guinea pig, would be cost prohibitive. Whether a constellation exists that would confer a transmissible phenotype to an H5N1 virus remains unknown.

Since their emergence, H5N1 viruses have diversified into many different clades and subclades that are not necessarily antigenically cross-reactive with one another (202). Although previous studies have been unable to identify transmissible viruses within this subtype, two recent studies found that a transmissible phenotype can be achieved with mutations alone or in combination with reassortment in clade 1 or clade 2.3.2 viruses (14, 15). The reassortment study used only a single constellation to test for transmission, and it is possible that many others could also

result in a transmissible phenotype between these two viruses. Given the great diversity between the clades, these studies highlight the need to continue research in H5N1 pandemic preparedness in order to identify the features that may contribute to transmissible viruses, and from which clades any potentially pandemic viruses may arise.

Although not as pathogenic as some of the H5N1 HPAI viruses, some H9N2 viruses have transmitted to humans, raising the possibility that these strains may become pandemic (203-205). In agreement with reported human cases, a panel of H9N2 viruses was observed to replicate in directly inoculated animals with a subset transmitting to direct contact animals. Although no transmission was observed in the respiratory contact animals, directed reassortment of an H9N2 virus with the internal genes of a seasonal, human H3N2 was shown to increase transmission to direct contact animals, highlighting an advantage to the virus of reassortment (196). Respiratory droplet transmission was only observed with this reassortant virus after serial passage and adaptation in the ferret model (13). With only a single gene constellation being tested in this study, however, it is important to note that other constellations could contribute to a transmissible phenotype as well. When the transmissible H9N2 surface genes were individually tested on the H1N1 pandemic backbone, an alternative constellation comprised of the transmissible H9 HA on an otherwise pandemic backbone was shown to be more transmissible than a virus with the H9N2 HA and NA on an otherwise pandemic backbone (206). Furthermore, when complex mixtures of reassortant viruses were challenged against one another through TBI, the H9 HA and pandemic NA pairing remained consistent in *in vivo* models,

suggesting that this combination is highly favored (197). While the seasonal and pandemic studies are not directly comparable, they suggest that the use of complex virus mixtures instead of a custom made constellation may produce a more transmissible virus.

This last study also highlighted an important distinction between *in vitro* and *in vivo* reassortment models. The same mixture that was used for constellation selection in the *in vivo* ferret model was also used to purify constellations by limiting dilutions *in vitro*. While both models selected for pandemic NP and NA genes, selection for PB2, PB1, PA, and NS was inconsistent (197). These data strongly suggest that different selective pressures are present in the *in vivo* and *in vitro* models, and calls into question the biological relevance of *in vitro* selection models used for the combinatorial, "brute force" methods of generating virus constellations in the laboratory setting.

The potential risk of an H7 pandemic virus has increased significantly since 2013 with the avian H7N9 outbreak in China. Similarly to the HPAI H5N1 viruses isolated since 1997, the H7N9 is a reassortant with the six internal genes derived from an avian H9N2 virus (207). Since its introduction into poultry, 137 people have been infected with 45 deaths as of October 2013 (208, 209). Although the H7N9 outbreak has garnered significant attention, these are not the first cases of human infection with H7 viruses. Some H7 viruses have acquired multibasic cleavage sites similar to those found in the HPAI and are highly pathogenic in poultry species (145). During some poultry outbreaks, H7 viruses have been known to infect humans. This was the case during an H7N7 outbreak in the Netherlands in 2003 in which 86 people were

confirmed to have been infected. Of these, a single person succumbed to acute respiratory distress syndrome and died. Although sustained transmission of this virus was not observed, transmission to three family members of infected individuals was observed to have occurred (210, 211). Zoonotic transmission of an HPAI H7N3 virus to humans during an outbreak in British Columbia has also been observed. In this case, there was neither contact transmission nor deaths associated with infection (212). Whether reassortment with circulating human or swine strains could increase the transmissibility of these viruses in humans is unknown. Nevertheless, viruses within this subtype have been identified as having pandemic potential and pose a significant threat to human health.

If past influenza pandemics hold any clues for future outbreaks, they are that reassortment with current circulating strains is most likely to contribute to the generation of influenza viruses with pandemic potential. Efficient and reproducible methods of generating these reassortants in biologically relevant models are required to identify these viruses. The studies herein examine reassortment from co-infection of seasonal strains with an emerging pandemic virus to produce complex populations of viral constellations. Population dynamics and constellation selection are then observed in a relevant animal model without artificial selection *in vitro*. Using these findings, the genetic elements required for gene selection are identified within a model segment observed to be under strong purifying selection. Using competitive mixture modes, two genes have been identified that promote selection of the entire model segment in the competition assays. Additionally, specific mutations in one of the genes were found to be sufficient to promote segment selection. Further analysis

of each gene within the model segment suggests possible mechanisms behind the fitness of the pandemic segment.

*2.5 Outline of dissertation*

Chapter 3: In Vivo Selection of H1N2 Influenza Virus Reassortants in the Ferret Model

- **Perez DR, Sorrell E, Angel M, Ye J, Hickman D, Pena L, Ramirez-Nieto G, Kimble B, Araya Y.** Fitness of Pandemic H1N1 and Seasonal influenza A viruses during Co-infection: Evidence of competitive advantage of pandemic H1N1 influenza versus seasonal influenza. PLoS Curr. 2009 Aug 24 [revised 2009 Aug 26];1:RRN1011.
- **Angel M, Kimble JB, Pena L, Wan H, Perez DR.** 2013. In vivo selection of H1N2 influenza virus reassortants in the ferret model. Journal of virology **87:**3277-3283.

Chapter 4: Role of the pandemic M1 and M2 genes in segment selection

- **Angel M, Li W, Perez DR.** Role of the pandemic M1 and M2 genes in M segment selection. In preparation.

Chapter 5: Towards *in vivo* reverse genetics: A recombinant bacmid rescue system for influenza virus in porcine cell types.

- **Angel M, Chen H, Sutton T, Perez DR.** Rescue of influenza viruses in porcine cell types. In preparation.

# Chapter 3: *In vivo* selection of H1N2 influenza virus reassortants in the ferret model

## 3.1 Introduction

Influenza A viruses (IAV) belong to the family *Orthomyxoviridae*, the genomes of whichare composed of eight, negative-sense, single-stranded RNA segments, all of which must be packaged into budding virions to form an infectious particle (145). IAVs have multiple strategies to increase their genetic diversity. For one, the error-prone viral RNA polymerase can introduce mutations into the viral genome through nucleotide misincorporation. While the majority of mutations are expected to be deleterious, some may provide the virus with an adaptive advantage. This process of drift evolution is the driving force behind the selection of immune escape mutants. As protective humoral responses are generally directed against the HA glycoprotein, most of the variability observed in influenza viruses is within the antigenic sites of this protein. Due to their segmented genomes, the genetic diversity of these viruses may also be increased through reassortment, in which multiple viruses infecting the same cell exchange their genomic content.

While the rapid antigenic drift of influenza viruses necessitates the frequent reformulation of vaccines, partial cross-reactivity and protection can be observed between adjacent formulations and seasons. Reassortment events, however, have historically introduced antigenically distinct subtypes for which there has been little cross protection from contemporary vaccine formulations. In 1957, reassortment between an avian H2N2 and the circulating H1N1 virus precipitated an H2N2 pandemic. The virus underwent further reassortment with an avian H3 virus to generate the H3N2 pandemic in 1968; in both cases, the avian PB1 gene segment was

donated to the pandemic virus. The swine-origin 2009 pandemic H1N1 virus (H1N1pdm) evolved via a complex series of reassortment events between classical swine H1N1, human H3N2 (H3N2s), and avian influenza viruses that is thought to have occurred in swine approximately 15 years prior to the outbreak in humans. In each of these three cases, reassortment led to the generation, selection, and establishment of viruses with internal gene cassettes containing segments from previously circulating viruses, indicating a contribution of these segments to viral fitness.

Reverse genetics has enabled the investigation of many, if not all, possible gene constellations existing between two viruses, but the combinatorial problem ($2^8$=256) of generating and characterizing each arrangement makes this approach heavily time consuming. Nevertheless, these studies usefully indicate that particular constellations may not be favored *in vitro*. Of more complex approaches, some have investigated reassortants arising from the transfection of multiple reverse genetic virus sets, while others have used co-infection to allow the viruses to reassort in a more natural way *in vitro*. While the significance of these experiments should not be understated, selection may largely depend on the ability of specific constellations to rescue and replicate *in vitro* and may not mimic the reassortment capacity and fitness of viruses *in vivo*.

With the rapid spread of the 2009 pandemic virus and its continual co-circulation and reassortment with seasonal human and swine strains, I investigated whether the ferret could be used to recapitulate reassortment events similar to those occurring in nature. Here, the reassortment potential arising from direct co-infection

of wild-type and reverse genetic reassortant viruses was examined. I report the generation of reassortant viruses between the 2009 pandemic and seasonal H3N2 viruses in the ferret model through co-infection and serial passage.

3.2 Materials and methods

**Cells and Viruses**

MDCK cells were cultured in Dulbecco's modified Eagle medium (Sigma-Aldrich, St. Louis, MO), supplemented with 25 mM HEPES (Sigma-Aldrich), 2 mM glutamine (Sigma-Aldrich), 10 mM HEPES (Invitrogen, Grand Island, NY), and 10% fetal bovine serum (FBS; Sigma-Aldrich), and were grown at 37 °C under 5% CO2. HEK 293T cells were cultured in Opti-MEM (Sigma-Aldrich) with 10% FBS and grown at 37 °C under 5% CO2. Viruses were titrated in tissue culture by endpoint dilution assays using the Reed-Muench method in Opti-MEM at 35°C (213). Viruses containing genes from A/Memphis/14/98 (H3N2) and A/Netherlands/602/2009 (H1N1pdm) were generated as previously reported (193). Virus stocks were produced in MDCK cells and sequenced with BigDye Terminator, version 3.1, Cycle Sequencing Kit 1 on a 3500XL Genetic Analyzer (Applied Biosystems, Carlsbad, CA) to confirm the gene constellations.

**Porcine Plasmid and Bacmid Construction**

The porcine RNA polymerase I promoter sequence was synthetically constructed from published sequence through Genetec and flanked with convenient restriction sites on the 5' and 3' ends, respectively (See Appendix Figure S1). The synthetic construct was subcloned into pDP-GLuc (NS) by digest with NotI and BstEII restriction enzymes to replace the human RNA polymerase I promoter to make pPIGv-GLuc(NS).

**Growth Kinetics**

MDCK cells were seeded at $8x10^5$ cells per well in a 6-well plate. Viruses were diluted to $8x10^2$ $TCID_{50}$/mL in media and overlaid onto cells. After 1 hour at 37˚C, the inoculum was removed, and the cells washed three times with PBS.

**Animal Studies**

Prior to infection, animals were confirmed negative for influenza virus by nucleoprotein (NP)-blocking enzyme-linked immunosorbent assay (ELISA; Synbiotics Co., San Diego, CA). Infection and transmission studies were carried out as previously described (196). Briefly, 5- to 7-month-old ferrets were inoculated intranasally with $1x10^6$ 50% tissue culture infective doses ($TCID_{50}$) of each surface reassortant virus in 500 µl and monitored for temperature and body weight daily. Nasal washes were performed daily, and infection was monitored using a Flu Detect Antigen Capture Test (Synbiotics Co.). Nasal turbinate, trachea, and lung tissues were harvested from two co-infected animals at 4 days postinfection (dpi). Tissues were homogenized in phosphate-buffered saline (PBS) (1:1, wt/vol) on a TissueLyser LT (Qiagen, Gaithersburg, MD). Additional samples were cut into 5-µm-thick sections and processed by Histoserv, Inc. (Germantown, MD), using a standard hematoxylin and eosin (H&E) staining protocol. During passages 2 to 7, ferrets for each lineage were housed in individual isolators and sampled daily for 5 days.

Nasal washes from 3 dpi of each passage were diluted 1:5 in PBS in a total volume of 500 µl and used to infect subsequent ferrets as before. For transmission studies, ferrets (n=2) were again inoculated intranasally with $1x10^6$ $TCID_{50}$ of virus in 500 µl. At 1 dpi, naïve animals (n=2 for each group) were placed in direct contact (DC) or

barrier-separated respiratory droplet contact (RC) with the infected animals. Animal studies were performed under protocols approved by the University of Maryland Institutional Animal Care and Use Committee.

**Quantitative RT-PCR**

Viral RNA was extracted from infected ferret nasal washes with a MagnaPure RNA HP II kit (Roche, Indianapolis, IN), per the manufacturer's recommendations. Reverse transcription was performed with avian myeloblastosis virus (AMV) reverse transcriptase (Promega, Madison, WI). Sample cDNAs were diluted 1:5 in EB buffer, and 2 μL of each were used for quantification. Sixteen minor groove binder (MGB) TaqMan assays were designed for each segment of the donor viruses using AlleleID 7 (Premier Biosoft, Palo Alto, CA) (214). Primers (Invitrogen) and TaqMan MGB probes (Applied Biosystems) were ordered from their respective manufacturers. Quantitative real-time PCR for each segment was performed on a LightCycler 480 (Roche) with the 2X TaqMan Universal PCR Master Mix (Applied Biosystems) with 1μM each primer and 250 nM probe in a final volume of 20μL (Table S4). Samples were heated at 50˚C for 2 min and then 95˚C for 10 min. Cycling proceeded as follows: 95˚C for 15 secs, 55˚C for 15 secs, 60˚C for 1 min, 72˚C for 1 sec for 45 cycles. Allelic copy numbers for either the seasonal or pandemic segment was determined by comparison to a plasmid based standard curve, which was generated for each assay.

*3.3 Results*

### 3.3.1 Reassortant influenza viruses carrying seasonal H3N2 and H1N1pdm gene segments replicate and transmit in ferrets

The pandemic H1N1 virus spread rapidly following its initial identification in mid-2009 and co-circulated with both seasonal H1N1 and seasonal H3N2 strains already present in the human population (Figure 3.1). The emergence of pandemic viruses in the 20th century was generally followed by reassortment with, and extinction of, the previously circulating strains (1957 and 1968), or co-circulation with these strains (1977). To determine if the H1N1pdm virus had a biological advantage over either of the seasonal strains or gained such a phenotype by reassortment with them, ferrets were co-infected with the H1N1pdm (A/California/04/2009) virus and one of two seasonal strains (A/Brisbane/59/2007 (H1N1) or A/Brisbane/10/2007 (H3N2)). At one day post infection, naïve contacts were introduced in both direct contact (DC) and barrier separated (aerosol contact, AC) to the infected animals. All cohorts (H1N1s::H1N1pdm, H3N2s::H1N1pdm) of infected, DC (Figure 3.2: A and B) and AC (Figure 3.2: C and D) animals shed virus for 5 to 7 days. Viral RNA from the directly infected and respiratory droplet contact animals was purified from ferret nasal washes on the first day and final day of shedding, respectively. Segment and virus specific primers for RT-PCR were then designed to amplify a region of one gene from a single virus in the co-infection pair. This was done for all 16 pairings (H1N1s vs H1N1pdm and H3N2s vs H1N1pdm). RT-PCR performed on the directly infected animals shows the presence of all 16 segments, 8 from each virus, indicating that these animals were successfully co-

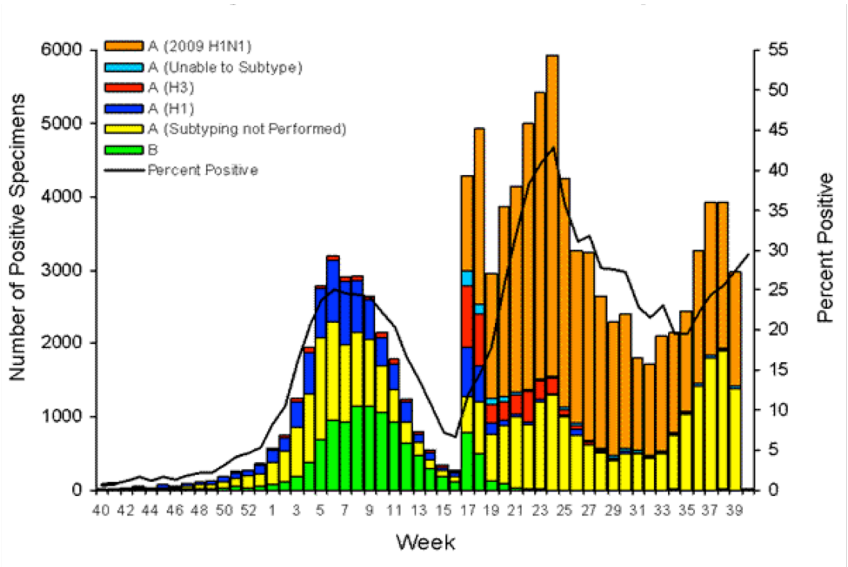


Figure 1.1: Surveillance data before and after the 2009 H1N1pdm outbreak. Seasonal H1N1 (Blue) dominance is observed prior to the outbreak followed by a period of co-circulation with the pandemic virus (orange) and extinction after the outbreak. The outbreak allowed for an expansion of the seasonal H3N2 virus (red), which was lost towards the end of the season. FluView, CDC.

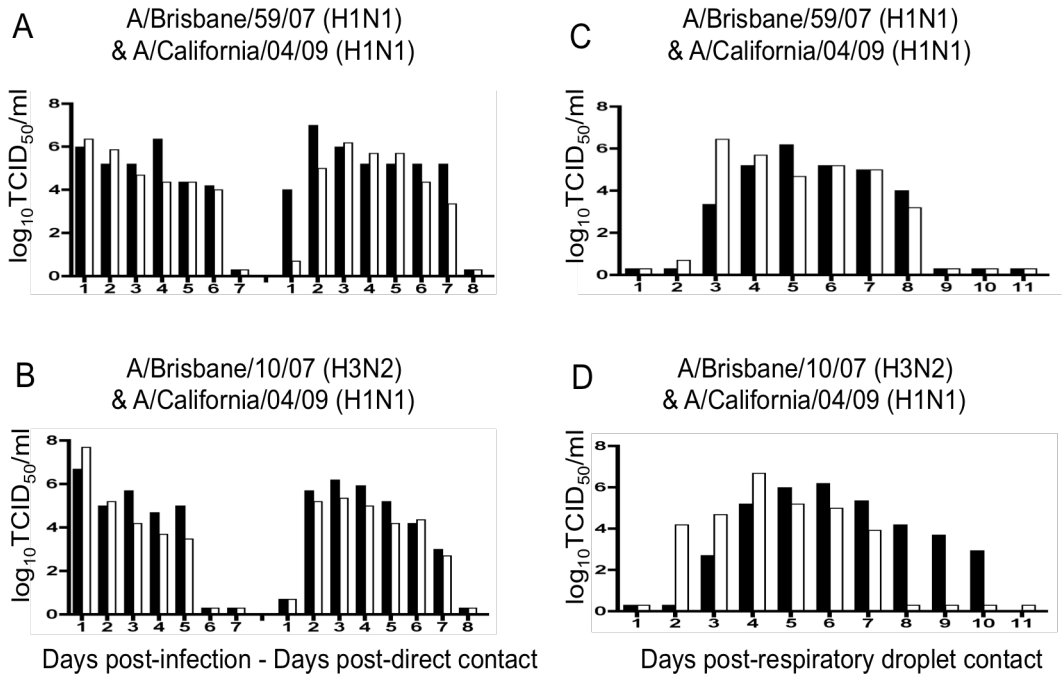


Figure 3.2: Transmission of seasonal and pandemic viruses following co-infection. A and B) Virus titers from directly inoculated (left) and direct contact (right) animals. C and D) Virus titers from respiratory droplet contact animals. A and C) Transmission groups of ferrets co-infected with the seasonal H1N1 and the pandemic H1N1. B and D) Transmission groups of ferrets co-infected with the seasonal H3N2 and the pandemic H1N1. N=2.

infected (Figure 3.3: C and F). Using the same method, the genetic composition of viruses shed from the respiratory droplet contacts was investigated to identify the most fit virus populations arising from co-infection. All animals in each virus pairing yielded the same result with a fully pandemic virus transmitting to respiratory droplet contacts preferentially to either seasonal or reassortment thereof (Figure 3.3: A,B and D,F). These results indicate that the pandemic virus has an apparent biological advantage over either of the seasonal strains used in this study in the ferret model. Additionally, the absence of seasonal segments in the respiratory droplet contacts suggests either a biological disadvantage to such reassortments or a limitation in the methods used to identify them. Variations in tissue and cell tropisms between the two strains may preclude reassortment. Reassortants arising from a co-infected cell are also expected to be in the minority compared to the inoculums. A moderate increase in fitness gained by reassortment may not be sufficient to overcome the dose and temporal advantage of the wild-type viruses to transmission.

Despite these observations, reassortment strains have sporadically been identified between viruses of the pandemic lineage and multiple others, mainly classical swine H1N1 and triple-reassortant swine H3N2 in swine. To reconcile these observations and our own reverse genetics were used to create recombinant 2:6 influenza viruses carrying two surface gene segments from one strain and six internal gene segments from another strain. To this end, a virus carrying the surface gene segments from the seasonal A/Memphis/14/98 (H3N2) strain and the six internal gene segments from the pandemic A/Netherlands/602/09 (H1N1pdm) was generated. In addition, a second virus carrying the H1N1pdm surface genes and the

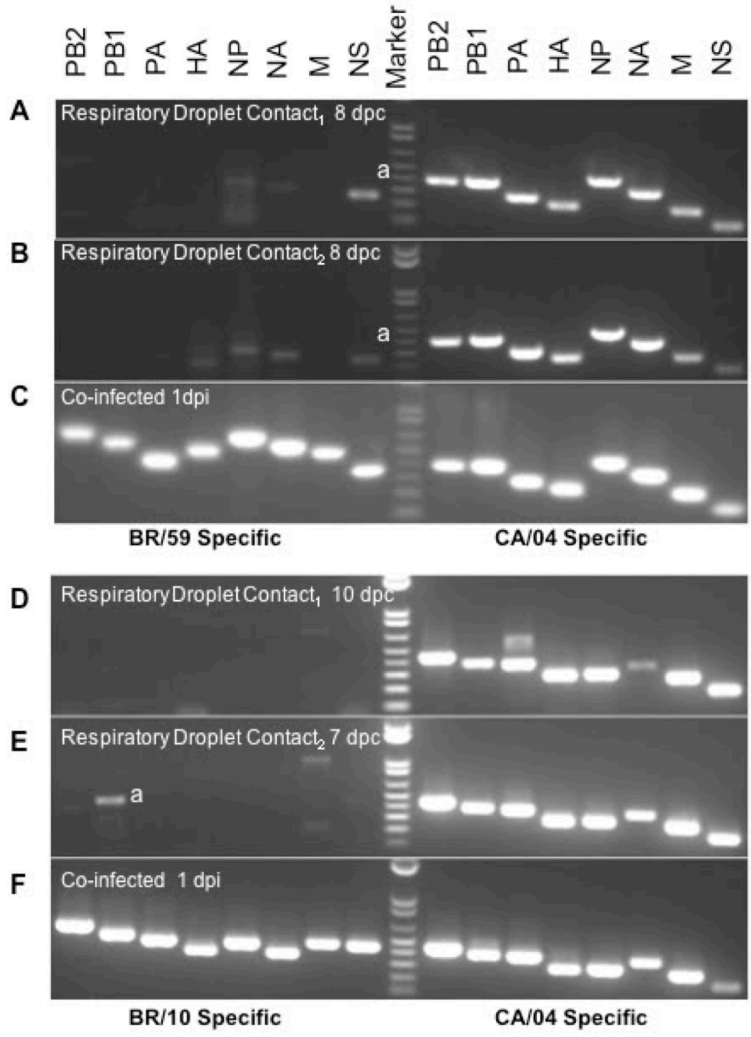


Figure 3.3: RT-PCR of viruses in respiratory droplet contacts for nasal wash genotyping. Genetic composition of respiratory droplet contacts from the A and B) H1N1s::H1N1pdm and D and E) H3N2s::H1N1pdm co-infections. C and F) Genetic composition of the directly infected animals on 1dpi, respectively. (a) denotes non-specific binding confirmed by sequencing the PCR product to eliminate suspicion of reassortment.

internal gene segments of the H3N2s using the strains mentioned above was made. These viruses are referred to as 2M98:6pdm and 2pdm:6M98, respectively (Figure 3.4).

The wild-type and reassortant viruses were then compared in a multiple-step infection cycle *in vitro*. MDCK cells were infected at a low multiplicity of infection (MOI of 0.001). While the wild-type H3N2s grew to significantly higher titers than the H1N1pdm virus, there was no discernible difference in peak titers (106.9 to 107.4 TCID50/ml) between the reassortant 2M98:6pdm and 2pdm:6M98 viruses. Interestingly, the initial growth kinetics of each reassortant virus mimicked that of the donor strain from which the internal genes were derived (Figure 3.4).

In order to test whether these viruses would replicate and transmit efficiently in ferrets, naïve animals were infected with $1 \times 10^6$ $TCID_{50}$ of either reassortant. At 1 dpi, additional animals were introduced in both direct and barrier-separated contact with the infected animal (13). Nasal washes were collected daily starting at 1 dpi, and sampling continued until the animals were negative by Flu Detect for 2 days. Directly infected animals shed for 5 to 6 days and transmitted to both direct contact and respiratory droplet contact animals equally well, suggesting no growth impairment of either virus in ferrets. Interestingly, transmission to respiratory droplet contact animals occurred more consistently with the 2M98:6pdm virus than with 2pdm:6M98 (Fig. 1.5A and B).

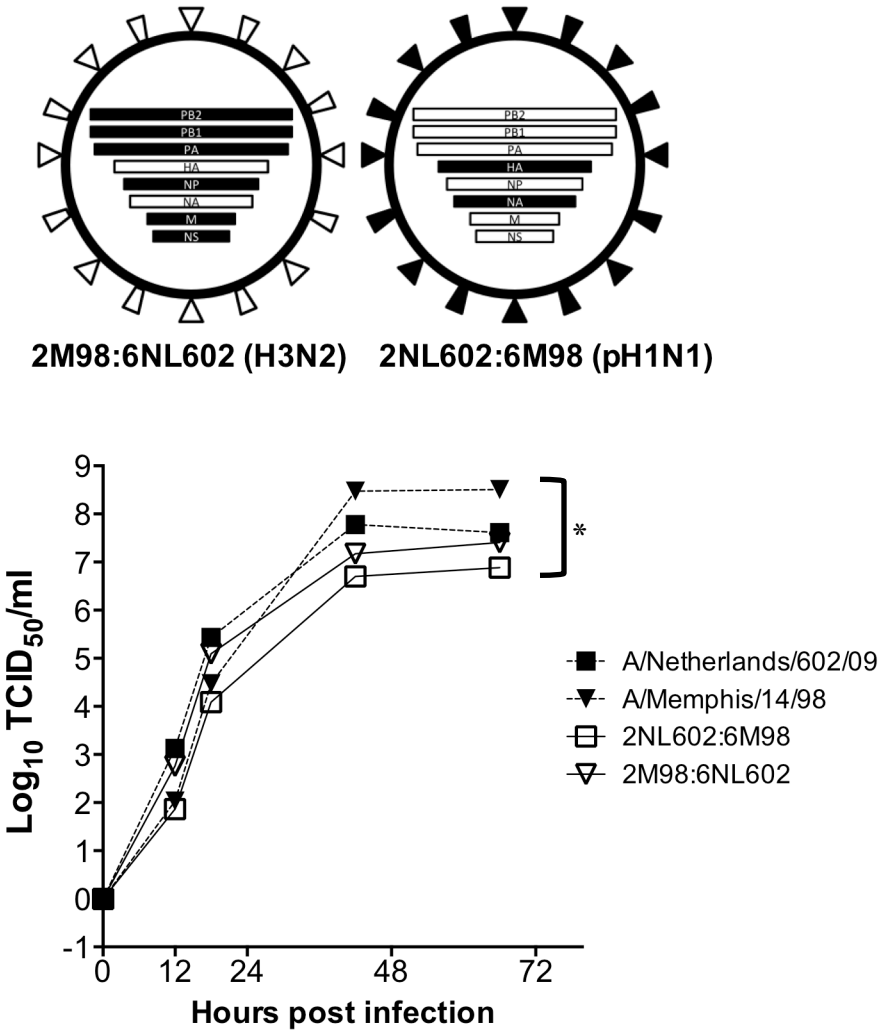


Figure 1.4: *In vitro* and *in vivo* characterization of parental viruses compared to 2:6 reassortants. A) Schematic diagram of 2:6 surface reassortant viruses. Black and white boxes indicate segments contributed from A/Netherlands/602/09 (pH1N1) and A/Memphis/14/98 (H3N2s), respectively. B) Multistep growth kinetics in infected MDCK cells (MOI=0.001) followed over time.

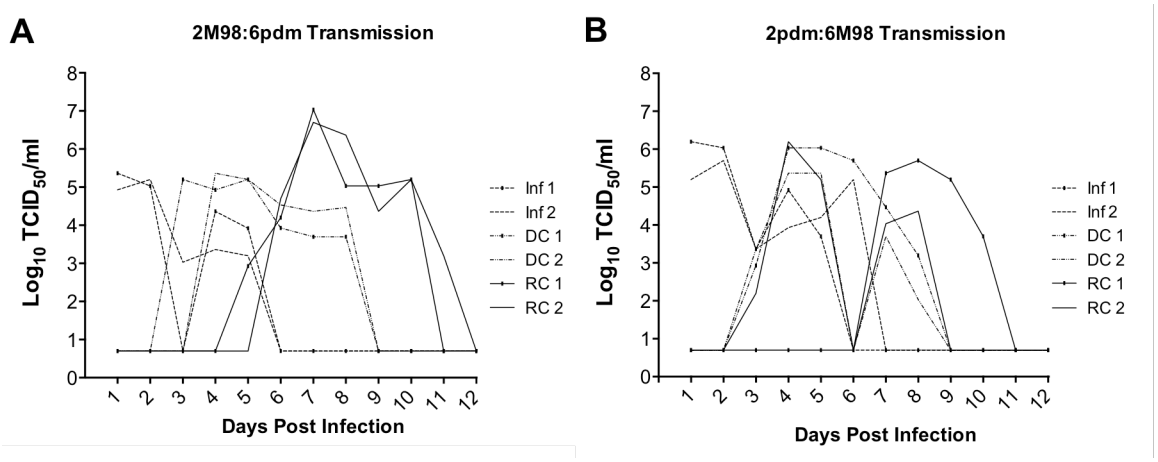


Figure 1.5: Transmission of parental 2:6 reassortant viruses. Ferrets (n=2/virus) were inoculated (Inf) with $1x10^6$ $TCID_{50}$ of either 2M98:6NL602 (H3N2) (A) or 2NL602:6M98 (pH1N1) (B). Direct contact (DC) and respiratory droplet contact (RC) animals (n=2/virus) were introduced at 24 hpi. Each curve represents a single ferret and its levels of virus shedding in nasal washes.

### 3.3.2 Selection of an H1N2 reassortant virus after serial passage in ferrets

To simulate a natural co-infection, naïve ferrets (n = 6) were inoculated with a mixture containing $1 \times 10^6$ $TCID_{50}$ of each surface reassortant virus. Sampling was performed as before. Although all animals shed virus for 5 to 6 days following infection, only moderate viral titers were observed in the nasal washes. To confirm that the ferrets were indeed infected with both viruses, sera were collected at 14 dpi and assayed for inhibitory antibodies against both donor hemagglutinin genes. While all animals seroconverted to both strains, each animal had consistently higher titers against the pandemic surface reassortant virus (2pdm:6M98) (Table S1). Whether this indicates that the 2pdm:6M98 pandemic reassortant has a replicative advantage or that it is simply more immunogenic is unknown. Viral RNA was then isolated from three of the infected animals at 3 dpi and genotyped with quantitative real-time reverse transcription-PCR (rRT-PCR). Importantly, genomic RNA for all 16 segments was isolated from each animal tested (Figure 3.6). Taken together, these data indicate that the co-infection was successful and both reassortant viruses were replicating in the infected animals.

As reassortment events occur in single cells within the infected host, the initial progeny resulting from an event may not represent a significant proportion of the total virus population, regardless of the fitness of the progeny relative to that of the parental viruses. We therefore reasoned that transmission could impose an unreasonably high selective barrier to small but biologically relevant initial populations of reassortant viruses. To that end, virus populations from the three

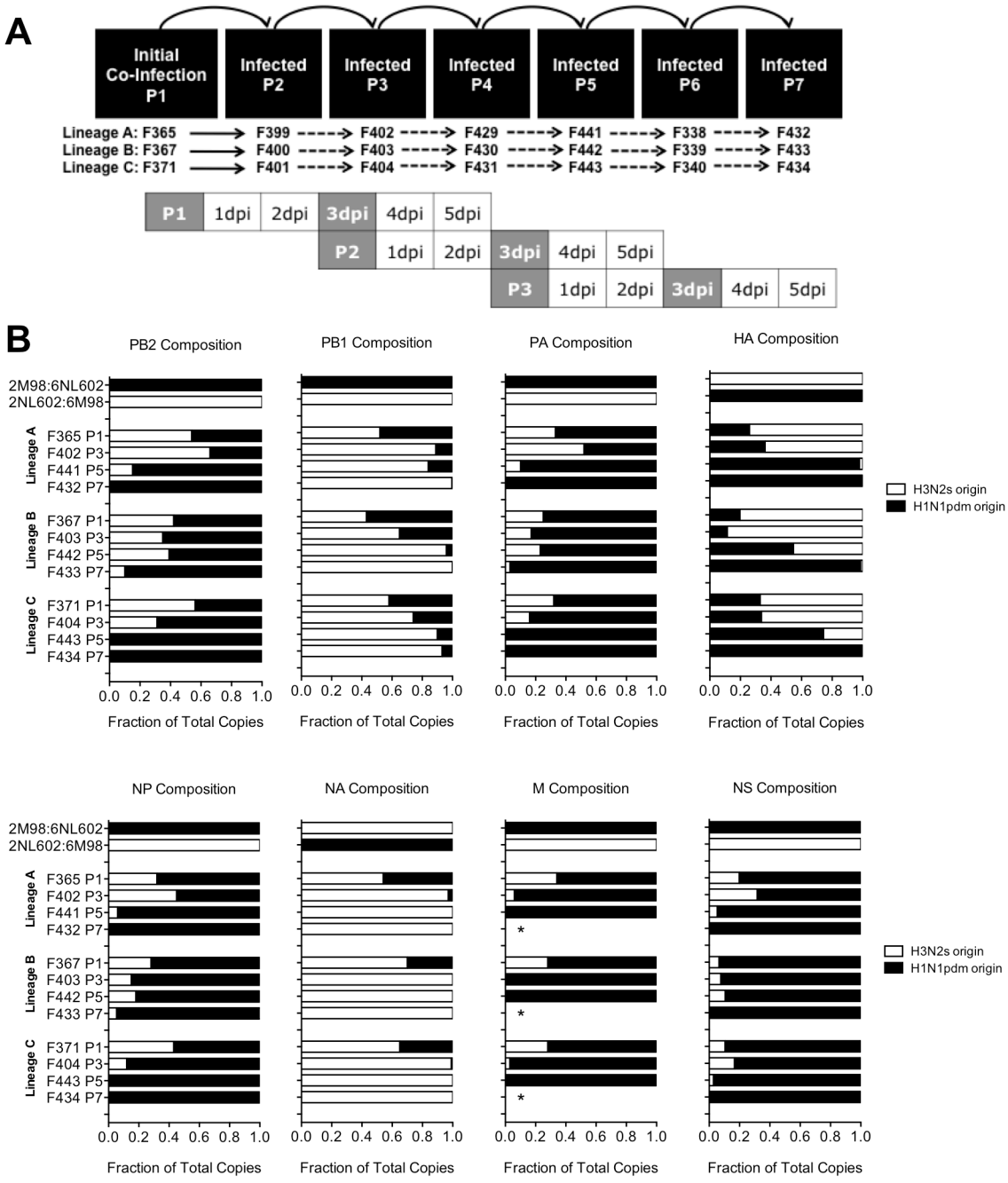


Figure 3.6: Passage schema and allele quantification over passage. A) Schema for passage and genotyping of co-infected nasal washes. Following infection, ferrets were sampled until 5 dpi. Nasal washes from 3 dpi were used to infect the subsequent passage. Animals comprising lineages A, B, and C were kept separate throughout the course of the experiment. B) Viral RNA from lineages A, B and C was purified from ferret nasal washes at 3 dpi from passage 1, 3, 5, and 7. Each of 8 segments from the 2 parental viruses was quantified by real-time RT-PCR with segment and virus specific Taqman MGB assays. The identification number for each ferret (F) is provided. Black bars represent relative amounts of pH1N1-origin copies for each particular segment, whereas white bars represent relative amounts of H3N2-origin copies for the same segment.

genotyped nasal washes were serially and independently passaged in ferrets directly from nasal washes of the preceding passage to create three lineages (A, B, and C) of passaged viruses (Figure 3.6A). This allowed for multiple rounds of replication, reassortment, and selection within the ferret based on constellation fitness without the loss of emerging and potentially better-fit constellations. Animals in each passage were infected with nasal washes (3 dpi) from the previous passage, housed in separate isolators, and sampled independently until 5 dpi. After 7 passages for each lineage had been completed, viral RNA from passages 3, 5, and 7 was obtained for further study (Figure 3.6B). Each allele for the 8 gene segments from the selected passages was quantified by real-time PCR to determine the ratio of the alleles in each. While both alleles for each segment were present in passage 1, all eight gene segments resolved to a single dominant allele by passage 7 (≥90%), with the extinction of several alleles below limits of detection (Figure 3.6B). The dominant genotype of the virus population at passage 7 was unique from both parental constellations. Moreover, all three lineages resolved to the same genotype, incorporating seasonal-origin PB1 and neuraminidase (NA) gene segments in an otherwise pandemic virus constellation despite being passaged independently from one another (Table S2).

### 3.3.3 Molecular changes associated with emergence of the dominant H1N2 reassortant viruses

To determine if the selection of an H1N2 virus was significantly favored, the dominant alleles of the passage 7 viruses were sequenced. The consensus sequences for all genes except HA remained unchanged after 7 serial passages in ferrets. The consensus sequences for HA, however, revealed mutations unique to each of the lineages whose emergence could be traced back to earlier passages within that lineage (Table S3). These results indicate that the H1N2 reassortant populations arose independently and consistently in each of the three lineages.

While endpoint genotyping of the populations selected *in vivo* at the end of multiple passages describes the most "fit" constellations to arise from co-infection, it yields little information on the population dynamics and selective pressures involved in reaching that endpoint. We therefore sought to examine segment fitness as a function of passage. While the majority of genes gradually resolved to the dominant alleles between passages 1 and 7, strong selection was observed for the seasonal neuraminidase and pandemic matrix gene segments. The seasonal neuraminidase accounted for 96% (A), 100% (B), and 99% (C) of segment 6 present in virus

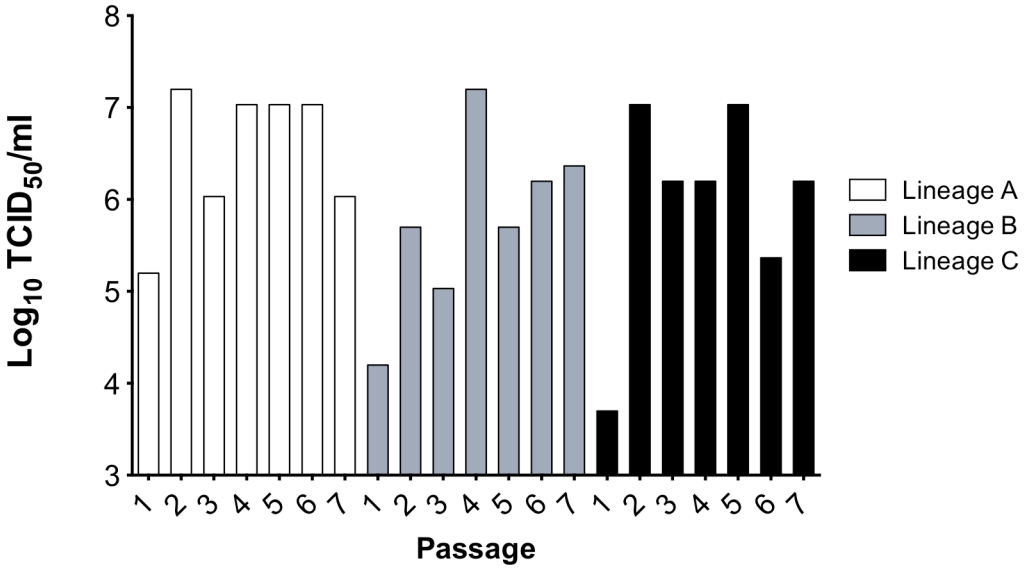


Figure 7: Virus shed into ferret nasal washes over passage. Ferret nasal washes from each lineage at 2 dpi are shown, and were generally representative of peak viral shedding for each passage.

populations at passage 3, while the pandemic matrix accounted for 94% (A), 100% (B), and 97% (C) of segment 7 present in the same passage. Although the seasonal-origin PB1 gene segment appears to be the dominant species in passage 7, its accumulation is not marked with a rapid extinction of the alternative allele (Figure 3.6B). A trend for an increase in infectivity was also observed during passage, concurrent with segment resolution (Figure 3.7). Despite a large initial infectious dose in passage 1, peak virus titers measured at 2 dpi remained low relative to levels at subsequent passages. While the infectious doses for passages 2 through 7 were generally 10- to 100-fold lower than the initial inoculant, peak shedding generally increased 100-fold over passage 1. Altogether, these results suggest strong selection for virus constellations and/or mutations that favor increased growth within the host.

### 3.3.4 Airborne transmission of the H1N2 reassortant virus

As both wild-type constellations have been shown to transmit efficiently in ferrets via respiratory droplets to contact animals (20, 21), we sought to determine whether serial passage without a transmission barrier resulted in selection for high-growth constellations to the detriment of transmissible species. To that end, two groups of ferrets were inoculated with passage 7 viruses. Lineages A and C were combined because rRT-PCR results determined that they were of similar genetic compositions. At 1 dpi, additional animals were introduced in direct and respiratory contact as before. In both groups, lineages A/C and B, infected animals shed to high titers for 6 to 8 dpi. Additionally, both groups transmitted to direct as well as respiratory droplet contacts efficiently (Figure 3.8).

At 4 dpi, lung, trachea, and nasal turbinate were collected for virus isolation and tissue pathology, and compared to samples from the initial co-infection experiment. Similar pathologies were observed in both co-infected and passage 7 infected animals, with moderate edema of the tracheal epithelium and moderate inflammation and infiltration in lung tissues (Figure 3.9A to F). Additionally, general similarity was observed in titers obtained from nasal turbinate, trachea, and lung tissues between the co-infection and passage 7 samples (Figure 3.9G).

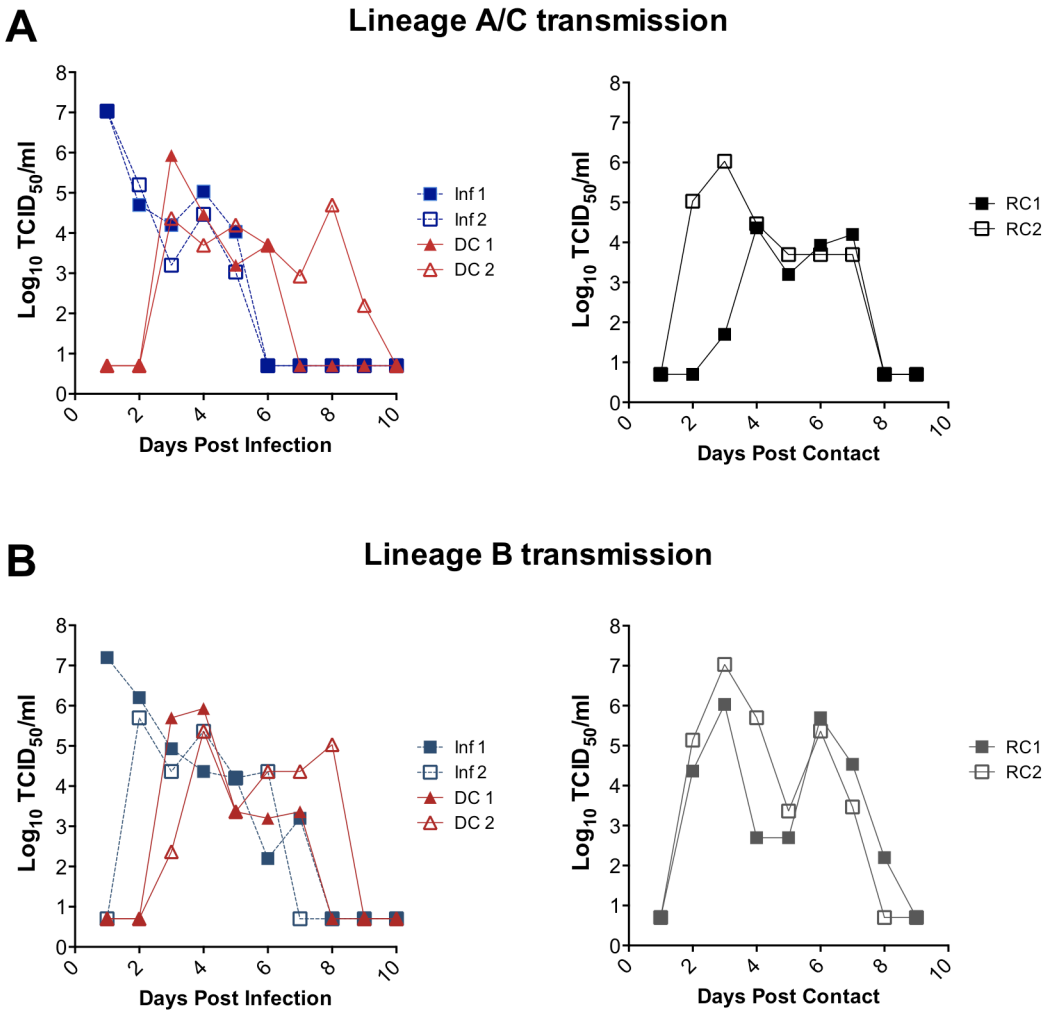


Figure 8**:** Transmission of Passage 7 viruses. Ferrets (blue lines, left panels) were inoculated with $1x10^6$ $TCID_{50}$ of either a passage 7 lineage A/C mixture (A) or lineage B (B). Direct contact (DC, red lines, left panels) and respiratory droplet contact animals (RC, black/grey lines, right panels) were introduced at 1 dpi. Levels of virus shedding in ferret nasal washes are shown over days post infections (left panels) or days post contact (right panels).

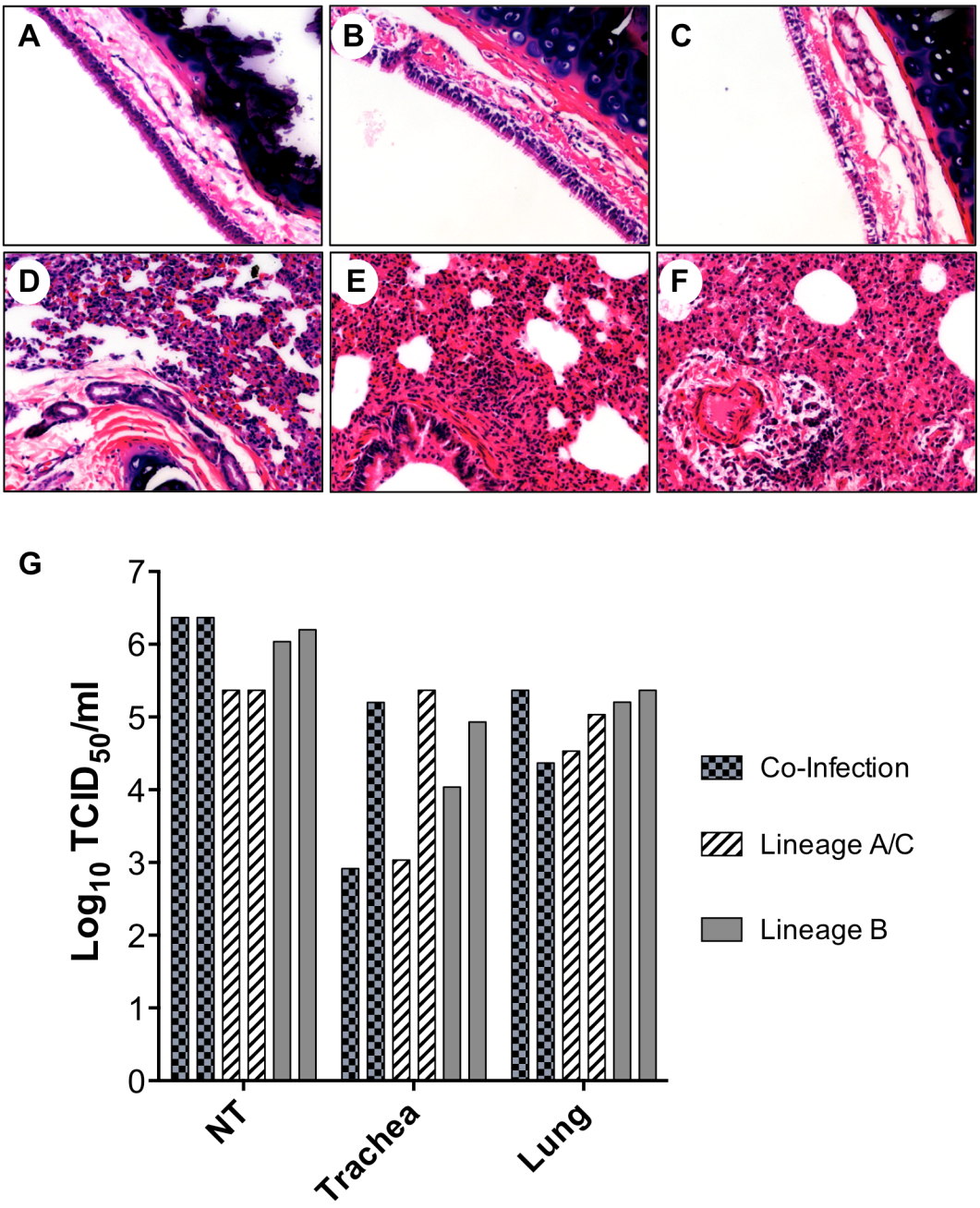


Figure 9 Tracheal and lung pathology in infected ferrets. Tracheal (A-C) and lung sections (D-F) from ferrets infected with P7 Lineage A/C mixture or P7 Lineage B, respectively. Tissues were collected at 4 dpi and treated for H&E staining as described in materials and methods. G) Virus titers in ferret nasal turbinates, tracheal, and lung tissues harvested from infected ferrets at 4 dpi. N=2.

*3.4 Discussion*

A relevant animal model to study reassortment could potentially provide information on gene segments especially adept for selection during influenza pandemics concurrent with established circulating strains. This study details the co-infection of ferrets to generate a reassortant virus with a constellation distinct from either parental strain. Real-time RT-PCR was used to determine the celerity of temporal selection on segment populations during a co-infection and subsequent serial passage. Our findings suggest not only that the ferret can be used to study reassortment but also that the ferret model can rapidly select for constellations currently being observed in nature.

The ferret has long been used as an animal model to study influenza virus infection, pathogenesis, and transmission and may in many respects recapitulate disease phenotypes observed in human cases (16, 17). Additionally, many novel laboratory-generated constellations are often tested in ferrets as a marker for these traits (99, 159). However, how best to generate these constellations has been the subject of rigorous debate. While reassortment studies performed *in vitro* may shed light on constellations compatible for high replicative fitness, combinations well suited for replication and transmission in the host may be underrepresented or lost entirely in these systems. In vivo co-infection studies using relevant animal models have been limited. In one of the few examples, inoculation of ferrets with a highly pathogenic H5N1 virus and a seasonal H3N2 virus demonstrated that reassortment *in vivo* occurred, but the experiment was unable to produce constellations capable of

transmission in this model (159). Reassortment between two viruses relies on infection of not only the same host in general but also the same tissues and cells within that host. If cell tropisms between the viruses differ in the host, the probability of generating reassortant viruses is diminished regardless of constellation fitness in tissue culture. The selection of H1N2 viruses in the ferret suggests an overlap in tropisms between the seasonal and pandemic strains used in this study in a manner that is difficult to reproduce *in vitro*.

Reassortment in swine between the 2009 pandemic virus and a variety of other strains has been widely reported. Most relevant to this study are those strains identified between the pandemic H1N1 and swine-lineage H3N2 strains in pigs that have shown sporadic transmission to humans. Of note are the H3N2 variant (H3N2v) lineage viruses, which have been shown to replicate efficiently and transmit in both swine and ferrets (215, 216). These strains specifically contain the pandemic M segment and the swine H3N2 lineage PB1 and N2, which were donated from an H3N2s virus in the 1990s.

While many of the other pandemic reassortant isolates contain a wide variety of constellations, the vast majority have been found to harbor the pandemic M segment (215, 217-219). Rapid selection for the M segment of the pandemic virus, while encouraging for the model, was not entirely unexpected. In tissue culture selection systems, it has been shown that this M segment reproducibly outcompetes the seasonal H3N2 counterpart after serial passage through limiting dilutions (198). While the selection was not as strong, this system also identified seasonal PB1 and NA segments as genetically fit progeny resulting from a mixed transfection. This may

indicate a selective pressure in the host that is not present *in vitro* and may not be indicative of constellation compatibility. Other studies have shown through directed reassortment that the pandemic matrix segment increases contact transmission in cooperation with the pandemic N1 in swine and ferret models (220, 221). Speculation on the role of the pandemic M1 suggests a morphological advantage to aerosol transmission. Despite this, pandemic M reassortants were consistently generated by direct serial passage without the introduction of an aerosol transmission barrier, indicating that other interactions may play a significant role in the selection of this segment. While the precise mechanism of segment selection remains unclear, the advantages of the process to the virus are evident. The rapid selection of specific gene segments in our study highlights the utility of the ferret as an *in vivo* model to study the viral and host factors contributing to reassortment. In addition to other indicators, this model could also facilitate the risk assessment of potentially pandemic viruses.

# Chapter 4: Role of the pandemic M1 and M2 genes in segment selection

## *4.1 Introduction*

We and others have previously shown that the M gene from the 2009 swine-origin pandemic virus is favored in reassortment upon co-infection with a prototypical seasonal H3N2 in the ferret, a model for human pathogenesis and transmission (198, 222). Others have shown that the pandemic M gene increases transmission in swine in cooperation with the neuraminidase gene (221). With the re-introduction of the pandemic virus into swine, the pandemic M gene has been introduced into other influenza strains, most notably the H3N2v viruses (215). Given these observations, our current interest is in understanding the genetic basis for pandemic M gene selection during reassortment.

The M segment encodes for at least two proteins. The first encodes for the M1 viral capsid protein and is produced from the primary transcript. The second protein encodes for the M2 ion channel and is the product of mRNA splicing. Both genes are translated from the same start codon and share eight amino acids on their N-terminal end. There is an additional overlap of 42 nucleotides in each open reading frame after the M2 donor site before M1 is terminated. While strong selection was observed for the pandemic M segment in co-infection studies, the contribution of each gene encoded within that segment is unclear.

While M1 has been reported to modulate the morphology and transmissibility of influenza viruses, little has been done to show which contributions, if any, M2 makes to viral fitness in the context of transmission or reassortment. Here, the role of

the pandemic M1 and M2 in segment selection is investigated in the context of a co-infection. I have found that both the pandemic M1 and M2 genes are independently sufficient to promote selection of the entire M segment *in vitro* and *in vivo* against a seasonal M segment. Single, pandemic-like mutations in the seasonal M2 gene were also found to promote selection of the entire segment in a competitive mixture against the wild-type seasonal M segment. Further examination of the pandemic M1 suggests that it may contribute to neuraminidase activity. As the pandemic M segment has been shown to increase the pathogenicity and transmissibility of reassortants in cooperation with NA, it is imperative for pandemic preparedness to understand the underlying mechanism by which this segment is selected for during reassortment.

*4.2 Materials and methods*

**Cell Culture and Virus Infection**

MDCK and PK(15) cells were cultured in Dulbecco's modified Eagle medium (Sigma-Aldrich, St. Louis, MO) supplemented with 25 mM HEPES (Sigma-Aldrich), 2 mM glutamine (Sigma-Aldrich), 10 mM HEPES (Invitrogen, Grand Island, NY), and 10% fetal bovine serum (FBS; Sigma-Aldrich) and were grown at 37 °C under 5% CO2. HEK 293T cells were cultured in Opti-MEM (Sigma-Aldrich) supplemented with 10% FBS and 1% Antibiotic/Antimycotics solution (OptiMEM+AB, Sigma) and grown at 37 °C under 5% CO2. For co-infections, MDCK cells were seeded into 6-well plates at a density of $8x10^5$ cells/well in Opti-MEM+AB and incubated at 37˚C for 24 hours. Prior to infection, cells were washed with PBS in triplicate, and infected at $1x10^5$ $TCID_{50}$/virus in 1mL. For viral growth kinetics and limiting dilutions, 96-well plates were seeded at $2.4x10^4$ cells/well in OptiMEM+AB and incubated at 37˚C for 24 hours. Serial, 10-fold dilutions were made in OptiMEM+AB. Of these, 200µL of each dilution were transferred to the 96-well plate in quadruplicate. For each infection scheme, cells were incubated at 37˚C for 72 hours before the supernatant was harvested or assayed.

**Virus Rescue**

Transfections for virus rescue were performed in co-culture, either HEK293T/MDCK (4:1). Cells were seeded in DMEM in the presence of serum 24 hours prior to transfection. Transfection mixtures were generally prepared with 1µg DNA/plasmid/gene segment in OptiMEM and TransIT-LT1 (2µL/µg DNA, Mirus, Madison, WI) in a total volume of 200µL, and incubated for 30 minutes. For

example, 6µg of DNA was transfected for a plasmid encoding 6 reverse genetic cassettes. Media would be exchanged for 1mL OptiMEM+AB, and the transfection mixture would be added drop wise to each well. At 6 hours post transfection (hpt), the transfection mixture would be replaced with 1mL OptiMEM-AB. At 24 hpt, 2mL of OptiMEM-AB supplemented with 3µg TPCK-treated Trypsin (Worthington Biochemical, Lakewood, NJ) would be added to each well of the transfection. Unless otherwise noted, all transfections were incubated at 37˚C under 5% CO2.

**Ferret Co-infections**

Ferrets in this study were 8- to 10- months old, and obtained from Triple F Farms (Sayre, PA). Animals were co-infected at $1x10^5$ $TCID_{50}$/virus in a total volume of 500µL. Nasal washes were performed daily, and infection was monitored using a Flu Detect Antigen Capture Test (Synbiotics Co.) until 3dpi. Nasal washes from 3 dpi of each passage were diluted 1:5 in PBS in a total volume of 500 µl and used to infect subsequent ferrets as before. For transmission studies, ferrets (n=2) were again inoculated intranasally with $1x10^6$ $TCID_{50}$ of virus in 500 µl. At 1 dpi, naïve animals (n=2 for each group) were placed in direct contact (DC) or barrier-separated respiratory droplet contact (RC) with the infected animals. Animal studies were performed under protocols approved by the University of Maryland Institutional Animal Care and Use Committee.

**Sanger sequencing of M gene amplicons**

RNA was isolated from 200µL tissue culture supernatant using the RNeasy isolation kit according to the manufacturer's recommendations. Transcription of cDNA was performed using AMV reverse transcriptase (Promega) with 10µM Uni12

primer (AGCAAAAGCAGG) in a final volume of 20µL. The entire M segment was amplified using M-1F and M-1027R as previously described (223). PCR products were gel purified and sequenced using the BigDye Terminator v3.1 Cycle Sequencing Kit (Applied Biosystems).

**Deep Sequencing of M Gene Amplicons**

RNA was isolated from ferret nasal washes and purified on the MagnaPure LC as before. Transcription of cDNA was performed with Superscript III Reverse Transcriptase using 10µM of primer M13-M 681F. A portion of the M gene then amplified with GoTaq 2X Green Master Mix (Promega) using 500nM barcoded primers Lib-L M13-GS Fwd and Lib-L M Rev (See Table S5). Cycling conditions were as follows: 95˚C for 2 mins, 35 x (95˚C for 20 secs, 56˚C for 15secs, 72˚C for 3 mins), and 72˚C for 10 mins. The 316bp Amplicons were gel purified, and 340ng ($1x10^{12}$ copies) of each was pooled together in a total volume of 10x(number of libraries) to a final concentration of $1x10^{11}$ copies/µL. The pooled library was diluted down to $1x10^{6}$ copies/µL. An aliquot was heat denatured at 95˚C for 2 mins before being snap cooled on ice. A final volume of 20µL of the library was loaded onto DNA capture beads, 2 copies/bead. An emPCR was then prepared with the capture beads following the manufacturer's recommendations in the emPCR Amplification Method Manual, Lib-L (Roche). Following the sequencing run, reads mapped against 4 references: M98_WT (cgaatgggGgtgcagatgcaAcgattcaagtgaCccGctTgt), NL602_WT (cgaatgggAgtgcagatgcaGcgattcaagtgaTccTctCgt), M98-NL602 (cgaatgggGgtgcagatgcaAcgattcaagtgaTccTctCgt), or NL602-M98 (cgaatgggAgtg

cagatgcaGcgattcaagtgaCccGctTgt). Percent composition for each sample was then determined from the output in the Reference Status file.

**Virus-based Neuraminidase Activity Assay**

Neuraminidase activity assays were performed essentially as previously described with minor modifications (224). Briefly, 96-well plates were coated in fetuin (20µg/mL, Sigma-Aldrich, St. Louis, MO) in PBS, 100µL/well and incubated overnight at 4˚C. The following day, plates were blocked with PBST-BSA (PBS, 0.05% Tween-20, 0.5% BSA) for 1 hour at room temperature. Excess BSA was removed by washing twice with PBST-High (PBS, 0.5% Tween-20). After viruses were were titer normalized to $1x10^6 TCID_{50}$/mL, two-fold serial dilutions were made in PBST-BSA supplemented with $CaCl_2$ and $MgCl_2$, 1mM each. To the fetuin-coated plate was added 100µL of each virus dilution. Cleavage of the fetuin substrate was allowed to occur for 18 hours at 37˚C and then washed 6 times in PBST-High. HRP-labeled lectin from peanuts (Sigma-Aldrich) was diluted to 2µg/mL in PBST-Low (PBS, 0.05% Tween-20) and 100µL added to each well following the incubation. The lectin was allowed to bind cleaved substrate for 2 hours at room temperature followed by 6 washes to remove unbound lectin. One 8mg OPD (o-Phenylenediamine dihydrochloride, Sigma-Aldrich) tablet was was dissolved in 25mL OPD buffer (50mM dibasic sodium phosphate, 25mM citric acid) and supplemented with 10µL 30% hydrogen peroxide. The peroxidase reaction was initialized by adding 100µL of the OPD buffer to each well and allowed to proceed for 20 minutes at room temperature. The reaction was quenched by the addition of 100µL 1M sulfuric acid. NA activity was determined by reading the OD490 of each well.

**M2 Activity Assay**

M2 activities were determined as previously described with modifications (225). Briefly, 293T were seeded in 96-well plates at a density of $7.1x10^4$ cells/well and allowed to recover at 37˚C overnight. A 10X common buffer (CB) was prepared from NaCl (1.4M), KCl (53mM), $MgSO_4$ (5.5mM), $CaCl_2$ (18mM), and D-glucose (55mM) in 500mL. Low and High pH buffers (1X) were prepared by adding MES or HEPES to a final concentration of 15mM and adjusted to pH 5.5 or 7.4, respectively. Cells were washed with 100µL High Buffer and imaged at pH=7.4. The buffer was then exchanged to adjust the pH to 5.5, and each well was imaged continuously for 8 minutes. The mean change from initial fluorescence was then calculated for each M2, and the rate and plateau were calculated for each.

*4.3 Results*

### 4.3.1 Pandemic M segment results in better replication over the seasonal segment

In previous reports, we have identified a selective advantage of the pandemic M segment during co-infection studies with a seasonal H3N2 virus. The M segment of IAV encodes for two proteins: M1, the primary transcript, and M2, a splice variant. To determine the effects of each gene on viral replication, a panel of viruses was generated containing either wild-type seasonal and pandemic M segments, or chimeras of the two in the H1N2 background selected for in ferret co-infections (222). To create these, the M1 open reading frame from NL602 (pandemic) was fused to the downstream M2 sequence from M98 (seasonal) by overlapping fragment extension (Figure 4.1). The resultant segment produced a chimeric vRNA species containing a 5' and 3' end of pandemic and seasonal origins, respectively (Chimera A, Figure 4.3A). Additionally, the inverse configuration was cloned containing an M1 of seasonal origin and the M2 from the pandemic virus (Chimera B).

To determine if increased growth kinetics could be responsible for the competitive advantage of the pandemic M segment, MDCK were infected at an MOI=0.001 ($8x10^2$ $TCID_{50}$) with either wild-type or chimeric M segment viruses, and time points were taken at 10, 24, 48 and 72 hours post infection. Although all viruses grew to high titers, the wild-type pandemic M segment virus grew to significantly higher titers over the course of the experiment compared to the wild-type seasonal M segment virus. Although not significant, viruses with chimeric M segments grew to intermediate titers (Figure 4.2). This may suggest that both M1 and M2 from the

pandemic segment contribute in some way to increased replication in this virus background.

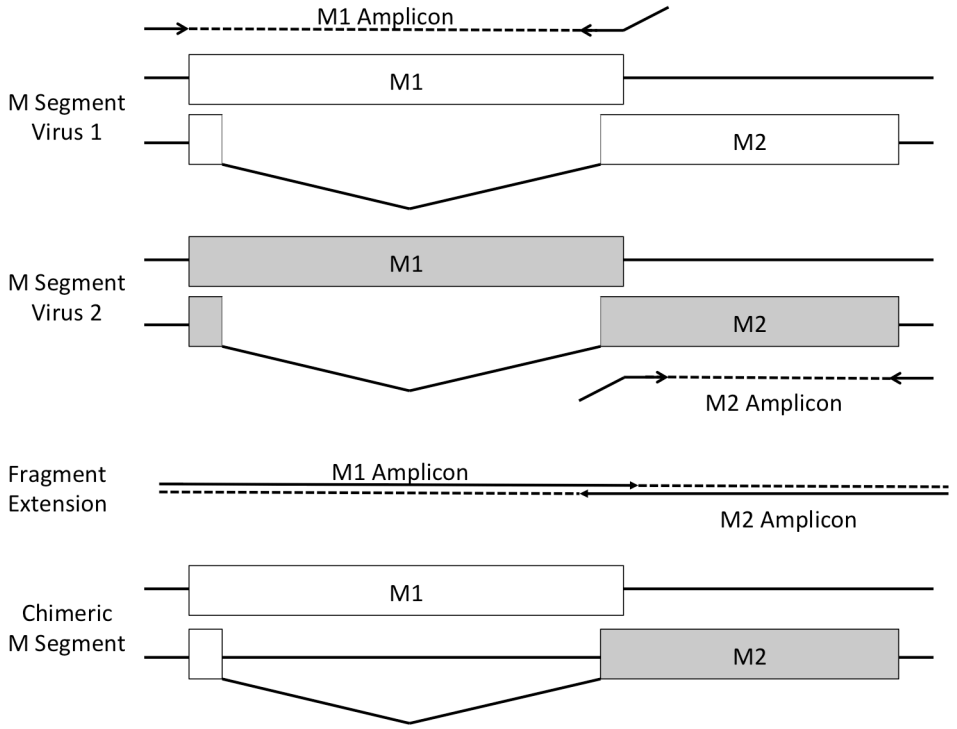


Figure 4.1: Construction of chimeric M segments. Fragments for either M1 or M2 were amplified with overlapping primers. Each fragment was used as a template to amplify a full length, chimeric M segment by fragment extension.

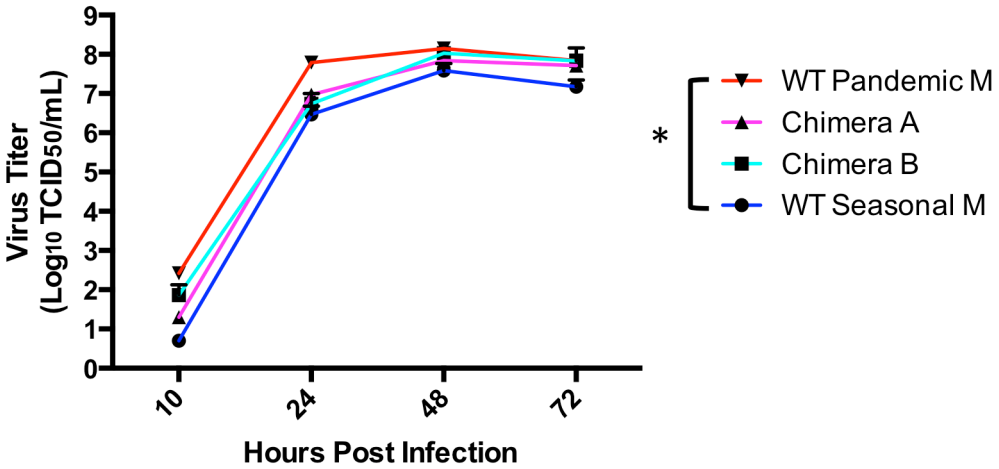


Figure 4.2: Growth kinetics of wild-type and chimeric M segment viruses. Multistep growth kinetics (MOI=0.001) in MDCK cells over 72 hours. N=3. 2-way ANOVA statistical analysis shown.

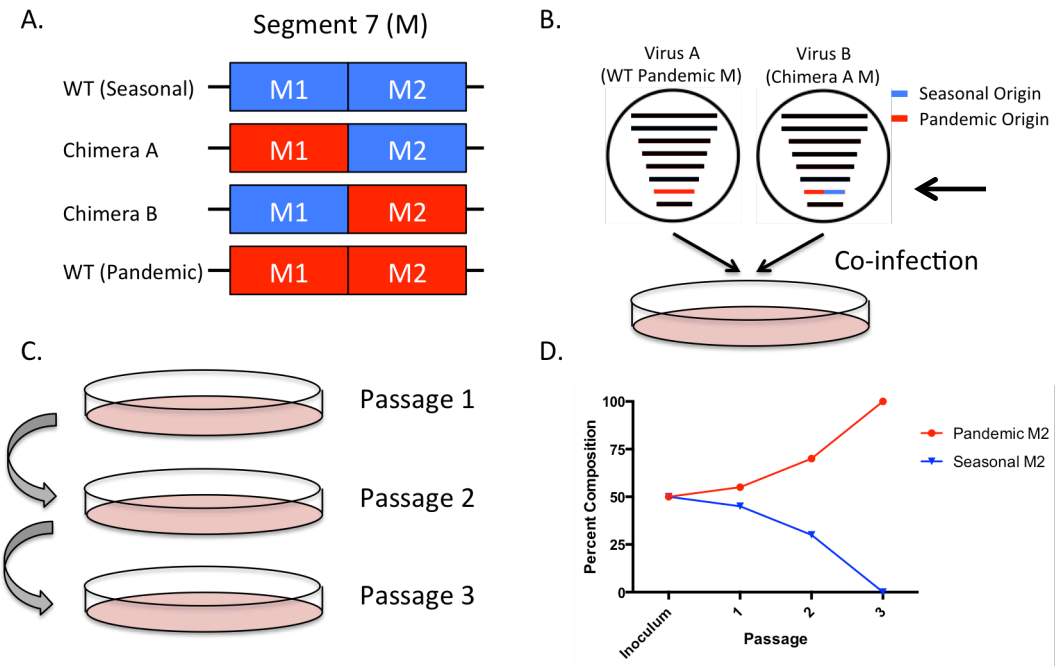


Figure 4.3: Competitive mixture model to identify segment fitness. A) Chimeras constructed from seasonal and pandemic M segments differ in the genetic origins of their M1 and M2 genes. B) In this example, viruses rescued from either wild-type pandemic or chimera A M segments in an otherwise identical segment composition are mixed together and used to co-infect MDCK cells or ferrets (not shown). Both M segments encode for the pandemic M1 gene (red) and differ in the genetic origin of the M2 gene. C) Viruses are allowed to grow for 72 hours and then passaged two subsequent times, allowing for segment competition effectively between the pandemic and seasonal M2 genes. D) The composition of each M segment, represented by the non-identical gene, is quantified either by Sanger sequencing SNP analysis or 454 sequencing of tissue culture supernatant or ferret nasal washes, respectively.

Table 3: Direct competition of chimeric M segments in vitro

| | Wild Type Virus | | Chimeric Virus | | Major Population (Ratio of Replicates) |
|---|---|---|---|---|---|
| | M1 | M2 | M1 | M2 | |
| Group A | Seasonal | Seasonal | Seasonal | **Pandemic** | Chimera (3/3) |
| Group B | Pandemic | Pandemic | Pandemic | **Seasonal** | Wild-type (3/3) |
| Group C | Seasonal | Seasonal | **Pandemic** | Seasonal | Chimera (3/3) |
| Group D | Pandemic | Pandemic | **Seasonal** | Pandemic | Wild-type (3/3) |
| | Virus 1 | | Virus 2 | | Major Population (Ratio of Replicates) |
| | M1 | M2 | M1 | M2 | |
| Group E | Seasonal | Pandemic | Pandemic | Seasonal | Virus 1 (1/3)<br>Virus 2 (2/3) |

### 4.3.2 Segments containing either the pandemic M1 and M2 outcompete the seasonal alleles *in vitro*

In previous studies, selection for the pandemic origin M segment was observed to occur rapidly in *in vivo* co-infection experiments. As the origins of each gene within the M segment may play a role in viral replication, competitive co-infections between viruses with wild-type and chimeric M segments were performed to identify which gene contributed to segment selection *in vitro*. MDCK cells were infected with $1x10^5$ $TCID_{50}$ of each virus pair in triplicate. At 3 dpi, supernatant from each well was passaged by serial dilution in MDCK cells to select for the most abundant population. The last positive dilution for each replicate was identified by RBC hemagglutination, and sequenced to identify the origin of the M2 gene segment. Co-infection of a wild-type seasonal M gene with a chimera containing the M2 from

the pandemic virus resulted in the selection of the chimeric gene segment (Table 3, group A). Alternatively, co-infection of a wild-type pandemic M gene with a chimeric virus encoding a seasonal M2 resulted in the selection of the wild-type pandemic segment (Table 3, group B).

The reciprocal experiment was also performed in which the M1 alleles were compared while holding the M2 gene constant. Selection was observed for the pandemic M1 chimeric segment when co-infected with a wild-type seasonal M virus (Table 3, group C). Conversely, co-infection of a wild-type pandemic virus with a chimeric M1 seasonal virus selected for the wild-type pandemic M segment (Table 3, group D). Altogether, these results suggest that both M1 and M2 genes from the pandemic virus confer a selective advantage to reassortant viruses *in vitro*.

### 4.3.3 Segments containing the pandemic M1 and M2 genes outcompete the seasonal alleles *in vivo*

To confirm these *in vitro* findings, ferrets were used to determine if the same phenotype was observed *in vivo*. Five ferrets were co-infected with $1x10^5$ $TCID_{50}$ of each virus pair as described (Figure 4.3A and table 3), and nasal washes were collected for 3 days. At 3dpi, nasal washes from infected ferrets were diluted 1:5 and serially passaged into 5 additional animals. This was repeated again for a total of 3 independent passages and 9 total days of virus replication for each virus pair. Viral RNA was extracted from ferret nasal washes, and M gene cDNA was prepared from each sample. A region spanning the M1/M2 gene overlap was barcoded with 454 lib-

L compatible primers and amplified for sequencing. Reads were reference mapped in order to identify the major M segment population and the overall percent composition of each M segment allele. Although an attempt was made to co-infect at equivalent doses by titer, the percent composition identified in the inoculum was skewed for all virus pairs, possibly due to inaccuracies in viral titrations or differences in the infectivity of each virus. Despite this, co-infection of wild-type M segment viruses with chimeras differing in either M1 or M2 yielded interesting results for the role of the these genes in M segment selection. Over the course of the 9-day infection, ferrets co-infected with a wild-type seasonal M segment virus and chimera A selected for the chimera, which contains the pandemic M1 gene (Figure 4.4A). Conversely, ferrets co-infected with a wild-type pandemic M segment and chimera B, containing a seasonal M1, selected for the wild-type segment (Figure 4.4B). Although the M segment population quickly resolved, these data may indicate a selective disadvantage of the seasonal M1 allele and suggest that the pandemic M1 allele is sufficient to drive selection of the entire M segment during a co-infection. The inverse experiment was also performed to determine the contributions, if any, of the M2 origin to segment selection using competitive mixtures of wild-type and chimeric M segment viruses. Ferrets co-infected with a wild-type seasonal M segment virus and the chimera B segment virus, selected for the chimeric virus, which contained the pandemic M2 allele (Figure 4.4C). Conversely, ferrets co- infected with a wild-type pandemic M segment virus and the chimera A segment virus, containing the seasonal M2, selected for the wild-type pandemic allele (Figure 4.4D). Although the initial composition of

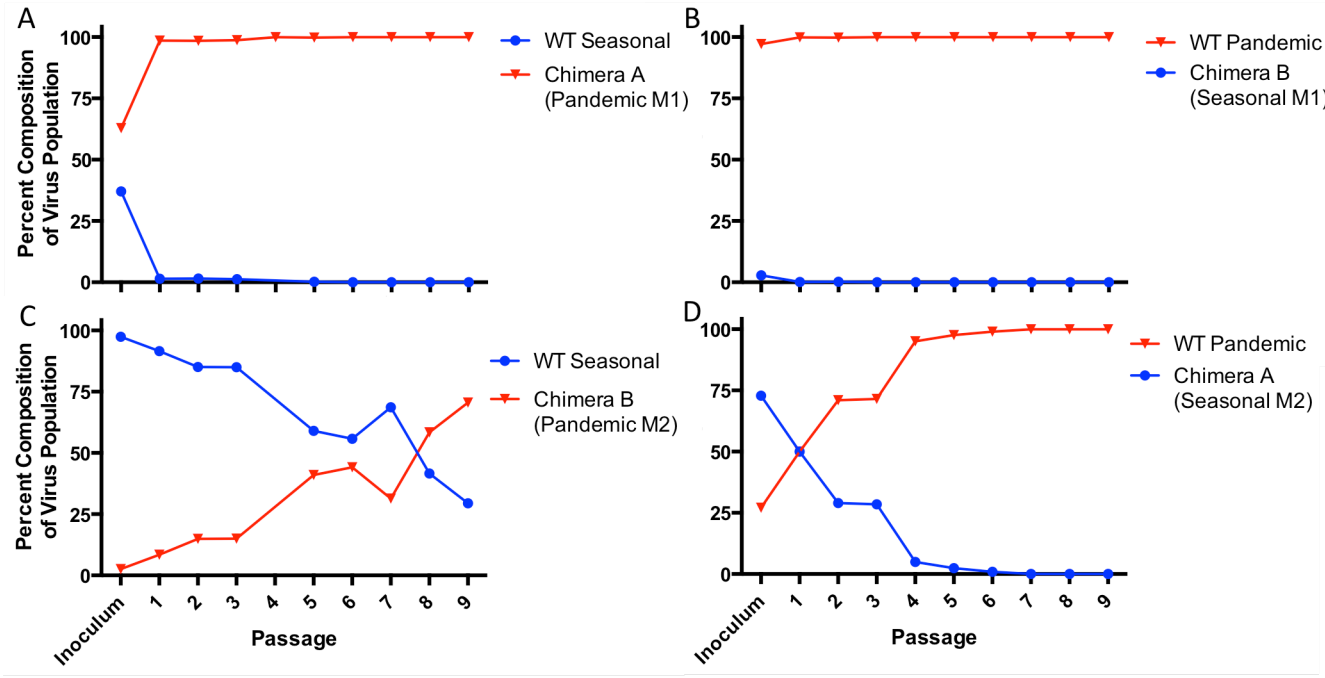


Figure 4.4: M gene allele selection *in vivo*. Ferrets were co-infected with viruses containing wild-type and chimeric M segments. Nasal washes were collected every day during 3 passages composed of 3 days each. Days post co-infection cover three passages, and are depicted as a single replication cycle. Percent composition of the wild-type allele in each co-infection was determined by 454 deep sequencing of an M gene amplicons. A and B) M1 contribution to M gene selection. C and D) M2 contribution to M gene selection.

each virus in each co-infection was skewed in the inoculum, the selection favored the minor initial population. These data indicate a strong and consistent selective preference for the pandemic M2 allele, and suggest that this allele is sufficient to drive the selection of the entire segment independent of the M1 gene origin.

### 4.3.4 Pandemic M genes overcome initial disadvantage to outcompete seasonal alleles

To overcome the difficulties in correlating virus titer to segment copy number, each virus pair in table 3 were mixed 1:1 at a calculated titer of $1x10^5$ $TCID_{50}$/mL. Viral RNA was again extracted, and cDNA was transcribed as previously described (223). The full length M gene was then amplified with universal primers, and the M1/M2 boundary was sequenced with a conserved, upstream primer. The ratio of each virus in the mixture was determined from the peak area of sequenced polymorphisms in the M genes using the polySNP software (226). To confirm previous results, the ratio generated from polySNP was used to repeat the co-infection at a ratio of 9:1 unselected to selected M segment based off of previous results. Once again, the inoculum was sequenced to determine the percent composition of each virus pair. Supernatant was harvested at 3 dpi and passaged two additional times at a dilution of 1:100 of the previous passage. The percent composition of M segments in each group at 3dpi for all three passages were determined by sequencing as before. In each case, the relative proportion of the previously selected segment in the inoculum was much less abundant than the previously unselected segment, and within a range of 16 to 26 percent of the overall M segments within the mixture (Figure 4.5). This is particularly

important in the M1 challenge groups where the more pandemic like segments were selected after being inoculated at a high starting frequency. As expected, all groups resolved to the genotypes previously observed both *in vitro* and *in vivo*, with either chimeric segment outcompeting the wild-type seasonal M segment, and the wild-type pandemic M segment outcompeting either chimeric. Taken together, these data suggest that selection of the pandemic M gene, at least in this constellation, is driven by both M1 and M2.

### 4.3.5 Both genes from the pandemic virus contribute to the selective advantage of the entire segment

To examine the relative contributions of either the pandemic M1 or M2 gene, viruses encoding either chimera were mixed at a 1:1 ratio as determined by titer. As before, these were used to co-infect both MDCK cells and ferrets. In cells, co-infection with each chimera resulted in the selection of the virus with the pandemic M1 and seasonal M2 (Table 3, group E), suggesting that a stronger selective contribution may exist for the pandemic M1. The same virus mixture was, however, used to co-infect ferrets, and the ratio of each chimera in the mixture was subsequently quantified. Deep sequencing of the mixture showed that the initial ratio of the pandemic M1/seasonal M2 chimera constituted a much higher proportion of the inoculum at 92%, placing the seasonal M1/pandemic chimeric segment at a significant disadvantage to selection (Figure 4.6B). This may have resulted in the observed frequencies of this chimera in tissue culture, and may not be indicative of a selective advantage of the

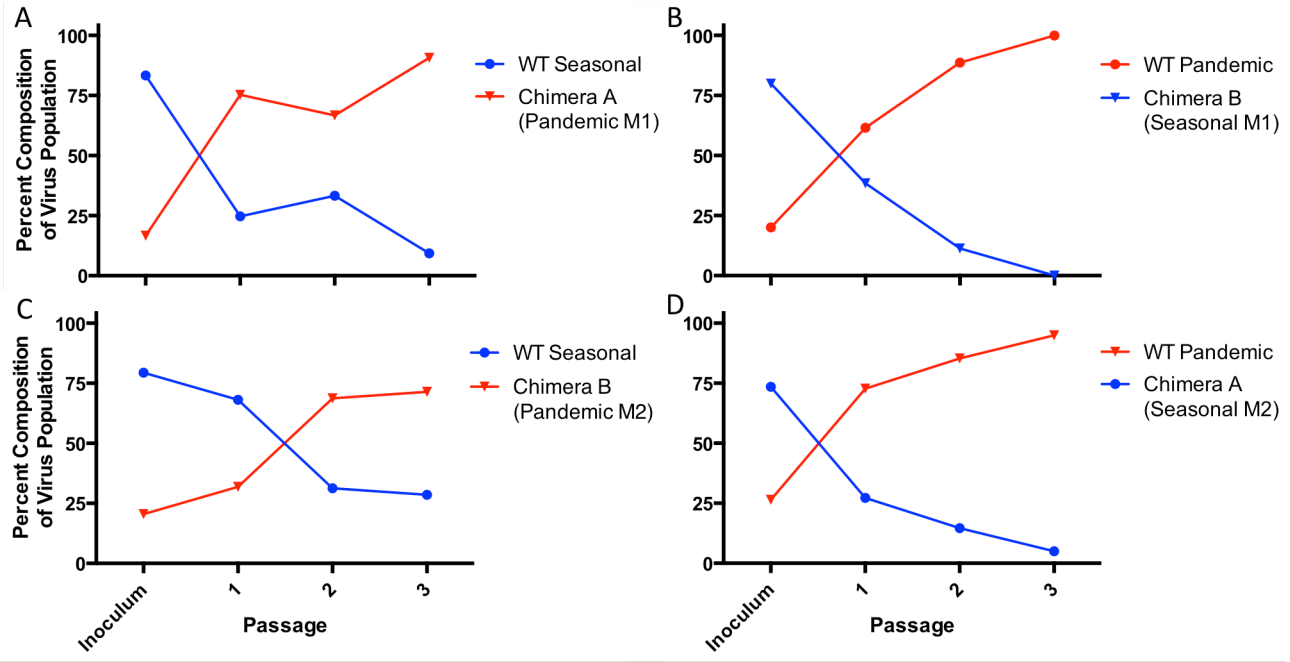


Figure 4.5: Quantified M gene allele selection *in vitro* with polySNP normalization. MDCK cells were co-infected with viruses containing wild-type and chimeric M segments. Supernatant was harvested at 72 hours post infection for quantification and additional virus passage. Percent composition of the wild-type allele in each co-infection was determined by Sanger sequencing of the M gene and polySNP. A and B) M1 contribution to M gene selection. C and D) M2 contribution to M gene selection.

pandemic M1/seasonal M2 chimera. Serial passage of this inoculum in ferrets, however, failed to extinguish the seasonal M1/pandemic M2 chimeric segment, which successfully recovered to 26% of the population by the end of the third passage in ferrets. The *in vitro* selection assay was repeated having quantified the chimeric viruses for co-infection with Sanger sequencing and polySNP. Interestingly, the percent composition of either chimera remained relatively static over three passages in MDCK (Figure 4.6A). Combined, these data suggest that neither chimera has a competitive advantage over the other, and that both the pandemic M1 and M2 genes contribute to the fitness of the entire segment.

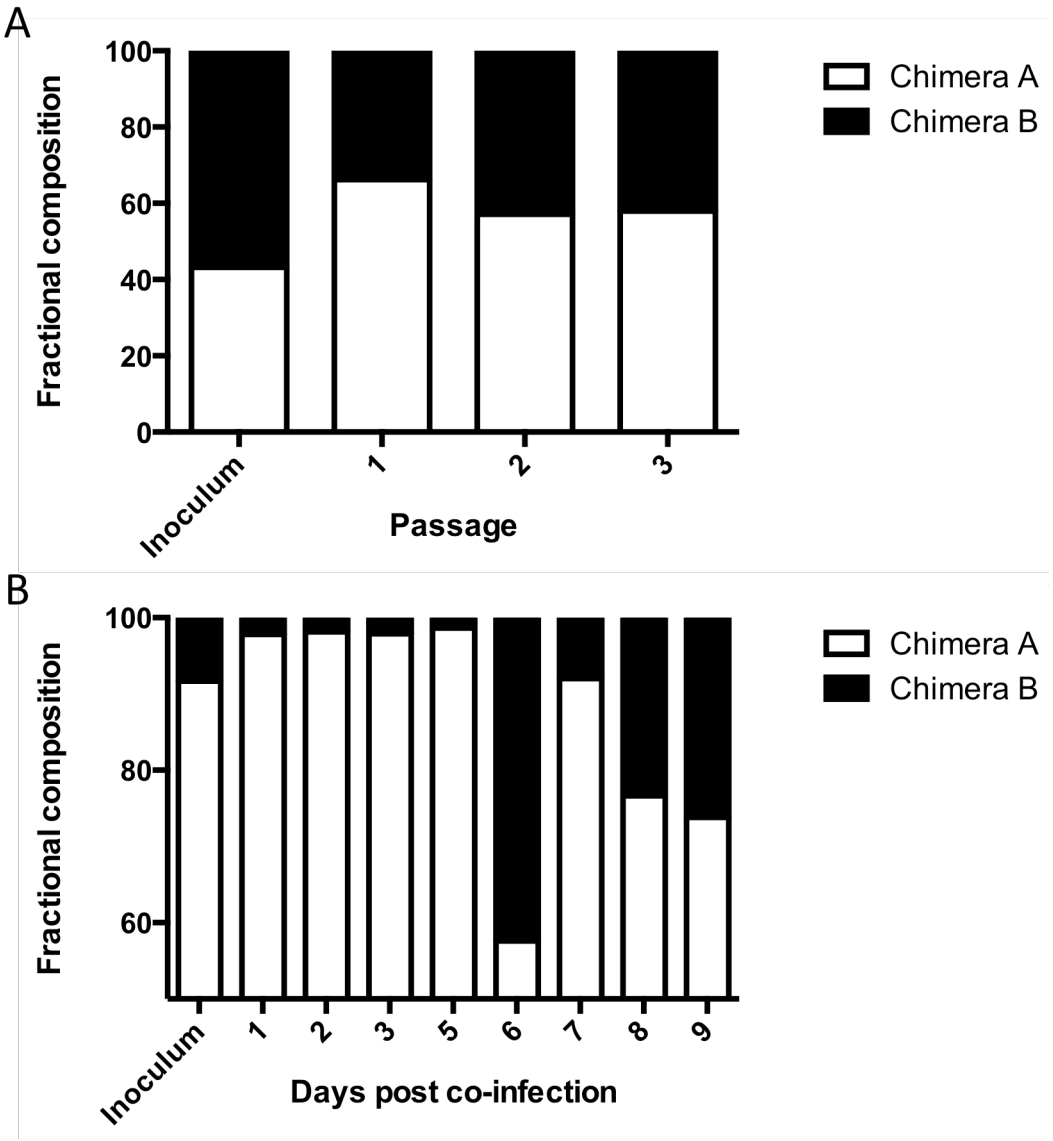


Figure 4.6: Chimeric M segment competitive mixtures. A) *In vitro* competition between chimeric M segment viruses normalized with polySNP. Inoculum and passages were quantified with polySNP. B) *In vitro* competition between chimeric M segment viruses normalized by titer (1x105 $TCID_{50}$ each). Inoculum and ferret nasal washes were quantified with 454 deep sequencing.

### 4.3.6 Characterization of the segment 7 dependence of NA activity

Since its emergence, the pandemic M segment has reassorted with swine lineage triple-reassortant H3N2 viruses between 4 to 10 times, suggesting an advantage in the field (227). Multiple *in vitro* and *in vivo* studies have also identified a preference for related neuraminidase genes to segregate with the pandemic matrix segment (198, 222). Furthermore, it has been suggested that these two segments cooperate to increase the transmissibility in swine (221). To further investigate the contribution of different M segment alleles to neuraminidase function, viruses were rescued with constellations similar to those produced by serial passaging in ferrets (Table 2), but with M segments originating from either a seasonal H3N2 (A/Memphis/14/1998) or the pandemic virus (A/Netherlands/602/2009) which had been previously selected for during reassortment and passaging. Although the identity of the N2 NA gene remained consistent throughout the experiment, viruses containing the pandemic M segment exhibited about a 4-fold higher NA activity compared to those containing a seasonal M segment (Figure 4.7A). To determine the genetic origin contributing to the difference in NA activity between these viruses, viruses containing M gene chimeras with M1 from a seasonal or pandemic origin and an M2 from the opposite origin of the M1 gene were examined. Although the NA activities were generally lower for these viruses, a 4-fold difference was also observed between the two viruses with the pandemic M1 gene conferring a higher NA activity (Figure 4.7B). These findings suggest that the pandemic M segment, and more specifically the pandemic M1, confer increased neuraminidase activity.

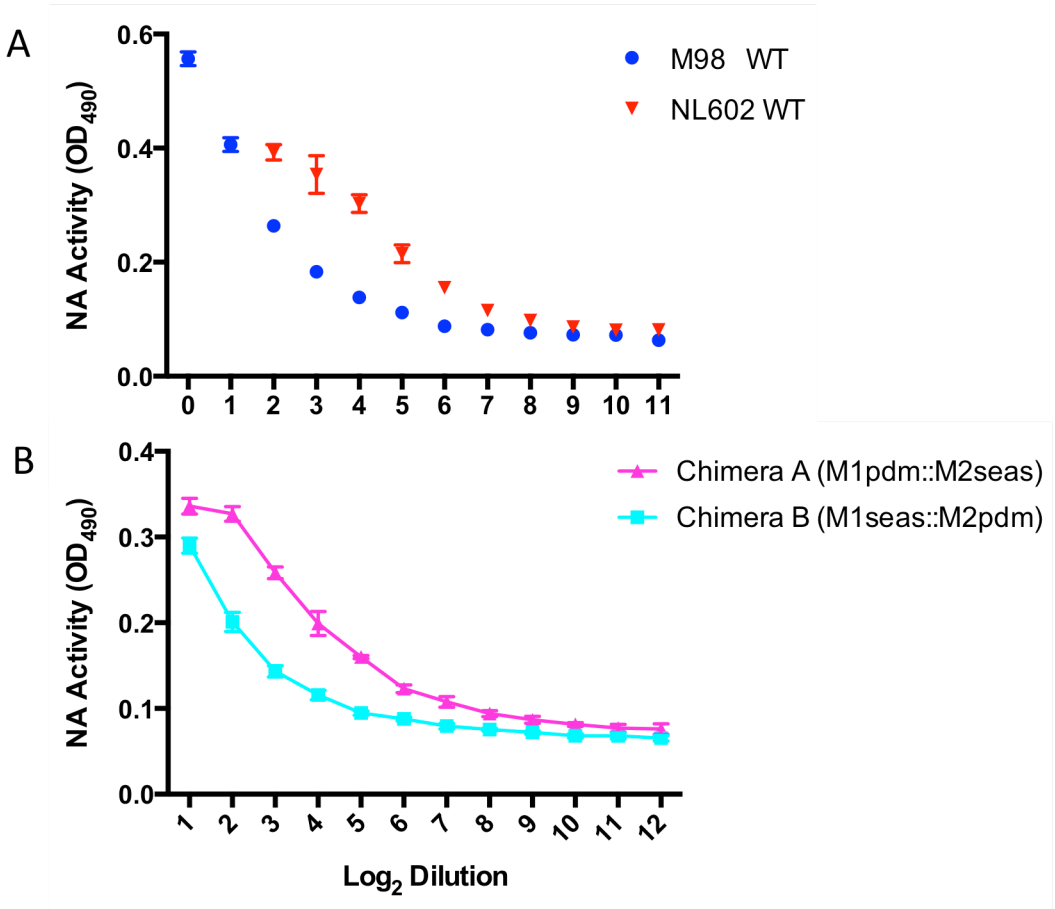


Figure 4.7: N2 NA dependence on M segment identity. Two-fold dilutions of viruses encoding either wild-type (A) or chimeric (B) M segments were incubated on plates coated with fetuin for 18 hours. After the incubation, the cleaved fetuin was bound by a peroxidase labeled peanut lectin, treated with the OPD substrate, and imaged on a spectrophotometer (N=3).

### 4.3.7 Characterization of M2 genes in seasonal and pandemic viruses

The M2 gene from the pandemic virus has been shown to undergo positive selection upon co-infection with a virus carrying the seasonal homolog. The underlying mechanism, however, remains unclear. Fifteen mutations exist between the seasonal and pandemic M2 genes that could speak to a possible mechanism, eleven of which occur after the overlapping reading frames between M1 and M2. To identify mutations that contribute to the selection of the pandemic M2 gene, the pandemic alleles corresponding to these eleven mutations, occurring in the transmembrane ion channel domain and the c-terminal domain, were engineered individually into an otherwise wild-type seasonal M segment. Of these, eight were viable for virus rescue. As before, these "pandemic-like" mutant viruses were challenged in a competitive mixture model in MDCK cells against viruses containing the wild-type seasonal M segment at an attempted ratio of 4:1, respectively. After 72 hours post infection, 300μL (1:10) of tissue culture supernatant was serially passed into MDCK cells. After 3 total passages, the percent composition of each segment was quantified for the inoculum and each passage using Sanger sequencing and polySNP. Of the eight mutations that were viable, those corresponding to L43T, H57Y, and K78Q resulted in the greatest increase in mutant segment percent composition over three passages (Figure 4.8).

The L43T mutation occurs within the transmembrane alpha helix of M2 near the proton gate. To determine if there were significant differences in the basic proton conductance activity of the two channels, the M2 ORF was cloned out of segment 7 into a protein expression plasmid, and its activity assayed using fluorescent

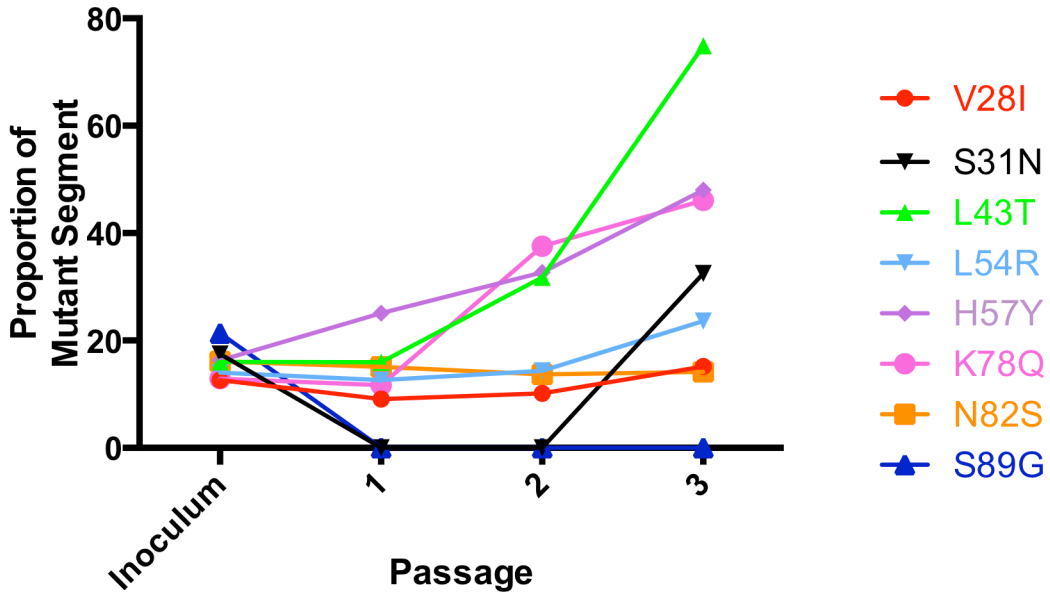


Figure 4.8: Mutant M segment competition model. Seasonal M segment viruses with the indicated mutations in M2 were mixed with viruses containing a wild-type seasonal M segment and serially passaged in MDCK cells. Each passage represents 72 hours of growth. Indicated is the proportion of mutant segment as a percentage of the total segment population.

quenching of EYFP as an intracellular pH sensor (225, 228). Plasmids for EYFP and M2 from either the seasonal or pandemic M2 genes was transfected into 293T cells. After 24 hours, the cells were washed with HEPES buffered saline at a pH of 7.4 and the fluorescence was quantified. The buffer was exchanged for MES buffered saline at a pH of 5.5, and the fluorescence was read every eight seconds for eight minutes until the signal stabilized (Figure 4.9). Both treatments lead to a decrease in fluorescent signal from EYFP compared to pH 7.4 controls, however cells transfected with the seasonal M2 lead to a more dramatic decrease in the intracellular pH compared to the pandemic M2. Although this is an indirect measurement of channel activity, it would suggest that the proton conductance activity of the seasonal M2 is higher than that of the pandemic M2.

The M2 protein has also been shown to slow protein traffic along the secretory pathways and stabilize HA during intracellular transport in a manner dependent on proton pump activity (106, 229, 230). To determine the effects of M2 on the secretion, cells were transfected with plasmids expressing a secreted Gaussia luciferase and M2 ion channels from either the seasonal or pandemic viruses. At 24 hours post transfection, both M2 proteins significantly decreased the expression of the secreted reporter gene compared to the empty vector control. The pandemic M2, however, decreased the total expression and secretion of GLuc to a greater extent. If the correlation between activity and protein expression through the secretory pathways is correct, these data would suggest, in contrary to the M2 activity assays, that the pandemic M2 conducted protons to a greater extent than the seasonal.

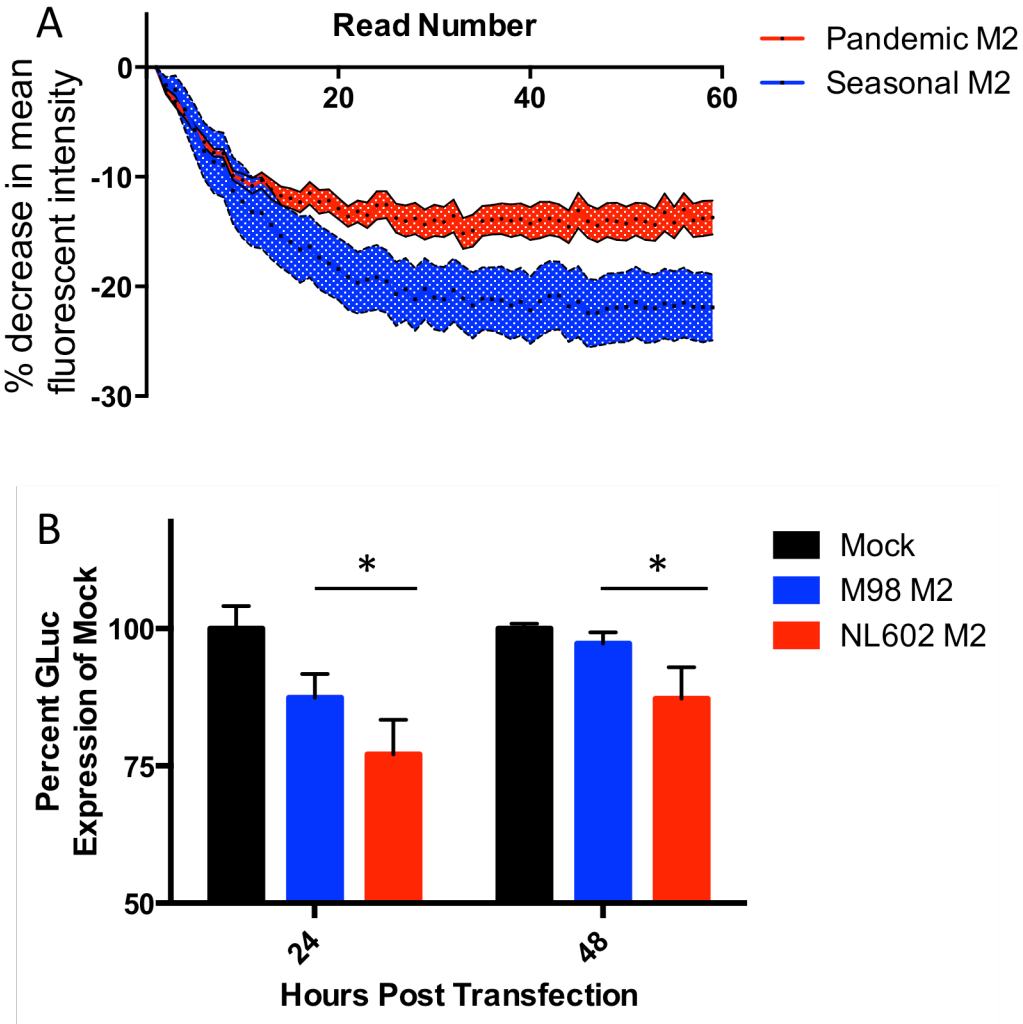


Figure 4.9: Characterization of M2 alleles. A) Plasmids encoding M2 genes from either the pandemic (red) or seasonal (blue) viruses were transfected into 293T cells along with pcDNA3-EYFP. At 24 hours post transfection, the pH of the media was adjusted to 5.5 with MES buffered saline, and the fluorescent intensity of each well was measured on a luminometer. B) Plasmid encoding M2 alleles were transfected into 293T cells together with pGLuc-NS, a secreted luciferase reporter. At 24 and 48 hours post transfection, luciferase activity was determined. Mock is empty vector (pcDNA3).

*4.4 Discussion*

Since its emergence, the 2009 pandemic virus has replaced the previously circulating H1N1 virus as the seasonal strain in humans, and is no longer observed by in the population through surveillance. Furthermore, the vaccine recommendations for trivalent and quadravalent vaccines no longer contain a 1977 "Russian Flu" lineage H1N1 strain in their formulations. A larger pool of immune susceptible hosts to the pandemic virus combined with immunological cross-reactivity of conserved H1 HA and N1 NA domains may account for the extinction of the seasonal H1N1, our work here and previously show that the pandemic HA and M are consistently selected for over seasonal strains in the absence of immune pressure suggesting a selective advantage of these genes.

The pandemic M gene has been found to cooperate with NA in transmission models, and confer increased activity NA activity in general (221, 231). Whether this is due to NA content, localization, or changes in viral morphology modulating both is unknown. Also unknown is whether the effect is strain or subtype specific. In our model, the M1 protein from the pandemic virus was sufficient to select for the entire M segment in competition assays with a seasonal allele. An increase in NA activity due to the pandemic M1 and not M2 was also found. An increase in sialidase activity would result in more efficient virion release from the plasma membrane post infection. This may contribute to higher replication kinetics, allowing the virus to spread more efficiently.

In addition to M1, the pandemic M2 protein was found to be sufficient for the selection of the entire M segment when challenged against a seasonal allele. Functional, albeit partially conflicting differences between the two M2 alleles were found. While an indirect activity assay indicates that the seasonal allele conducts protons more efficiently than the pandemic allele, the greater attenuation of the pandemic M2 protein on reporter secretion suggests the opposite. The lower level of proton conductance observed in the indirect activity assay may be the result of decreased surface expression of the pandemic M2 due to its effects on secretory pathways. Alternatively, the differences in observed activities could be attributed to different localization patters between the two proteins.

Several amino acid variations exist between the seasonal and the pandemic M2 proteins. Of note are the L43T, H57Y, and K78Q mutations, which gave mutant seasonal M segments a competitive advantage over the wild-type seasonal segment. The L43T mutation may play a role in ion channel conductance activity. Although not investigated here, it may influence a second proposed amantadine binding site on the lipid face of the transmembrane alpha helix by stabilizing the structure of the channel (232). Interestingly, this mutation is almost exclusively found within the pandemic M gene with few strains lacking it. The H57Y mutation completes the consensus for one of M2's CRAC motifs, however, mutation of this tyrosine has not been found to be detrimental to virus replication (233, 234). The K78Q occurs within a region of M2 that is important for viral assembly (235). Independently, these latter two mutations rescue very efficiently compared to some of the other M2 mutants (not shown), and together, they may modulate protein localization and viral budding.

Despite the functional characteristics described here for the pandemic M1 and M2 proteins, it is also entirely possible that the primary vRNA sequence of the pandemic M segment may contribute to the observed selective fitness of the pandemic segment, and not the gene products themselves. Large portions of the M segment coding sequence have been shown to be required for vRNA packaging into virions (183). Essere et al. showed that some silent mutations within the M1 packaging sequences and some non-silent mutations within M2 could affect the incorporation of other segments into the virion; however, mutational effects on M2 splicing, expression, and function were not performed to exclude a protein contribution to this phenotype (186).

Identification of the genetic determinants and mechanisms behind M segment selection is not purely academic. In addition to disrupting the classical TRIG cassette during the evolution of the 2009 pandemic virus, the segment has survived reassortment with swine H3N2 viruses to define a new lineage in pigs that has been reported to transmit to humans (215). Understanding the contributions that this segment lends to viral fitness could have a significant impact to human health and pandemic preparedness.

# Chapter 5: Towards *in vivo* reverse genetics: A recombinant bacmid rescue system for influenza virus in porcine cell types

## *5.1 Introduction*

Swine influenza was first recognized in pigs following the emergence of the 1918 "Spanish Flu" pandemic, and was first isolated in 1930 by Richard Shope (236). This "classical" swine virus (cH1N1) continued to circulate and evolve in pigs until the mid-1990s when a triple reassortant (tr) between a North American avian, a human H3N2, and the cH1N1 was identified (237). This new trH3N2 virus quickly reassorted again with the cH1N1's to produce a wide range of subtype constellations (H3N2, H1N1, H1N2, etc.), all with the same triple reassortant, internal gene cassette (TRIG) composed of avian-origin PB2 and PA genes, human-origin PB1, and swine-origin NP, M, and NS genes. The diversity of this virus pool has since been increased with the introduction and establishment of human-origin H1N1 and H1N2 viruses containing the TRIG cassette in United States swine populations (19).

The virulence of these viruses varies widely, but infection may result in fever, anorexia, and abortion in pregnant sows resulting in an overall decline in pork production for affected farms. A number of methods have been employed, however, to control this burden. Vaccination and biosecurity have become the most common method to prevent the spread of influenza and to ease the disease burden on the population. Today, inactivated influenza vaccines are commonly available and are designed to match the most common circulating strains. While these commercial vaccines are available, limited protection is observed in practice due to the antigenic and genetic diversity of influenza viruses circulating in pig populations (130-132). Furthermore, continued use of these commercial vaccines will most likely result in

immune pressure and antigenic divergence of circulating viruses necessitating the reformulation of commercial vaccines. For these reason, many swine producers have turned to autogenous vaccines to better match strains circulating within their own herds. The use of autogenous influenza vaccines have grown rapidly in recent years due to the diversity of viruses circulating in US pig populations (19). While they are not yet approved for use in swine, live-attenuated influenza vaccines (LAIV) have been shown to provide significant protection to homo- and heterosubtypic challenge in both human and swine models (132-136). While both autogenous and LAIV could fill an efficacy void left by commercial vaccines, their production still relies heavily on virus growth in eggs or tissue culture systems.

In order to increase the speed at which vaccines can be made available, a new system has been developed to deliver influenza reverse genetic cassettes encoding the virus into the host cell for expression. This system using recombinant baculovirus transducers is a "Trojan horse" approach to deliver reverse genetic cassettes encoding an influenza virus into host cells for expression and rescue.

Reverse genetic systems for generating influenza, and indeed many other negative sense viruses, have been available for many years. Transcription of the mRNA for these four viral proteins required for transcription and replication is typically done from a plasmid encoding a RNA polymerase II (pol II) promoter element upstream of cloned cDNA in a manner similar to host mRNA synthesis. Synthesis of the negative-sense, single-stranded, uncapped vRNAs can be accomplished by inserting a T7 RNA polymerase promoter directly upstream of viral cDNA cloned in the negative sense. The 3' end of the vRNA is formed by HDV

ribozyme cleavage (238). An alternative method to generate the uncapped vRNA utilizes host RNA polymerase I (pol I). RNA pol I is used by eukaryotic cells to produce uncapped ribosomal RNA. Transcription is terminated with the murine RNA polymerase I terminator (mTerm) to produce an RNA species with a defined start and stop, making it an attractive tool to generate influenza vRNA. As such, transcription of the eight vRNAs from a human pol I promoter, together with the previously mentioned protein expression plasmids, allows for the generation of influenza in 293T and a variety of other human derived cell types (192, 194). Bidirectional vectors have been made that contain both pol II and pol I promoters to drive expression of both RNA species from the same plasmid, thus eliminating the need for a 12 plasmid transfection (193). While efficient, the generation of influenza viruses by a pol I approach is thought to be species specific requiring a species match between the pol I promoter and the cell type (239). Although the porcine pol I promoter has been used to transcribe a viral-like reporter RNA (240), its utility as a reverse genetic platform remains unexplored. Herein, we describe the use of the previously reported porcine RNA pol I promoter (241) to produce an influenza reporter gene and influenza viruses in porcine cell types from a bidirectional vector.

*5.2 Materials and methods*

**Plasmids**

The NS 3'UTR-porcine RNA polymerase I promoter construct was synthesized from Genscript (Piscataway, NJ) with NotI and BstEII terminal sites for cloning (See appendix Figure S1). pPIG-GLuc(NS) was produced directly from pDP-GLuc(NS) by subcloning the synthetic construct into the NotI and BstEII sites, effectively replacing the human pol I promoter with the porcine pol I promoter. To make the generic reverse genetic vector pPIG2012, the vector portion of pPIG-GLuc(NS) was amplified with ATATCGTCTCGTCCCCCCCAACTTCGGAGGT CG and TATTCGTCTCGATCTACCTGGTGACAGAAAAGG and digested with BsmBI. A small double stranded oligonucleotide insert was generated by mixing /5Phos/GGGACGAGACGATATGAATTCTATTCGTCTCG and /5Phos/AGATCG AGACGAATAGAATTCATATCGTCTCG together and incubating at 95˚C for 1 minute, followed by a slow cool down to room temperature. This was then ligated into the digested PCR-generated vector. Viral segments from A/turkey/OH/ 313053/2004 (H3N2) were amplified and cloned into pPIG2012 in essentially the same manner as described in Hoffmann et al. (193, 223) with alternative reverse primers (See Appendix Table S6).

To generate the pΔFast-P6 construct, gene cassettes comprising the pCMV promoter, mTerm, cloned DNA, porcine pol I promoter, and bovine growth hormone polyadenylation signal were amplified from the individual reverse genetic plasmids with CMV Fwd (**[RS]**TGCCAAGTACGCCCCCTATTG) and BGH Rev (**[RS]**TGG

CCGATTCATTAATGCAGCTG) where [RS] represents one of the restriction enzymes used to clone into pΔFast (See Figure 5.6).

**Cells and Tissue Culture**

MDCK and PK(15) cells were cultured in Dulbecco's modified Eagle medium (Sigma-Aldrich, St. Louis, MO) supplemented with 25 mM HEPES (Sigma-Aldrich), 2 mM glutamine (Sigma-Aldrich), 10 mM HEPES (Invitrogen, Grand Island, NY), and 10% fetal bovine serum (FBS; Sigma-Aldrich) and were grown at 37 °C under 5% CO2. HEK 293T cells were cultured in Opti-MEM (Sigma-Aldrich) with 10% FBS and grown at 37 °C under 5% $CO_2$.

**Virus Rescue**

Transfections for virus rescue were performed in co-culture, either HEK293T/MDCK (4:1) or PK(15)/MDCK (4:1) as indicated. Cells were seeded in DMEM in the presence of serum 24 hours prior to transfection. Transfection mixtures were generally prepared with 1µg DNA/plasmid/gene segment in OptiMEM and TransIT-LT1 (2µL/µg DNA, Mirus, Madison, WI) in a total volume of 200µL, and incubated for 30 minutes. For example, 6 µg of DNA was transfected for a plasmid encoding 6 reverse genetic cassettes. Media would be exchanged for 1mL OptiMEM supplemented with 1X Antibiotics/Antimycotics Solution (OptiMEM-AB, Sigma), and the transfection mixture would be added drop wise to each well. At 6 hours post transfection (hpt), the transfection mixture would be replaced with 1mL OptiMEM-AB. At 24 hpt, 2mL of OptiMEM-AB supplemented with 3µg TPCK-treated Trypsin (Worthington Biochemical, Lakewood, NJ) would be added to each well of the

transfection. Unless otherwise noted, all transfections were incubated at 37˚C under 5% $CO_2$.

**Deep Sequencing of Bacmids**

Bacmids encoding Ty04 were sequenced essentially as described in the manufacturer's protocol for Lib-L chemistry with minor exceptions. Briefly, 500ng of bacmid DNA was nebulized to an upper fragment limit of ~1250bp. Barcoded adapters were obtained from IDT for RL014 and RL015. These were prepared following Roche TCB No. 2010-010 to a working stock concentration of 50µM/adapter. Following end repair of nebulized bacmids, adapters were ligated onto each fragment library. Samples were then size selected to a lower limit of ~500bp on Ampure XP beads (Beckman Coulter, Sykesville, MD). The quality of each library was determined using the FlashGel system (Lonza, Walkersville, MD). Libraries were quantified based on the 6FAM label on each adapter, and diluted to $1x10^7$ fragments/library. Finally, libraries were loaded into the emPCR reaction at a concentration of 3 fragments/bead. Following the sequencing run, reads were de novo aligned and reference mapped to expected sequences, and compared to known sequence for the bacmid and influenza reverse genetic inserts.

**Isolation of Baculovirus DNA**

Genomic DNA was isolated from baculovirus stocks using a modified TRIzol protocol. First, 250µL of baculovirus stock was treated with 20U DNaseI (NEB, Ipswich, MA) and incubated at 37˚C for 1 hr. Following digest, 750µL of TRIzol reagent (Life Tech) was added to each sample, mixed, and incubated at RT for 5 minutes. Added to each sample was 150µL of chloroform. Samples were shook

vigorously for 15 seconds, incubated at RT for 3 minutes, and spun at 12,000 x g for 30 minutes for phase separation. The aqueous upper phase was discarded, and 350µL of Back Extraction Buffer (4M guanidine thiocyanate, 50mM sodium citrate, 1M tris base) was added to each sample and centrifuged again at 12,000 x g for 30 minutes (242). The aqueous phase was removed to a new tube and precipitated with 250µL isopropanol at 12,000 x g for 15 minutes. The pellet was washed with 500µL 70% ethanol and precipitated at 12,000 x g for 15 minutes. Finally, the ethanol was removed and the pellet was allowed to air dry for 10 minutes before being eluted in 50µL of EB.

*5.3 Results*

### 5.3.1 Construction of a porcine pol I-driven uni- and bidirectional reverse genetic platform

A secreted Gaussia luciferase (GLuc) reporter construct has previously been developed within our lab to assay IAV polymerase function in 293T cells (243). The vector is composed of a human pol I promoter that expresses a negative sense clone of a GLuc ORF that is flanked by segment 8 terminal noncoding regions. Transcription is terminated immediately thereafter by a murine RNA pol I termination sequence. The viral-like RNA that is produced is recognized by the IAV polymerase as an influenza segment. In order to test the ability of a porcine RNA pol I promoter to drive expression of a similar viral-like RNA species in swine cells, the human promoter from the GLuc report vector was replaced with the porcine RNA pol I promoter (Figure 5.1). Porcine kidney cells (PK15) were then transfected with the porcine pol I IAV reporter plasmid along with RNA polymerase II expressed PB2, PA, and NP plasmids. As a control for IAV amplification, transfections were performed with or without the addition of a plasmid expressing PB1. As early as 12 hours post transfection (hpt), expression of the reporter gene was significantly greater in the presence of the full IAV polymerase compared to the negative control (Figure 5.2). These results suggest a viral-like RNA was efficiently transcribed from the porcine pol I promoter, which was then recognized and amplified by the IAV polymerase. RNA polymerase I promoters have been reported to be species specific. Indeed, little sequence homology exists between the human promoter used in

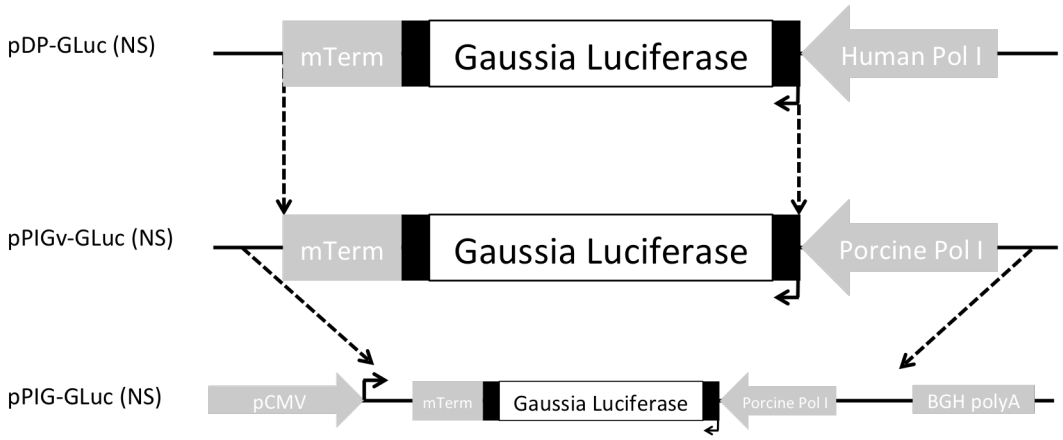


Figure 5.1: Schematic representation of porcine pol I-based influenza reverse genetic system. The murine polI termination signal and a GLuc reporter, flanked by NS noncoding regions (black boxes), was subcloned from the human pol I vector pDP-GLuc (NS) and placed in front of the porcine pol I promoter to construct a viral RNA expression vector, pPIGv-GLuc (NS). This cassette was then subcloned between a RNA pol II promoter and bovine growth hormone polyadenylation signal to construct a bidirectional vector, pPIG-GLuc (NS).

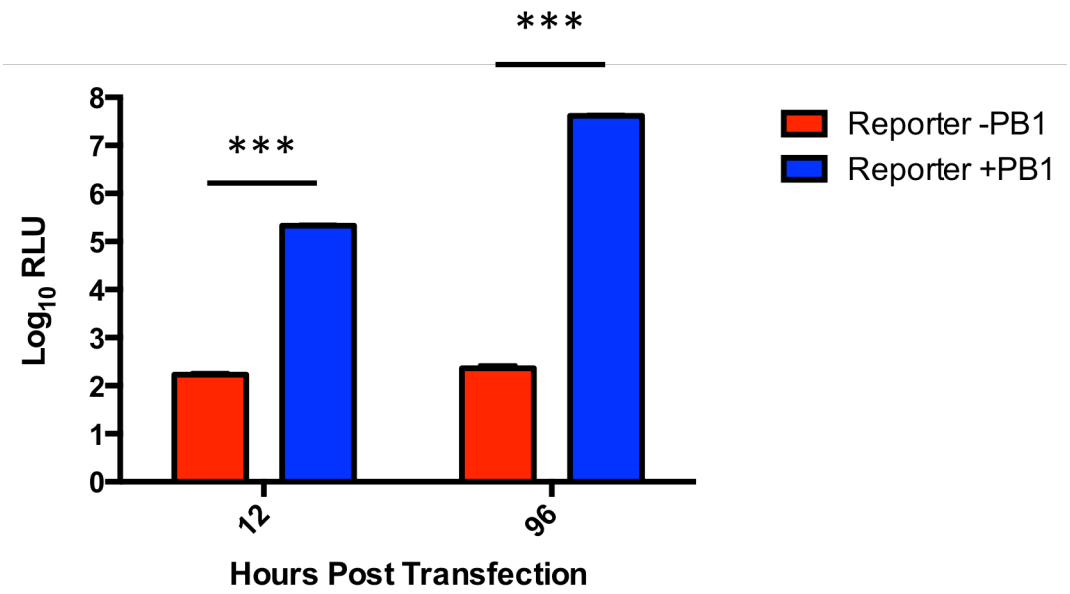


Figure 5.2: IAV amplification of vRNA-like reporter gene expressed from porcine RNA pol I promoter. $1x10^6$ PK(15) cells were transfected with 1µg pPIG-GLuc (NS) together with 1 µg of each plasmid expressing IAV PB2, PA, and NP. As a control for IAV amplification, transfections were done with or without the addition of PB1. Luciferase values represent fold change mock. p values < 0.001 at each time point.

pHW2000-like vectors and the porcine promoter used in this study. To examine the species specificity of the porcine promoter in multiple cell types, GLuc expression of the human and porcine pol I reporter vectors was determined in their cognate and reciprocal cell types. Surprisingly, both the human and porcine pol I reporters functioned well in both 293T and PK(15) cells. As expected, however, the human pol I promoter and the porcine pol I promoter functioned significantly more efficiently in the human and swine derived cell types, respectively (Figure 5.3). These results suggest that while a specific cell type may be preferred, an *in vivo* reverse genetic platform may be functional in more than the intended target.

Four proteins are sufficient and required to generate IAV from cloned cDNA; PB2, PB1, PA, and NP. The remainder of the genes need only to be expressed as vRNA in order for the polymerase complex to recognize, replicate, and perform mRNA transcription. Expression of these four proteins from "helper" plasmids in trans to replicate eight, co-transfected, pol I-derived, vRNA-like transcripts is common practice to generate IAV in tissue culture in a so called 12 plasmid (8 pol I + 4 pol II) system (192). Alternatively, cloned cDNA can be inserted into bidirectional vectors expressing the negative sense or positive sense, vRNA or cRNA from a RNA pol I promoter and the mRNA from an RNA pol II promoter (193, 244). This system requires that only eight plasmids be transfected in order to generate IAV *de novo*, and is the backbone of our rescue platform. To that end, the pCMV (RNA pol II) promoter and the bovine growth hormone polyadenylation signal (BGH polyA) were cloned upstream of the mTerm sequence and downstream of the porcine pol I cassette respectively to construct pPIG-GLuc(NS) (Figure 5.1). Efficient expression of mRNA

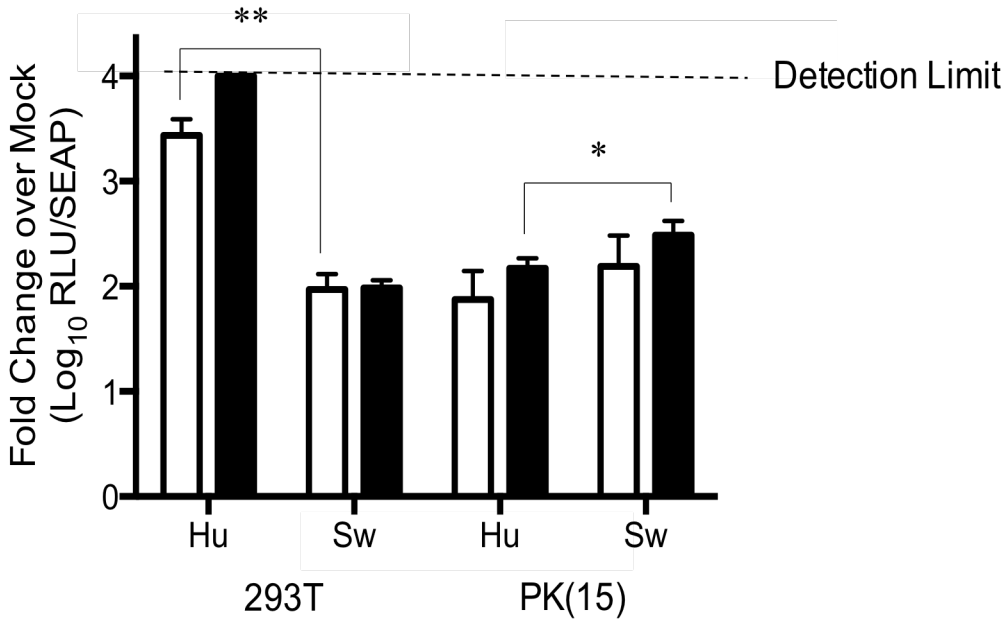


Figure 5.3: RNA Polymerase I activity in human and swine cell types. HEK293T or PK(15) cells were transfected with influenza-amplifiable GLuc vRNA reporter genes expressed from either a human (Hu) or Swine (Sw) RNA polymerase I promoter. The viral replication complex was reconstituted with PB2, PB1, PA, and NP expressed from pcDNA3.1 vectors. Luciferase activity was assayed at 24 (white) and 48 (black) hours post transfection. All transfections normalized to SEAP.

in eukaryotic cells requires the presence of both a 5' cap and a 3' polyadenylated tail. Proteins recognize both structures and each other through adapters to make a circular transcript that is read by the ribosome. The absence of either structure signals that the transcript may be regarded as foreign, and should be degraded by the cell. To determine if the mRNA expression cassette was functional, PK15 cells were transfected with the pol I reporter vector lacking a RNA pol II promoter, the reporter vector with the addition of the pCMV RNA pol II promoter, or the reporter vector containing both the pCMV promoter and the BGH polyA signal in the absence of the IAV polymerase. Expression of the reporter gene was increased by about 72-fold over the negative control in the presence of the CMV promoter, and by about 1000-fold with the addition of a polyadenylation signal (Figure 5.4). These results strongly suggest that the GLuc reporter gene is being expressed in the cell via a cap dependent manner, and that the mRNA expression cassette on the plasmid is functioning properly.

### 5.3.2 An eight plasmid, porcine pol I-driven rescue of influenza A virus in tissue culture

Having generated a bidirectional, porcine pol I-driven reverse genetic vector, we wanted to determine if a full influenza virus could be rescued from this vector in tissue culture. A/turkey/OH/313053/2004 (Ty/04), a swine-origin, triple reassortant H3N2 virus, has been characterized and attenuated in our lab to server as a master vaccine backbone (243). In addition to rescuing well from human pol I reverse genetic platforms, the wild-type virus induces a febrile response, macro- and microscopic pneumonic lesions, and severe clinical signs in inoculated pigs, making it an ideal candidate as a proof of principle for the porcine pol I rescue system. To facilitate the insertion of cloned IAV cDNA into the vector, the flu-amplifiable GLuc reporter was replaced with BsmBI cloning sites similar to those used in the pHW2000 vector. Each of the eight segments from Ty/04 were cloned into this porcine pol I, influenza reverse-genetic vector, pPIG2012 (Figure 5.5A). The full set of plasmids encoding Ty/04 were then transfected into PK15/MDCK co-culture to determine if this reverse genetic platform could in fact launch infectious virus *in vitro*. Following the addition of TPCK-treated trypsin at 24 hpt, a dramatic increase in viral replication was observed in transfected cells throughout 72 hpt (Figure 5.5B).

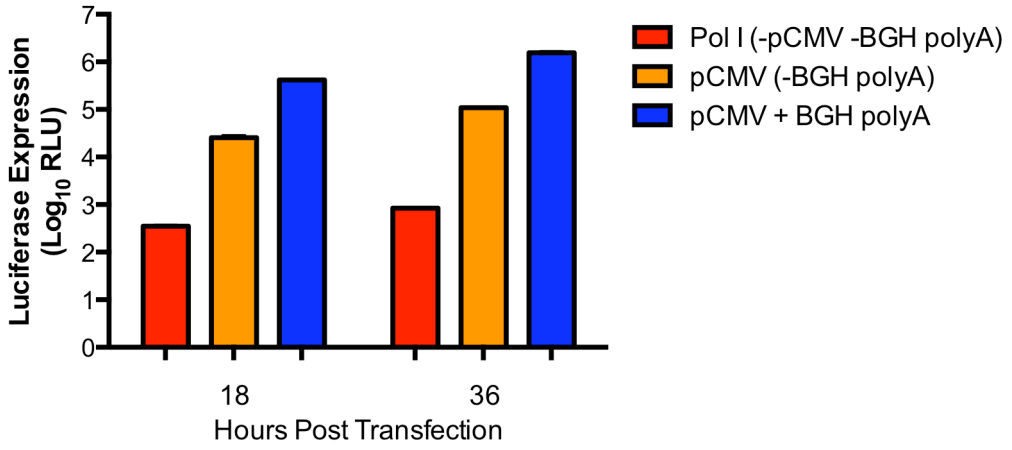


Figure 5.4: Contributions of the CMV early promoter and BGH polyadenylation signal to reporter expression. PK(15) cells were transfected with either the pPIGv-GLuc (NS) reporter containing only the RNA polymerase I promoter (red), an intermediate plasmid encoding both the RNA pol I and pCMV promoters (orange), or pPIG-GLuc (NS) containing the RNA polI, pCMV, and the BGH polyadenylation signal (blue). All results are normalized to background.

### 5.3.3 Construction of a bacmid and baculovirus vectored porcine pol I-driven influenza reverse genetic platform

Baculoviruses have been used to provide a platform for the expression of foreign proteins in large quantities for many years. Commercially available kits provide a rapid way to insert genes of interest into baculoviruses for expression in insect cells. To make these recombinant bacmids, foreign genes are inserted into a donor vector under the transcriptional control of the polyhedron promoter. The expression cassette, located within a mini-Tn7 element, is then transposed into a bacmid encoding the mini-attTn7 attachment site with the aid of a helper plasmid. The bacmid, bMON14272, encodes the genome of Autographa californica nuclear polyhedrosis virus (AcNPV), and is capable of launching infectious virus in insect cells. AcNPV baculoviruses have also been shown to be powerful transducers of foreign genes into a wide range of mammalian cell types (245, 246). This system was used with modification as the basis of a "Trojan horse" approach for the rescue of influenza virus *in vivo*.

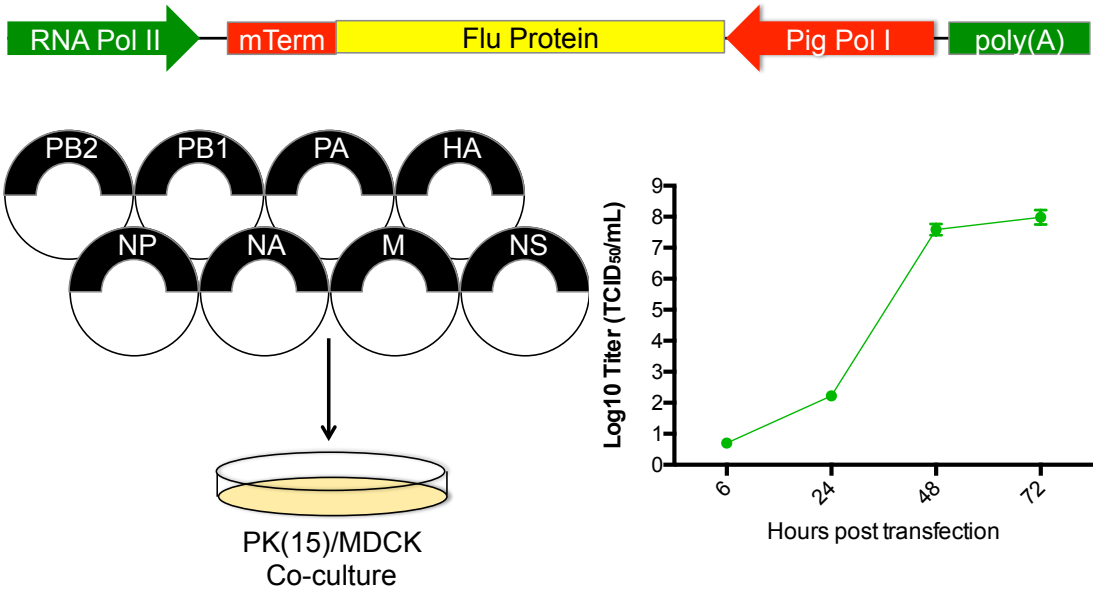


Figure 5.5: Swine based influenza reverse genetics. Schematic diagram of eight segments from A/turkey/Ohio/313053/2004 (trH3N2) cloned in between the murine termination sequence (mTerm) and the porcine polymerase I promoter in pPig2012 swine reverse genetics vector. These eight plasmids were transfected into PK(15)/MDCK co-culture which rescued virus to high titers after 72 hours (N=3).

The internal genes from Ty/04 were used as the backbone in this proof of principle. The virus rescues well in tissue culture, and causes mild to moderate disease signs in infected pigs, which may serve as disease signs for *in vivo* rescue. Additionally, the attenuated strain protects very well in homo- and heterologous challenge. To construct the backbone donor vector, reverse genetic cassettes from each individual pPIG2012 plasmid (PB2, PB1, PA, NP, M, and NS) were amplified from the start of the pCMV promoter to the end of the BGH polyA signal, and cloned into one of the restriction sites in the pΔFast donor vector (Figure 5.6). As the donor vector became more and more unstable with the addition of more influenza cassettes, construction was done in two parts, cloning PB2, PB1 and PA in to one vector (pΔFast-P1), and NS, NP, and M into another (pΔFast-P2). The latter cassettes were then subcloned into the former vector as one large piece to generate a pΔFast-P6 (Ty04) donor vector containing the six internal genes of Ty04 (Figure S1).

Although the individual reverse genetic plasmids are stable in bacteria, the addition of each gene cassette into pΔFast resulted in a higher occurrence of unstable clones. To confirm that each plasmid during the construction process was stable, each was tested for functionality. With the exception of M, the activity of the internal genes cloned into pΔFast can be assayed with a minireplicon system. Each pΔFast construct was transfected into PK(15) cells with the porcine Gaussia luciferase reporter, pPIG-GLuc(NS), and supplemented with individual plasmids required for

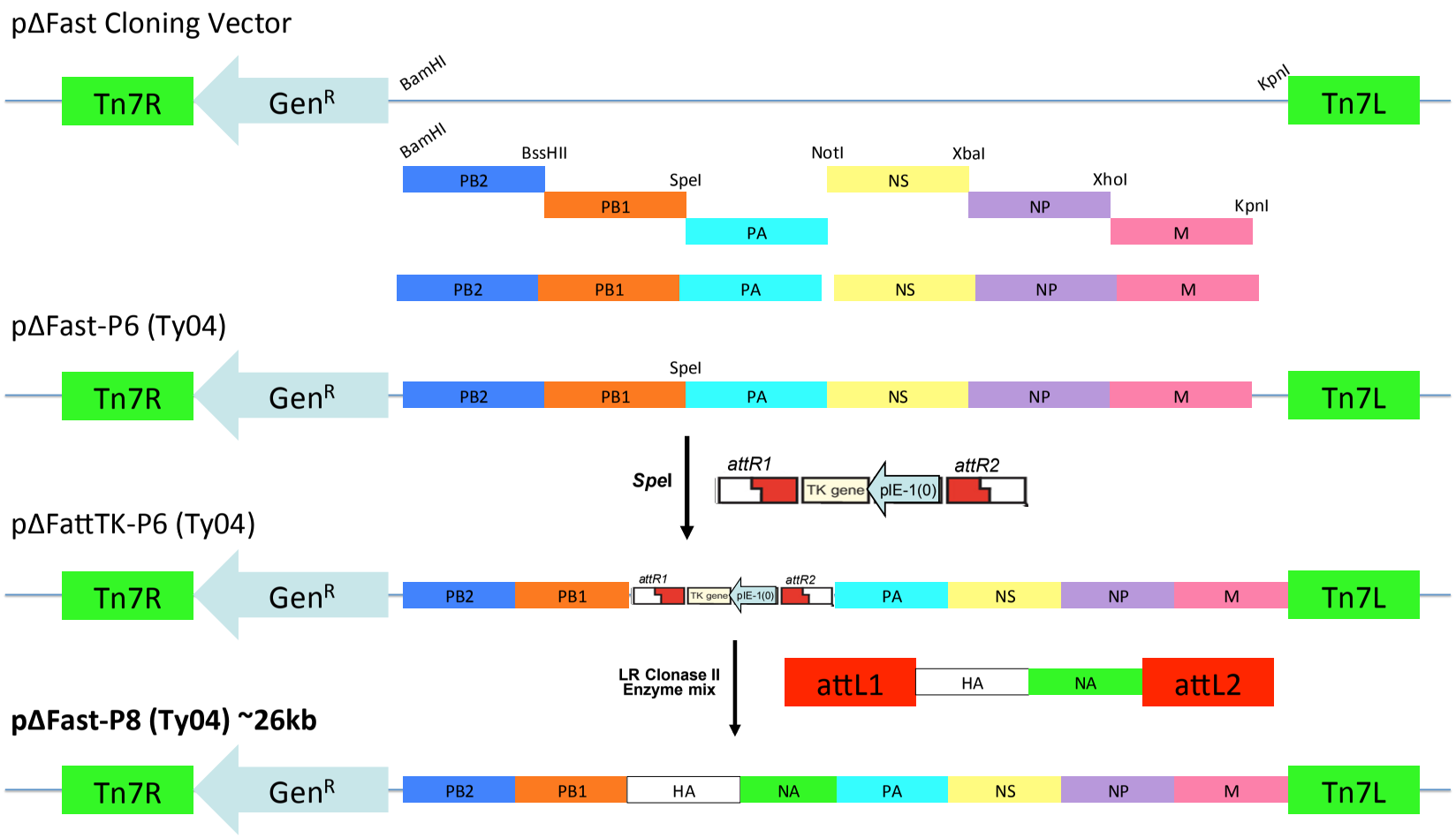


Figure 5.6: Strategy for consolidating the reverse genetic cassettes for Ty04 into pΔFast.

influenza segment replication (PB2, PB1, PA or NP). For example, pΔFast-P1.2 contains reverse genetic cassettes for PB2 and PB1. The minireplicon was restored with the addition of pPIG-PA and pPIG-NP. Each construct was assayed for activity at 24 and 48 hours post transfection. In each case, constructs exhibited significant activity above the negative control, indicating that the encoded reverse genetic cassettes were functional (Figure S4). Additionally, when a construct containing the NS cassette was transfected into cells, the resultant luciferase activity increased significantly over the transfections that lacked NS. This increase in activity in the presence of the NS plasmid suggests that amplification of the reporter gene is mediated by the viral polymerase, as NS1 has been shown to stimulate viral mRNA gene expression at the detriment to host cell messages (247).

In order to generate a plasmid encoding the six internal genes of Ty04, the fragment encoding the NS, M, and NP cassettes was subcloned into pΔFast-P1.3. This plasmid was termed pΔFast-P6, and contains the reverse genetic cassettes required for the expression of the backbone segment mRNAs and vRNAs. To test for the proper expression of internal genes, this construct was transfected into PK(15) cells along with the flu amplifiable GLuc reporter. After 24 hours post transfection, the polymerase expressed of the pΔFast-P6 promoter expressed GLuc to comparable levels compared to those produced by the transfection of six pPIG reverse genetic plasmids encoding the same genes (Figure 5.7A). The same experiment was performed in which PK(15)/MDCK co-cultures were transfected with the pΔFast-P6 plasmid, supplemented with pPIG plasmids encoding HA and NA to test for virus rescue. As expected, virus was rescued at comparable levels to the positive control in

which cells had been transfected with eight individual reverse genetic, pPIG plasmids (Figure 5.7B). This data suggests that the internal genes from Ty04, cloned into the

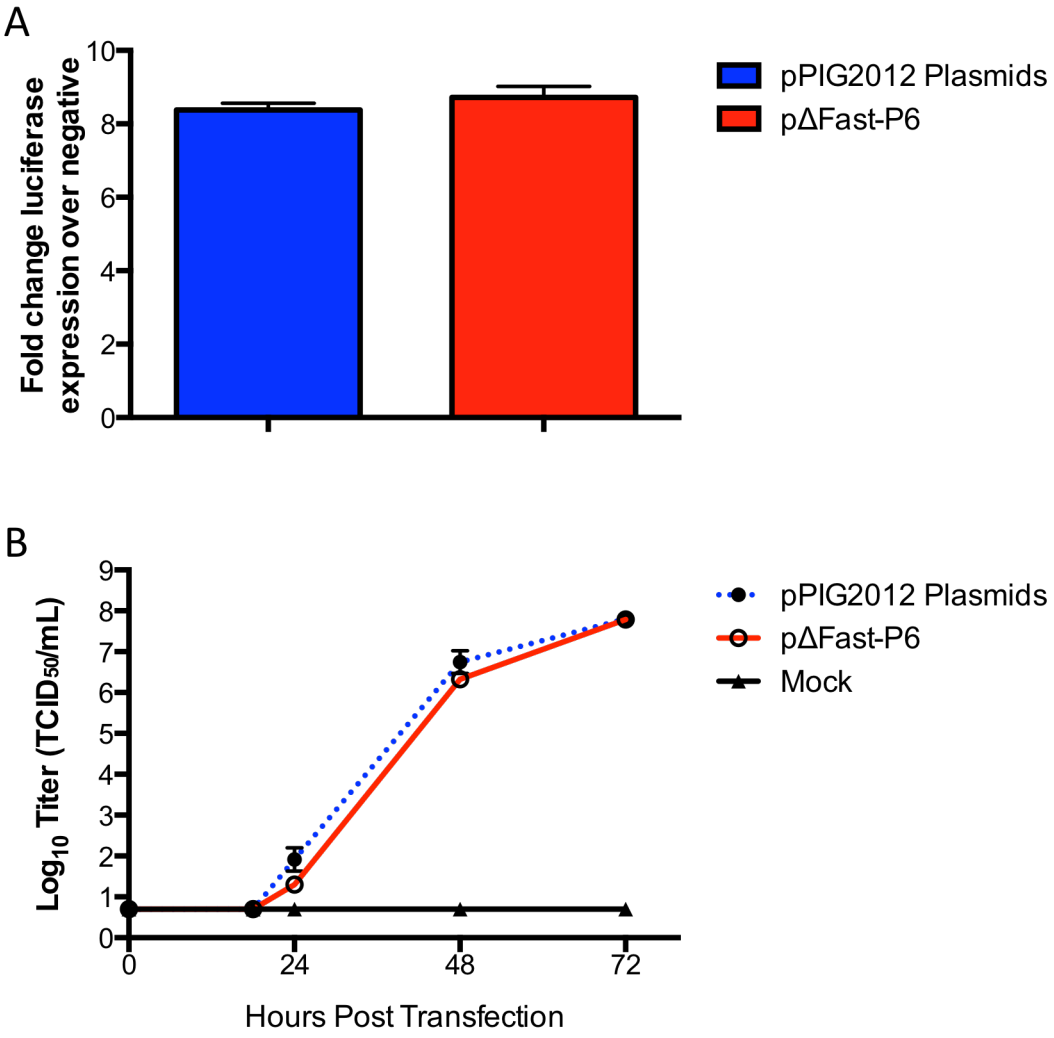


Figure 5.7: Characterization of pΔFast-P6 (Ty04) backbone vector. A) PK(15) cells were transfected with either 6 µg pΔFast-P6 (Ty04) or the copy number equivalent genes in pPIG2012. At 24 hpt, supernatant was harvested and assayed for luciferase activity (N=2). B) Virus rescue of 6 µg pΔFast-P6 (Ty04) or equivalent genes in pPIG2012 complemented with pPIG-HA and pPIG-NA in PK(15)/MDCK co-culture (4:1 ratio, N=3). Aliquots from 4 time points were titrated by $TCID_{50}$ in MDCK cells.

baculovirus entry vector, functionally produce mRNA and vRNA for each gene from a single plasmid.

The majority of vaccines currently produced use only the HA and NA of the circulating strain, and the internal genes generally come from a master donor strain. For human influenza vaccines, these strains are either A/PuertoRico/8/1934 (H1N1) for the inactivated vaccines, or A/AnnArbor/6/60 (H2N2) for the live-attenuated vaccines. To enable the rapid exchange of surface antigens in the baculovirus system, the pΔFast-P6 plasmid was further modified by the insertion of a constitutively expressed thymidine kinase gene flanked by lambda phage attR1 and attR2 sites (pΔFast-P6Tkatt, ~19.6 kbp), enabling this vector to be compatible with the Gateway cloning system. The HA and NA reverse genetic cassettes from Ty04 were subcloned into pENTR-1A in a similar manner as the remaining genes into pΔFast. The complete reverse genetic system containing all eight genes for Ty04 was subsequently generated through recombination of the pENTR-HANA Gateway cassette into pΔFast-P6TKatt. This pΔFast-P8 plasmid was about 26 kbp in size, and efficiently rescued influenza virus after transfection into PK(15) cells (Figure 5.9). The Bac-to-bac baculovirus system offers a convenient method of generating recombinant baculoviruses quickly from inserts cloned into the pFastBac vector and its derivatives, such as pΔFast. The system is based on the bMON14272 baculovirus shuttle vector, which encodes a modified AcMNPV genome containing a mini-F replicon and an attachment site for the Tn7 transposon (248). To generate the recombinant bacmid encoding the complete reverse genetic system for Ty04, pΔFast-P8 (Ty04) was transfected into DH10Bac, which contained the shuttle vector together

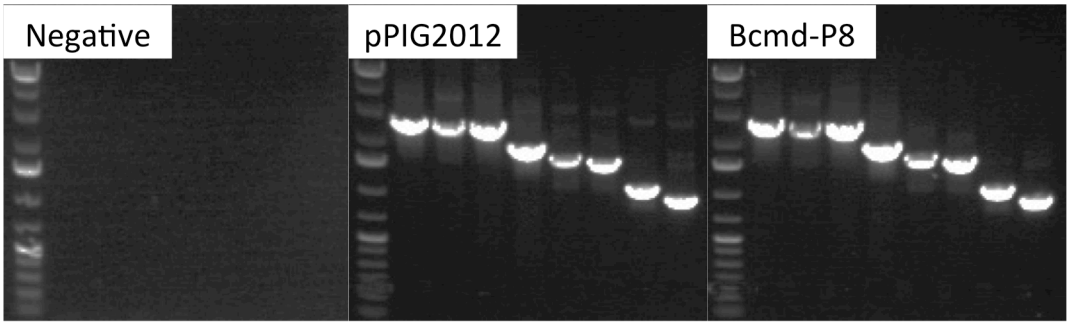

Figure 5.8: Amplification of the influenza genome from Bcmd-P8. Each of the eight genes from A/turkey/Ohio/313053/2004 (trH3N2) were amplified with universal primers and separated on a 0.75% agarose gel. The negative panel shows the results of PCR without template. Initial lane in each panel contains 1kb Plus DNA latter.

with the components required for Tn7 integration. Bacmids containing the Tn7 insert from pFast-P8 (Ty04) were selected for on kanamycin and gentamycin LB agar plates. PCR of the bacmid indicates that each influenza gene from Ty04 is present in the transposed bacmid (Figure 5.8). To determine the stability of the viral sequence, 454 libraries were prepared from the bacmid, and the influenza gene inserts were sequenced in their entirety. Each gene was found to be present in the bacmid by sequencing, and no high confidence mutations were observed to have been introduced between the initial pPIG2012 vectors and the final bacmid (Table 4). Additionally, no deletions were observed to have occurred suggesting that the final bacmid product is stable despite the highly repetitive promoter regions of the reverse genetic cassettes.

Bacmid DNA (Bcmd-FluRG) was transfected into mammalian tissue co-culture to determine whether the reverse genetic cassettes were functional for virus rescue. The DNA copy numbers of the bacmid and the pΔFast-P8 plasmid were normalized to that of pPIG-PB2 (Ty04), which contains $1.76x10^{11}$ copies / µg. This corresponded to 31.5µg and 4.94µg of the bacmid and pΔFast-P8 plasmid DNA, respectively. Supernatant from each transfection was titrated every 24 hours for 3 days. Although the bacmid DNA was delayed in its amplification, virus titers in the supernatant recovered to similar levels as the controls by 3 days post transfection (Figure 5.9). It should also be noted that the bacmid transfection was hindered by DNA precipitation and a high toxicity due to the amount of transfection reagent used. Regardless, the bacmid encoding Ty04 reverse genetic cassettes is competent for the rescue of influenza in tissue culture.

Table 4: Sequencing statistics of bacmid cloned influenza genes

| | PB2 | PB1 | PA | HA | NP | NA | M | NS |
|---|---|---|---|---|---|---|---|---|
| Coverage | 100% | 100% | 100% | 100% | 100% | 100% | 100% | 100% |
| Percent Identity[1] | 100% | 100% | 100% | 100% | 100% | 100% | 100% | 100% |
| Number of Reads | 7325 | 6941 | 6385 | 4904 | 5239 | 4459 | 3411 | 3007 |
| Average Depth[2] | 412 | 398 | 382 | 372 | 416 | 391 | 379 | 379 |

1 Compared to sequence of pPIG2012 plasmids

2 Depth of unique reads

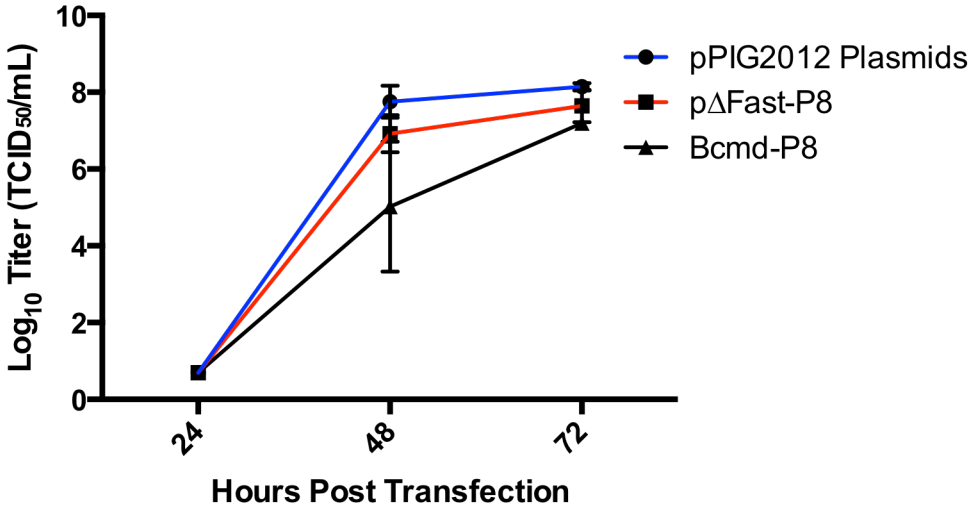


Figure 5.9: Rescue kinetics of complete reverse genetic constructs. 293T/MDCK co-cultures were transfected with either eight pPIG2012 plasmids (blue), a single pΔFast plasmid encoding all eight influenza gene cassettes (red), or a bacmid containing all eight influenza gene cassettes (black) from Ty04 under the control of the swine polymerase I vector (N=3). Copy numbers of plasmids (each gene) and bacmids were normalized to the amount of pPIG-PB2 in 1µg.

Rescue of influenza virus from eight plasmid systems are efficient, and has become routine in many labs. DNA in the transfection generally reaches $10^5$ copies of each plasmid per cell. This ensures that cells receive, on average, many copies of each plasmid in the eight-plasmid set. As a single bacmid contains the complete complement of gene cassettes required to rescue influenza virus, we reasoned that transfection of the bacmid and subsequent virus rescue would be more efficient than the standard eight-plasmid transfection scheme. To do this, transfections were performed as before, but $2.8x10^{10}$ copies of either the bacmid DNA or each of the eight pPIG2012 plasmids encoding Ty04. This represents a 6.4x reduction in the amount of DNA previously used, and is about the limit at which virus can be consistently rescued from the bacmid. For the bacmid, this transfection consists of 5µg total DNA while the individual plasmids range from 159ng (pPIG-PB2) to 115ng (pPIG-NS) depending on the length of the influenza gene insert. Similar peak titers were observed for both the bacmid transfection and the pPIG2012 transfection. Although the difference was not significant, the bacmid tended to grow to higher titers than the eight-plasmid transfection (Figure 5.10). Rescue of the bacmid was also more consistent with the bacmid with 3/3 replicates rescuing virus compared to the eight-plasmid transfection, which only had 2/3 replicates rescue. These results may suggest that while the bacmid contributes a complete reverse genetic, any gain in efficiency may be modulated by other factors such as transfection efficiency or nuclear transport of such a large DNA molecule.

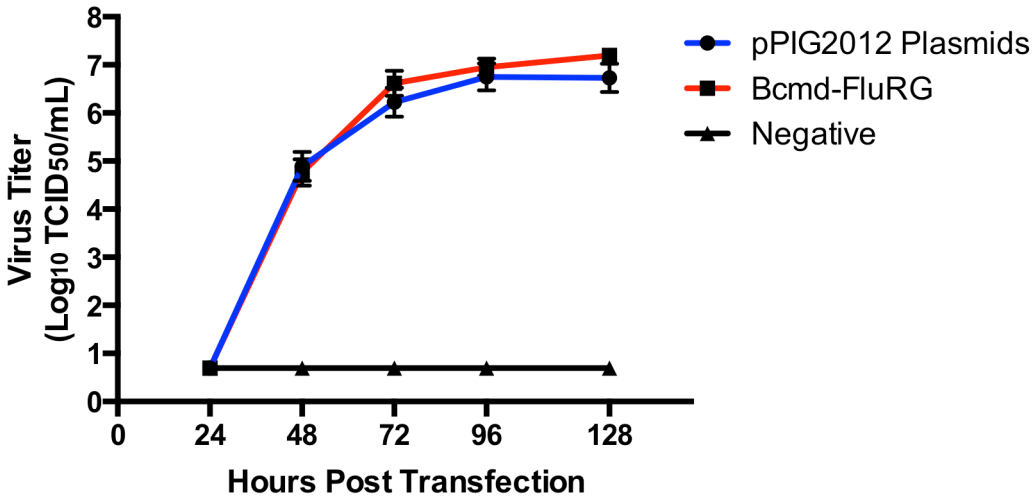


Figure 5.10: Low copy rescue of influenza virus. Bacmid or eight pPIG2012 plasmids were transfected into 293T/MDCK co-culture at $2.78x10^{10}$ copies of either the bacmid or each plasmid. Supernatant was harvested every 24 hours for 128 hours and titrated on MDCK. N=3.

Bcmd-FluRG also contains the information required to rescue AcNPV baculovirus in insect cell culture. This allows for an additional mode of reverse genetic competent DNA entry into target cells as baculoviruses have been shown to be strong transducers of mammalian cell types (245). To determine if the Bcmd-FluRG DNA could indeed generate baculovirus, bacmid DNA was transfected into Sf9 insect cells. At 96 hours post transfection, the supernatant was collected, clarified with low speed centrifugation, and treated with DNaseI to remove any contaminating bacmid DNA from the transfection. DNA protected within virions was then purified, and each of the eight influenza genes encoded within the baculovirus genome was amplified with full-length primers (Figure 5.11A). The transfected cells were also fixed and stained for gp64, a baculovirus surface glycoprotein (Figure 5.11B). Baculovirus was passaged 4 subsequent times, and DNA prepared as before. Again, PCR amplification indicates the presence of all eight influenza reverse genetic cassettes within the genome of the baculvirus (Figure 5.11A). Together, these data indicate that the Bcmd-FluRG bacmid is competent for the rescue of baculovirus containing the reverse genetic cassettes required for the rescue of influenza virus, and that these cassettes are stable over multiple passages.

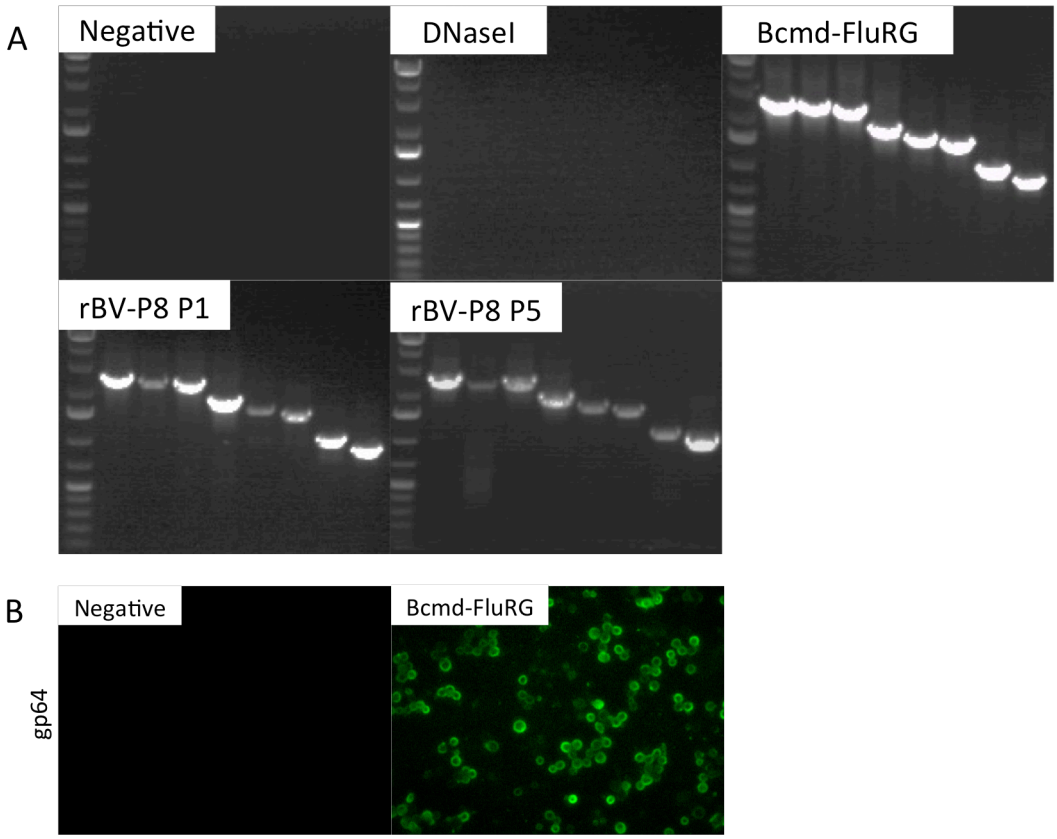


Figure 29: Rescue of rBV-P8 baculovirus encoding influenza reverse genetic cassettes. A) PCR amplification of baculovirus vectored influenza reverse genetic cassettes using full length, gene specific primers. DNaseI control is growth media spiked with 1µg bacmid DNA. B) Immunofluorescent staining of baculovirus gp64 on the surface of insect Sf9 cells.

*5.4 Discussion*

Evidence suggests that swine play a major role in the adaptation of influenza viruses from the avian reservoir into the human population. This is indeed the case in the most recent pandemic in which viruses from the classical swine H1N1, 1967-derived H3N2 human, and North American avian lineages converged in swine to produce the 2009 swine-origin pandemic virus. It is therefore reasonable to assert that swine health and human health are intimately intertwined, and that protection of swine heard from influenza viruses may have a direct influence on emerging pandemic viruses in humans. While biosecurity and vaccination provide the best means of protection in production facilities, a high degree of antigenic diversity within currently circulating and emerging strains complicate vaccination efforts. Vaccines must be produced quickly and reliably without changing the antigenicity of the seed strain. Although the advent of reverse-genetics for influenza virus has enabled vaccines to be produced much more quickly, seed stocks must ultimately be propagated in traditional substrates such as tissue culture or embryonated eggs. Vaccine candidate viruses also may not be well adapted for growth in these non-natural substrates, as was the case for the 2009 human H1N1 vaccine, and adapting for high growth strains may adversely affect the intended antigenicity of the vaccine stock (249). Despite the experience with traditional vaccine production and access to more recent technology, vaccination of humans during the 2009 pandemic did little to significantly ameliorate the impact of the pandemic. Next generation vaccines must be able to be produced rapidly, in high yields, and with high antigenic fidelity to the circulating strains. Here, we propose either a DNA or a baculovirus-based vaccine for

the production of influenza viruses in swine cells with the intent of producing an *in vivo* reverse genetic vaccine. Cloned cDNA from a triple reassortant swine virus, Ty04, was introduced into a reverse genetic vector and transcribed into a viral-like RNA species under the control of a porcine RNA polymerase I promoter. The reverse genetic cassettes for each of the eight segments, consisting of the RNA polymerase II promoter, the cloned cDNA segment, the porcine RNA polymerase I promoter, and the bovine growth hormone polyadenylation signal, were serially cloned into a single shuttle vector and transposed into a bacmid encoding the AcNPV genome. We have shown that this bacmid is capable of rescuing both influenza and baculovirus in mammalian and insect cell culture, respectively.

Single plasmid rescue strategies have been described previously in the literature (250). In our experience, these large plasmids with repetitive promoter sequences are unstable in E. coli, and the cassettes are often lost. Bacterial artificial chromosomes (BACs), such as bMON14272 used here, are based off of the F factor and are maintained at low copy numbers thus increasing the stability of the DNA (251). Our strategy also allows for the rapid exchange of surface antigens by using the Gateway cloning system, and doesn't require ligations into large vectors. Given the higher cloning capacity of the BAC compared to traditional plasmids, we can envision the introduction of additional genes to act as immune modulators, increasing the response to the rescued virus.

# Chapter 6: Conclusions and future prospectives

Influenza A virus continues to circulate in human, swine, and avian reservoirs as well as many others. Understanding how these viruses share information between these reservoirs to create new strains is a vital part of not only influenza research, but also to pandemic preparedness. The four IAV pandemics and many of the outbreaks during the past century have highlighted the need for this understanding, and require further research to determine which gene constellations and mutations favor transmission and expansion of new viruses to and through a new reservoir, and ultimately into the human population. In this dissertation, we have used the ferret animal and competitive co-infection models to identify genes of significant interest during reassortment between two model viruses from two important genetic lineages. First, ferrets were co-infected with two wild-type viruses to identify highly favored constellations arising from reassortment. While reassortant strains were not identified in this study, we were able to conclude that the virus from the 2009 swine-origin pandemic had a significant fitness advantage during transmission to respiratory contact animals over either the seasonal H1N1 or H3N2 viruses. In fact, the latter two viruses could not be identified at all in the nasal washes of respiratory contact animals by RT-PCR. Although reassortants were not identified either, we suspect that they were present at such a low level to preclude their transmission to contact animals in the background of a wild-type, pandemic infection. Their relative fitness to the pandemic virus may have been obscured by the methods used to perform the transmission study.

Given the apparent fitness advantage of the pandemic virus over the seasonal strains, we next sought to determine if reassortment between these viruses was possible. We hypothesized that if the pandemic virus truly had a fitness advantage over the seasonal strains, and if reassortment was possible in the ferret model then co-infection of reverse genetic "surface" reassortants would regenerate a fully pandemic constellation. We also removed the requirement for aerosol transmission which may have served as a high selective barrier to the establishment of alternative constellations in the first experiment, and serially passaged entire populations of replicating viruses from the nasal washes of ferrets. After serial passage, we found that reassortment had occurred and that three independent infections had resulted in the same H1N2 constellation with seasonal PB1 and NA genes in an otherwise pandemic virus. These finding suggest the ferret, traditionally used to model human influenza virus infection, can be used to study reassortment. More importantly, the selection of the seasonal NA and pandemic M strongly are consistent with viruses currently being isolated in the field.

Having observed that the pandemic M segment was rapidly selected for during co-infections, we wanted to determine the genetic determinants responsible for segment selection. Chimeras were made between the seasonal and pandemic M segments and rescued in the previously described H1N2 constellation. Competitive co-infections were then performed *in vitro* and *in vivo* with viruses encoding either a wild-type or chimeric M segment. Using this strategy, we were able to show that both M1 and M2 genes from the pandemic virus were sufficient to independently drive selection of the entire M segment when challenged against a similar seasonal

segment. Additionally, it was observed that a wild-type pandemic segment had a clear selective advantage over either of the chimeric segments, which encoded only a single pandemic M1 or M2 gene, again suggesting that both M1 and M2 contribute to the observed preference for the pandemic M allele in that constellation. Further studies of the pandemic M1 and M2 proteins are required to determine the mechanisms by which they promote the selection of this gene. Direct measurements of the ion channel activities and protein localization studies could shed light on a possible mechanism.

While the pandemic M and seasonal NA segments have been observed to segregate together and cooperate with each other, the responsible mechanisms remain unclear (198, 221, 222). We've observed through neuraminidase activity assays that the M1 protein may operate to increase the apparent activity of the neuraminidase. This may not be a direct affect on the enzymatic properties of the protein, but rather indirectly through additional NA incorporation into or concentration of NA protein within a portion of the virion.

Swine play an important role in the adaptation of viruses from the avian to the human reservoir. Moreover, their increased susceptibility to viruses from both reservoirs makes swine an important nexus of reassortment between avian, human, and endemic swine viruses. Controlling the introduction and movement of new isolates within this species therefore has a direct influenza on human health, and may play a role in pandemic prevention. Current inactivated vaccines may not be sufficient to protect against newly introduced HA antigens, and current autogenous vaccines that protect individual herds may not grow efficiently in egg substrates.

Here, we have developed a new vaccine platform that is tailored specifically to swine for the purpose of generating virus *de novo* through either DNA transfection or baculovirus transduced introduction of reverse-genetic elements directly into swine cells. Our approach does not require virus to be grown in artificial substrates, and can rapidly accommodate new HA and NA antigens into an already well characterized viral backbone. A new, bi-directional influenza reverse genetic backbone was constructed using the porcine polymerase I promoter to drive transcription of a viral RNA-like product. We found that influenza virus could be successfully generated in tissue culture from an eight-plasmid transfection using this vector.

Using this reverse genetic vector, we envision a new generation of species specific, tailor-made, DNA or baculovirus-transduced vaccines for use in swine. We have transferred the eight reverse genetic cassettes required for the rescue of influenza virus into a single bacmid. In addition to being stable, HA and NA segments can be exchanged rapidly to update the antigenicity of the vaccine. The bacmid rescues influenza virus in mammalian cell culture, and baculovirus containing the reverse genetic cassettes in insect cell culture. Baculoviruses are currently used to produce many vaccines, including FluBlok, which is a protein subunit vaccine produced from baculovirus. Here, however, we envision the novel use of the baculovirus to transduce porcine cells and generate virus *in vivo*. Using either a DNA or baculovirus vaccine approach could decrease the reliance on classical methods used to produce influenza virus vaccines. We have shown that influenza virus can be rescued from the recombinant bacmid. We have also shown that the influenza

cassettes are stable during baculovirus passage. Further work, however, is required to show that influenza virus can be generated from baculovirus transduction.

# Appendix

Table S1: Hemagglutination inhibition titers following co-infection

| | Seasonal Titers | | Pandemic Titers | |
|---|---|---|---|---|
| | 0 dpi | 14 dpi | 0 dpi | 14 dpi |
| Infected | <10, <10, <10, <10<br><10[†], <10[†] | 160, 160, 80, 160 | <10, <10, <10, <10<br><10[†], <10[†] | 640, 640, 320, 640 |

[†] Animals euthanized on 4 dpi for tissue collection.

Table S2: Majority genotype of passage 7 viruses

| | PB2 | PB1 | PA | HA | NP | NA | M | NS |
|---|---|---|---|---|---|---|---|---|
| Lineage A | Pandemic | **Seasonal** | Pandemic | Pandemic | Pandemic | **Seasonal** | **Pandemic** | Pandemi |
| Lineage B | Pandemic | **Seasonal** | Pandemic | Pandemic | Pandemic | **Seasonal** | **Pandemic** | Pandemi |
| Lineage C | Pandemic | **Seasonal** | Pandemic | Pandemic | Pandemic | **Seasonal** | **Pandemic** | Pandemi |

Seasonal: A/Memphis/14/98 (H3N2) origin; Pandemic: A/Netherlands/602/2009 (H1N1p) origin
Bold indicating segments for which there was strong selection by real-time PCR.

Table S3: Lineage consensus sequences of pandemic HA during passage

| | Position | Inoculum | P1 | P3 | P5 | P7 |
|---|---|---|---|---|---|---|
| Lineage A | HA1 137 | A | A | A | A/T | T |
| | HA2 47 | E | E | E | E/K | K |
| Lineage B | HA2 55 | I | I | I | I | I/V |
| Lineage C | HA1 252 | V | V | V/M | V/M | M |

**Table S4: Taqman Primer and MGB Probe Sets for Quantitative RT-PCR of Influenza Gene Alleles**

| Gene | | Seasonal Primers (A/Memphis/14/1998 (H3N2)) | Pandemic Primers (A/Netherlands/602/2009 (H1N1)) |
|---|---|---|---|
| PB2 | Forward | GRGATGGTGGACATTCTTAG | CCAGGAGGAGAAGTGAGA |
| | Reverse | GAAGGATGAGCTGATTCTCA | GCACATTTCCAAGAGAGATG |
| | Probe | 6FAM-CCATTGCAGCCTT | VIC-TGCTGACACTGCT |
| PB1 | Forward | GGAGTAACAGTGATAAAGAACAA | GCAGAGAGAGGCAAGTTA |
| | Reverse | TCTCCTCTATGGCACCTATA | CTCCTAGCTAAAGTTTCAACAAA |
| | Probe | 6FAM-TGGACCAGCAACA | VIC-ATCGCAACACCTG |
| PA | Forward | CCAAGACCAATCAAACTTCC | CCGATTTGAGATAATTGAAGGAA |
| | Reverse | CCTTCTCCTTCGTGACTTG | CCTGTTGTGTTACATATACTGTTC |
| | Probe | 6FAM-ATCAGCGGTCCAA | VIC-ACCGAATCATGGC |
| HA | Forward | CTTCCAAAATAAGAAATGGGAC | TGCTGGATCTGGTATTATCA |
| | Reverse | GGCACATCATAAGGGTAAC | ATCGGATGTATATTCTGAAATGG |
| | Probe | 6FAM-AGCCTACAGCAAC | VIC-AGTCCACGATTGC |
| NP | Forward | CGGTCTTATGAACAGATGGA | AGTGGGCATGACTTTGAA |
| | Reverse | TGCACATTTGGATGTAGAATC | CTGGGTTTTCATTTGGTCTC |
| | Probe | 6FAM-TCGCCAGAATGCA | VIC-TGACCACTTGGCT |
| NA | Forward | SAGGAAACTGAAGTCTKGTG | GAGCTGTCCTATTGGTGAA |
| | Reverse | TAGGCATGAGATTGATGTCC | CCATCATGACAAGCACTTG |
| | Probe | 6FAM-TGAGCCTGTTCCA | VIC-AGCGACTGACTCA |
| M | Forward | GGCAACAACCAATCCATTA | GATGCAGCGATTCAAGTG |
| | Reverse | CCTGACTAGCAATCTCCA | AGACGATCAGTAATCCACAATA |
| | Probe | 6FAM-TGCCTGCTCACTT | VIC-TCGTCATTGCAGC |
| NS | Forward | AGGCACTTAAAATGACCATG | TCACGAGACTGGTTCATG |
| | Reverse | ACCAGTTTCTTGACAATTCC | GTTCGCTTTCAGTACTATGTTC |
| | Probe | 6FAM-TCCACACCTGCTT | VIC-CAATCGCACGCAA |

**Table S5: Primers for M Amplicon Deep Sequencing**

| Reverse Transcription Primer | |
|---|---|
| M13-M 681F | AACAGCTATGACCATGTTGGGACTCATCCTAGCTCCAGT |

| Amplification Primers | |
|---|---|
| Lib-L M13-GS Fwd | CCATCTCATCCCTGCGTGTCTCCGAC**TCAG**[MID]AACAGCTATGACCATG |
| Lib-L M Rev | CCTATCCCCTGTGTGCCTTGGCAGTCTCAGCCGTAGAAGGCCCTCTTTTC |

| MID Sequences | | | |
|---|---|---|---|
| MID001 | ACACGACGAC | MID021 | CGACGACGCG |
| MID002 | ACACGTAGTA | MID022 | CGACGAGTAC |
| MID003 | ACACTACTCG | MID023 | CGATACTACG |
| MID004 | ACGACACGTA | MID024 | CGTACGTCGA |
| MID005 | ACGAGTAGAC | MID025 | CTACTCGTAG |
| MID006 | ACGCGTCTAG | MID026 | GTACAGTACG |
| MID007 | ACGTACACAC | MID027 | GTCGTACGTA |
| MID008 | ACGTACTGTG | MID028 | GTGTACGACG |
| MID009 | ACGTAGATCG | MID029 | ACACAGTGAG |
| MID010 | ACTACGTCTC | MID030 | ACACTCATAC |
| MID011 | ACTATACGAG | MID031 | ACAGACAGCG |
| MID012 | ACTCGCGTCG | MID032 | ACAGACTATA |
| MID013 | AGACTCGACG | MID033 | ACAGAGACTC |
| MID014 | AGTACGAGAG | MID034 | ACAGCTCGTG |
| MID015 | AGTACTACTA | MID035 | ACAGTGTCGA |
| MID016 | AGTAGACGTC | MID036 | ACGAGCGCGC |
| MID017 | AGTCGTACAC | MID037 | ACGATGAGTG |
| MID018 | AGTGTAGTAG | MID038 | ACGCGAGAGA |
| MID019 | ATAGTATACG | MID039 | ACGCTCTCTC |
| MID020 | CAGTACGTAC | MID040 | ACGTCGCTGA |

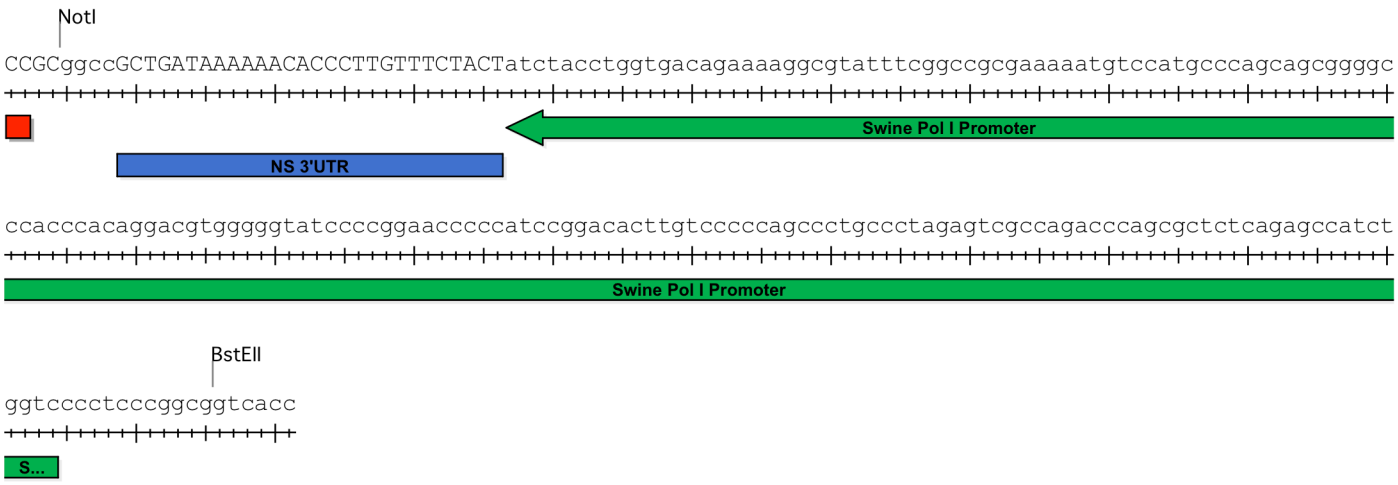


Figure S1: Sequence of the synthetic porcine RNA polymerase I promoter. The 3' noncoding region from A/guineafowl/HongKong/WF10/1999 (H9N2) NS, NotI, and BstEII restriction sites were added for convenience.

Table S6: Universal primers for the cloning of IAV into pPIG2012

| Gene | Forward Primer | | Reverse Primer | |
|---|---|---|---|---|
| PB2 | Ba-PB2 1F | TATTGGTCTCAGGG**AGCGAAAGCAGGTC** | BaPIG-PB2 2341R | ATATGGTCTCGAGAT**AGTAGAAACAAGGTCGTTT** |
| PB1 | Bm-PB1 1F | TATTCGTCTCAGGG**AGCGAAAGCAGGCA** | BmPIG-PB1 2341R | ATATCGTCTCGAGAT**AGTAGAAACAAGGCATTT** |
| PA | Ba-PA 1F | TATTGGTCTCAGGG**AGCGAAAGCAGGTAC** | BaPIG-PA 2233R | ATATGGTCTCGAGAT**AGTAGAAACAAGGTACTT** |
| HA | Aar-HA 1F | TATTCACCTGCCTCAGGG**AGCAAAAGCAGGGG** | AarPIG-NS890R | |
| NP | Ba-NP 1F | TATTSGTCTCAGGG**AGCAAAAGCAGGGTA** | BaPIG-NP 1565R | ATATGGTCTCGAGAT**AGTAGAAACAAGGGTATTTTT** |
| NA | Bm-NA 1F | TATTSGTCTCAGGG**AGCAAAAGCAGGAGT** | BmPIG-NA 1413R | ATATCGTCTCGAGAT**AGTAGAAACAAGGAGTTTTTT** |
| M | Bm-M 1F | TATTSGTCTCAGGG**AGCAAAAGCAGGTAG** | BmPIG-M 1027R | ATATCGTCTCGAGAT**AGTAGAAACAAGGTAGTTTTT** |
| NS | Aar-NS 1F | TATTSGTCTCAGGG**AGCAAAAGCAGGGTG** | AarPIG-NS 890R | ATAT**CACCTGC**TATGAGAT**AGTAGAAACAAGGGTGTTTT** |

Sequences of primers used to amplify genes from Ty/04 for cloning into pPIG2012. Primer sequence encodes the 12 conserved and 13 conserved nucleotides on the 5' and 3' end of the cDNA, respectively shown in bold. Additional sequence specific for individual genes is underlined. 5' of all conserved sequences is a BsmBI (Bm), BsaI (Ba), or AarI (Aar) restriction site for cloning.

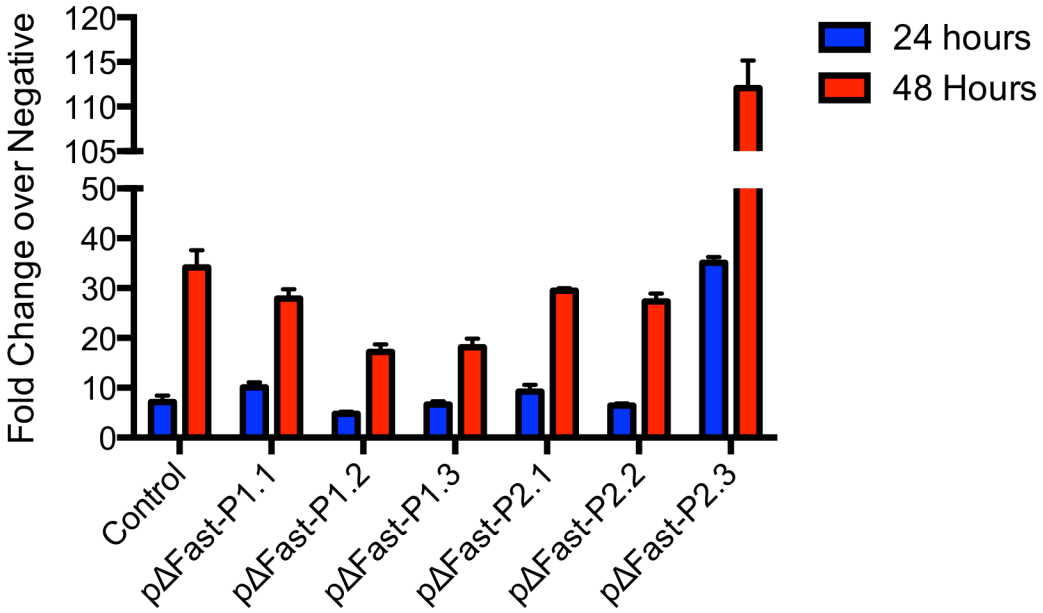


Figure S2: **Luciferase activity of pΔFast constructs**. Plasmids containing 1, 2, or 3 genes from A/turkey/Ohio/313035/2004 (H3N2) were transfected into PK(15) cells together with plasmids to complement the full vRNP luciferase amplicon. For example, P1.1 (PB2), P1.2 (PB2, PB1) were complemented with pPIG-PB1 + pPIG-PA or pPIG-PA, respectively, together with pPIG-. P1.3 (PB2, PB1, PA) required no complementation. All P1 constructs were transfected with pPIG-NP and pPIG-GLuc. P2.1 (NP), P2.2 (NP, M), and P2.3 (NP, M, NS) were all transfected with pPIG-GLuc and complemented with pPIG-PB2, pPIG-PB1, and pPIG-PA.

# References


1. **Organization WH** April 2009 2009, posting date. Influenza (Seasonal) Fact Sheet. [Online.]

2. **Presti RM, Zhao G, Beatty WL, Mihindukulasuriya KA, da Rosa AP, Popov VL, Tesh RB, Virgin HW, Wang D.** 2009. Quaranfil, Johnston Atoll, and Lake Chad viruses are novel members of the family Orthomyxoviridae. Journal of virology **83:**11599-11606.

3. **Baltimore D.** 1971. Expression of animal virus genomes. Bacteriol Rev **35:**235-241.

4. **McGeoch D, Fellner P, Newton C.** 1976. Influenza virus genome consists of eight distinct RNA species. Proceedings of the National Academy of Sciences of the United States of America **73:**3045-3049.

5. **Mjaaland S, Rimstad E, Falk K, Dannevig BH.** 1997. Genomic characterization of the virus causing infectious salmon anemia in Atlantic salmon (Salmo salar L.): an orthomyxo-like virus in a teleost. Journal of virology **71:**7681-7686.

6. **Cox NJ, Kendal AP.** 1976. Presence of a segmented single-stranded RNA genome in influenza C virus. Virology **74:**239-241.

7. **Epizooties OId** 2013, posting date. Manual of Diagnostic Tests for Aquatic Animals 2013: Diseases of fish. [Online.]

8. **Workenhe ST, Wadowska DW, Wright GM, Kibenge MJ, Kibenge FS.** 2007. Demonstration of infectious salmon anaemia virus (ISAV) endocytosis in erythrocytes of Atlantic salmon. Virol J **4:**13.

9. **Moneke E, Ikede BO, Kibenge FS.** 2005. Viremia during infectious salmon anemia virus infection of Atlantic salmon is associated with replicating virus in leucocytes. Dis Aquat Organ **66:**153-157.

10. **Workenhe ST, Kibenge MJ, Wright GM, Wadowska DW, Groman DB, Kibenge FS.** 2008. Infectious salmon anaemia virus replication and induction of alpha interferon in Atlantic salmon erythrocytes. Virol J **5:**36.

11. **Webster RG, Bean WJ, Gorman OT, Chambers TM, Kawaoka Y.** 1992. Evolution and ecology of influenza A viruses. Microbiol Rev **56:**152-179.

12. **Palese P.** 2004. Influenza: old and new threats. Nature medicine **10:**S82-87.

13. **Sorrell EM, Wan H, Araya Y, Song H, Perez DR.** 2009. Minimal molecular constraints for respiratory droplet transmission of an avian-human H9N2

influenza A virus. Proceedings of the National Academy of Sciences of the United States of America **106:**7565-7570.

14. **Imai M, Watanabe T, Hatta M, Das SC, Ozawa M, Shinya K, Zhong G, Hanson A, Katsura H, Watanabe S, Li C, Kawakami E, Yamada S, Kiso M, Suzuki Y, Maher EA, Neumann G, Kawaoka Y.** 2012. Experimental adaptation of an influenza H5 HA confers respiratory droplet transmission to a reassortant H5 HA/H1N1 virus in ferrets. Nature **486:**420-428.

15. **Herfst S, Schrauwen EJ, Linster M, Chutinimitkul S, de Wit E, Munster VJ, Sorrell EM, Bestebroer TM, Burke DF, Smith DJ, Rimmelzwaan GF, Osterhaus AD, Fouchier RA.** 2012. Airborne transmission of influenza A/H5N1 virus between ferrets. Science **336:**1534-1541.

16. **Smith W, Andrewes CH, Laidlaw PP.** 1933. A VIRUS OBTAINED FROM INFLUENZA PATIENTS. The Lancet **222:**66-68.

17. **Smith H, Sweet C.** 1988. Lessons for human influenza from pathogenicity studies with ferrets. Rev Infect Dis **10:**56-75.

18. 2010. Manual of Diagnostic Tests and Vaccines for Terrestrial Animals: Swine Influenza. World Organization for Animal Health.

19. **Vincent AL, Ma W, Lager KM, Janke BH, Richt JA.** 2008. Swine influenza viruses a North American perspective. Advances in virus research **72:**127-154.

20. **Calder LJ, Wasilewski S, Berriman JA, Rosenthal PB.** 2010. Structural organization of a filamentous influenza A virus. Proceedings of the National Academy of Sciences of the United States of America **107:**10685-10690.

21. **Noda T, Sagara H, Yen A, Takada A, Kida H, Cheng RH, Kawaoka Y.** 2006. Architecture of ribonucleoprotein complexes in influenza A virus particles. Nature **439:**490-492.

22. **Schulze IT.** 1973. Structure of the Influenza Virion, p. 1-55. *In* Max A. Lauffer FBBKM, Kenneth MS (ed.), Advances in virus research, vol. Volume 18. Academic Press.

23. **Compans RW, Content J, Duesberg PH.** 1972. Structure of the ribonucleoprotein of influenza virus. Journal of virology **10:**795-800.

24. **Yasuda J, Nakada S, Kato A, Toyoda T, Ishihama A.** 1993. Molecular assembly of influenza virus: association of the NS2 protein with virion matrix. Virology **196:**249-255.

25. **Lamb RA, Choppin PW.** 1981. Identification of a second protein (M2) encoded by RNA segment 7 of influenza virus. Virology **112:**729-737.

26. **Lamb RA, Zebedee SL, Richardson CD.** 1985. Influenza virus M2 protein is an integral membrane protein expressed on the infected-cell surface. Cell **40:**627-633.

27. **Moss B, Keith JM, Gershowitz A, Ritchey MB, Palese P.** 1978. Common sequence at the 5' ends of the segmented RNA genomes of influenza A and B viruses. Journal of virology **25:**312-318.

28. **Skehel JJ, Hay AJ.** 1978. Nucleotide sequences at the 5' termini of influenza virus RNAs and their transcripts. Nucleic acids research **5:**1207-1219.

29. **Robertson JS.** 1979. 5' and 3' terminal nucleotide sequences of the RNA genome segments of influenza virus. Nucleic acids research **6:**3745-3757.

30. **Hsu MT, Parvin JD, Gupta S, Krystal M, Palese P.** 1987. Genomic RNAs of influenza viruses are held in a circular conformation in virions and in infected cells by a terminal panhandle. Proceedings of the National Academy of Sciences of the United States of America **84:**8140-8144.

31. **Honda A, Ueda K, Nagata K, Ishihama A.** 1987. Identification of the RNA polymerase-binding site on genome RNA of influenza virus. J Biochem **102:**1241-1249.

32. **Desselberger U, Racaniello VR, Zazra JJ, Palese P.** 1980. The 3' and 5'-terminal sequences of influenza A, B and C virus RNA segments are highly conserved and show partial inverted complementarity. Gene **8:**315-328.

33. **Cheong HK, Cheong C, Choi BS.** 1996. Secondary structure of the panhandle RNA of influenza virus A studied by NMR spectroscopy. Nucleic acids research **24:**4197-4201.

34. **Baudin F, Bach C, Cusack S, Ruigrok RW.** 1994. Structure of influenza virus RNP. I. Influenza virus nucleoprotein melts secondary structure in panhandle RNA and exposes the bases to the solvent. EMBO J **13:**3158-3165.

35. **Chenavas S, Estrozi LF, Slama-Schwok A, Delmas B, Di Primo C, Baudin F, Li X, Crepin T, Ruigrok RW.** 2013. Monomeric nucleoprotein of influenza A virus. PLoS pathogens **9:**e1003275.

36. **Rees PJ, Dimmock NJ.** 1981. Electrophoretic separation of influenza virus ribonucleoproteins. The Journal of general virology **53:**125-132.

37. **Zvonarjev AY, Ghendon YZ.** 1980. Influence of membrane (M) protein on influenza A virus virion transcriptase activity in vitro and its susceptibility to rimantadine. Journal of virology **33:**583-586.

38. **Biswas SK, Nayak DP.** 1996. Influenza virus polymerase basic protein 1 interacts with influenza virus polymerase basic protein 2 at multiple sites. Journal of virology **70:**6716-6722.

39. **Perez DR, Donis RO.** 1995. A 48-amino-acid region of influenza A virus PB1 protein is sufficient for complex formation with PA. Journal of virology **69:**6932-6939.

40. **Obayashi E, Yoshida H, Kawai F, Shibayama N, Kawaguchi A, Nagata K, Tame JR, Park SY.** 2008. The structural basis for an essential subunit interaction in influenza virus RNA polymerase. Nature **454:**1127-1131.

41. **Sugiyama K, Obayashi E, Kawaguchi A, Suzuki Y, Tame JR, Nagata K, Park SY.** 2009. Structural insight into the essential PB1-PB2 subunit contact of the influenza virus RNA polymerase. EMBO J **28:**1803-1811.

42. **Detjen BM, St Angelo C, Katze MG, Krug RM.** 1987. The three influenza virus polymerase (P) proteins not associated with viral nucleocapsids in the infected cell are in the form of a complex. Journal of virology **61:**16-22.

43. **Gonzalez S, Zurcher T, Ortin J.** 1996. Identification of two separate domains in the influenza virus PB1 protein involved in the interaction with the PB2 and PA subunits: a model for the viral RNA polymerase structure. Nucleic acids research **24:**4456-4463.

44. **Romanos MA, Hay AJ.** 1984. Identification of the influenza virus transcriptase by affinity-labeling with pyridoxal 5'-phosphate. Virology **132:**110-117.

45. **Ulmanen I, Broni BA, Krug RM.** 1981. Role of two of the influenza virus core P proteins in recognizing cap 1 structures (m7GpppNm) on RNAs and in initiating viral RNA transcription. Proceedings of the National Academy of Sciences of the United States of America **78:**7355-7359.

46. **Engelhardt OG, Smith M, Fodor E.** 2005. Association of the influenza A virus RNA-dependent RNA polymerase with cellular RNA polymerase II. Journal of virology **79:**5812-5818.

47. **Li ML, Rao P, Krug RM.** 2001. The active sites of the influenza cap-dependent endonuclease are on different polymerase subunits. EMBO J **20:**2078-2086.

48. **Plotch SJ, Bouloy M, Ulmanen I, Krug RM.** 1981. A unique cap(m7GpppXm)-dependent influenza virion endonuclease cleaves capped RNAs to generate the primers that initiate viral RNA transcription. Cell **23:**847-858.

49. **Barcena J, Ochoa M, de la Luna S, Melero JA, Nieto A, Ortin J, Portela A.** 1994. Monoclonal antibodies against influenza virus PB2 and NP polypeptides interfere with the initiation step of viral mRNA synthesis in vitro. Journal of virology **68:**6900-6909.

50. **Dias A, Bouvier D, Crepin T, McCarthy AA, Hart DJ, Baudin F, Cusack S, Ruigrok RW.** 2009. The cap-snatching endonuclease of influenza virus polymerase resides in the PA subunit. Nature **458:**914-918.

51. **Yuan P, Bartlam M, Lou Z, Chen S, Zhou J, He X, Lv Z, Ge R, Li X, Deng T, Fodor E, Rao Z, Liu Y.** 2009. Crystal structure of an avian influenza polymerase PA(N) reveals an endonuclease active site. Nature **458:**909-913.

52. **Lazarowitz SG, Choppin PW.** 1975. Enhancement of the infectivity of influenza A and B viruses by proteolytic cleavage of the hemagglutinin polypeptide. Virology **68:**440-454.

53. **Klenk HD, Rott R, Orlich M, Blodorn J.** 1975. Activation of influenza A viruses by trypsin treatment. Virology **68:**426-439.

54. **Bottcher-Friebertshauser E, Freuer C, Sielaff F, Schmidt S, Eickmann M, Uhlendorff J, Steinmetzer T, Klenk HD, Garten W.** 2010. Cleavage of influenza virus hemagglutinin by airway proteases TMPRSS2 and HAT differs in subcellular localization and susceptibility to protease inhibitors. Journal of virology **84:**5605-5614.

55. **Klenk HD, Garten W.** 1994. Host cell proteases controlling virus pathogenicity. Trends Microbiol **2:**39-43.

56. **Stieneke-Grober A, Vey M, Angliker H, Shaw E, Thomas G, Roberts C, Klenk HD, Garten W.** 1992. Influenza virus hemagglutinin with multibasic cleavage site is activated by furin, a subtilisin-like endoprotease. EMBO J **11:**2407-2414.

57. **Veits J, Weber S, Stech O, Breithaupt A, Graber M, Gohrbandt S, Bogs J, Hundt J, Teifke JP, Mettenleiter TC, Stech J.** 2012. Avian influenza virus hemagglutinins H2, H4, H8, and H14 support a highly pathogenic phenotype. Proceedings of the National Academy of Sciences of the United States of America **109:**2579-2584.

58. **Palese P, Compans RW.** 1976. Inhibition of influenza virus replication in tissue culture by 2-deoxy-2,3-dehydro-N-trifluoroacetylneuraminic acid (FANA): mechanism of action. The Journal of general virology **33:**159-163.

59. **Palese P, Tobita K, Ueda M, Compans RW.** 1974. Characterization of temperature sensitive influenza virus mutants defective in neuraminidase. Virology **61:**397-410.

60. **Hirst GK.** 1942. The Quantitative Determination of Influenza Virus and Antibodies by Means of Red Cell Agglutination. The Journal of experimental medicine **75:**49-64.

61. **Varghese JN, Laver WG, Colman PM.** 1983. Structure of the influenza virus glycoprotein antigen neuraminidase at 2.9 A resolution. Nature **303:**35-40.

62. **Colman PM.** 1994. Influenza virus neuraminidase: structure, antibodies, and inhibitors. Protein Sci **3:**1687-1696.

63. **Enami M, Enami K.** 1996. Influenza virus hemagglutinin and neuraminidase glycoproteins stimulate the membrane association of the matrix protein. Journal of virology **70:**6653-6657.

64. **Tian C, Gao PF, Pinto LH, Lamb RA, Cross TA.** 2003. Initial structural and dynamic characterization of the M2 protein transmembrane and amphipathic helices in lipid bilayers. Protein Sci **12:**2597-2605.

65. **Ito T, Gorman OT, Kawaoka Y, Bean WJ, Webster RG.** 1991. Evolutionary analysis of the influenza A virus M gene with comparison of the M1 and M2 proteins. Journal of virology **65:**5491-5498.

66. **Pinto LH, Holsinger LJ, Lamb RA.** 1992. Influenza virus M2 protein has ion channel activity. Cell **69:**517-528.

67. **Lamb RA, Lai CJ.** 1980. Sequence of interrupted and uninterrupted mRNAs and cloned DNA coding for the two overlapping nonstructural proteins of influenza virus. Cell **21:**475-485.

68. **Neumann G, Hughes MT, Kawaoka Y.** 2000. Influenza A virus NS2 protein mediates vRNP nuclear export through NES-independent interaction with hCRM1. EMBO J **19:**6751-6758.

69. **Krug RM, Etkind PR.** 1973. Cytoplasmic and nuclear virus-specific proteins in influenza virus-infected MDCK cells. Virology **56:**334-348.

70. **Hale BG, Randall RE, Ortin J, Jackson D.** 2008. The multifunctional NS1 protein of influenza A viruses. The Journal of general virology **89:**2359-2376.

71. **Garcia-Sastre A, Egorov A, Matassov D, Brandt S, Levy DE, Durbin JE, Palese P, Muster T.** 1998. Influenza A virus lacking the NS1 gene replicates in interferon-deficient systems. Virology **252:**324-330.

72. **Bergmann M, Garcia-Sastre A, Carnero E, Pehamberger H, Wolff K, Palese P, Muster T.** 2000. Influenza virus NS1 protein counteracts PKR-mediated inhibition of replication. Journal of virology **74:**6203-6206.

73. **Thanos D, Maniatis T.** 1995. Virus induction of human IFN beta gene expression requires the assembly of an enhanceosome. Cell **83:**1091-1100.

74. **Greenspan D, Palese P, Krystal M.** 1988. Two nuclear location signals in the influenza virus NS1 nonstructural protein. Journal of virology **62:**3020-3026.

75. **Kim T, Kim TY, Lee WG, Yim J, Kim TK.** 2000. Signaling pathways to the assembly of an interferon-beta enhanceosome. Chemical genetic studies with a small molecule. The Journal of biological chemistry **275:**16910-16917.

76. **Ludwig S, Wang X, Ehrhardt C, Zheng H, Donelan N, Planz O, Pleschka S, Garcia-Sastre A, Heins G, Wolff T.** 2002. The influenza A virus NS1 protein inhibits activation of Jun N-terminal kinase and AP-1 transcription factors. Journal of virology **76:**11166-11171.

77. **Chen W, Calvo PA, Malide D, Gibbs J, Schubert U, Bacik I, Basta S, O'Neill R, Schickli J, Palese P, Henklein P, Bennink JR, Yewdell JW.** 2001. A novel influenza A virus mitochondrial protein that induces cell death. Nature medicine **7:**1306-1312.

78. **Chakrabarti AK, Pasricha G.** 2013. An insight into the PB1F2 protein and its multifunctional role in enhancing the pathogenicity of the influenza A viruses. Virology **440:**97-104.

79. **Pena L, Vincent AL, Loving CL, Henningson JN, Lager KM, Li W, Perez DR.** 2012. Strain-dependent effects of PB1-F2 of triple-reassortant H3N2 influenza viruses in swine. The Journal of general virology **93:**2204-2214.

80. **Jagger BW, Wise HM, Kash JC, Walters KA, Wills NM, Xiao YL, Dunfee RL, Schwartzman LM, Ozinsky A, Bell GL, Dalton RM, Lo A, Efstathiou S, Atkins JF, Firth AE, Taubenberger JK, Digard P.** 2012. An overlapping protein-coding region in influenza A virus segment 3 modulates the host response. Science **337:**199-204.

81. **Alexander DJ.** 2000. A review of avian influenza in different bird species. Veterinary microbiology **74:**3-13.

82. **Ito T, Couceiro JN, Kelm S, Baum LG, Krauss S, Castrucci MR, Donatelli I, Kida H, Paulson JC, Webster RG, Kawaoka Y.** 1998. Molecular basis for the generation in pigs of influenza A viruses with pandemic potential. Journal of virology **72:**7367-7373.

83. **Matlin KS, Reggio H, Helenius A, Simons K.** 1981. Infectious entry pathway of influenza virus in a canine kidney cell line. The Journal of cell biology **91:**601-613.

84. **Han X, Bushweller JH, Cafiso DS, Tamm LK.** 2001. Membrane structure and fusion-triggering conformational change of the fusion domain from influenza hemagglutinin. Nat Struct Biol **8:**715-720.

85. **Bullough PA, Hughson FM, Skehel JJ, Wiley DC.** 1994. Structure of influenza haemagglutinin at the pH of membrane fusion. Nature **371:**37-43.

86. **Zhirnov OP, Grigoriev VB.** 1994. Disassembly of influenza C viruses, distinct from that of influenza A and B viruses requires neutral-alkaline pH. Virology **200:**284-291.

87. **Bui M, Whittaker G, Helenius A.** 1996. Effect of M1 protein and low pH on nuclear transport of influenza virus ribonucleoproteins. Journal of virology **70:**8391-8401.

88. **O'Neill RE, Jaskunas R, Blobel G, Palese P, Moroianu J.** 1995. Nuclear import of influenza virus RNA can be mediated by viral nucleoprotein and transport factors required for protein import. The Journal of biological chemistry **270:**22701-22704.

89. **Wu WW, Sun YH, Pante N.** 2007. Nuclear import of influenza A viral ribonucleoprotein complexes is mediated by two nuclear localization sequences on viral nucleoprotein. Virol J **4:**49.

90. **Boulo S, Akarsu H, Ruigrok RW, Baudin F.** 2007. Nuclear traffic of influenza virus proteins and ribonucleoprotein complexes. Virus Res **124:**12-21.

91. **Moore MS, Blobel G.** 1993. The GTP-binding protein Ran/TC4 is required for protein import into the nucleus. Nature **365:**661-663.

92. **Moore MS, Blobel G.** 1994. Purification of a Ran-interacting protein that is required for protein import into the nucleus. Proceedings of the National Academy of Sciences of the United States of America **91:**10212-10216.

93. **Moroianu J, Hijikata M, Blobel G, Radu A.** 1995. Mammalian karyopherin alpha 1 beta and alpha 2 beta heterodimers: alpha 1 or alpha 2 subunit binds nuclear localization signal and beta subunit interacts with peptide repeat-containing nucleoporins. Proceedings of the National Academy of Sciences of the United States of America **92:**6532-6536.

94. **Gabriel G, Klingel K, Otte A, Thiele S, Hudjetz B, Arman-Kalcek G, Sauter M, Shmidt T, Rother F, Baumgarte S, Keiner B, Hartmann E, Bader M, Brownlee GG, Fodor E, Klenk HD.** 2011. Differential use of importin-alpha isoforms governs cell tropism and host adaptation of influenza virus. Nature communications **2:**156.

95. **Tarendeau F, Boudet J, Guilligay D, Mas PJ, Bougault CM, Boulo S, Baudin F, Ruigrok RW, Daigle N, Ellenberg J, Cusack S, Simorre JP, Hart DJ.** 2007. Structure and nuclear import function of the C-terminal domain of influenza virus polymerase PB2 subunit. Nat Struct Mol Biol **14:**229-233.

96. **Huet S, Avilov SV, Ferbitz L, Daigle N, Cusack S, Ellenberg J.** 2010. Nuclear import and assembly of influenza A virus RNA polymerase studied in live cells by fluorescence cross-correlation spectroscopy. Journal of virology **84:**1254-1264.

97. **MacDonald LA, Aggarwal S, Bussey KA, Desmet EA, Kim B, Takimoto T.** 2012. Molecular interactions and trafficking of influenza A virus polymerase proteins analyzed by specific monoclonal antibodies. Virology **426:**51-59.

98. **Li C, Hatta M, Watanabe S, Neumann G, Kawaoka Y.** 2008. Compatibility among polymerase subunit proteins is a restricting factor in reassortment between equine H7N7 and human H3N2 influenza viruses. Journal of virology **82:**11880-11888.

99. **Maines TR, Chen LM, Matsuoka Y, Chen H, Rowe T, Ortin J, Falcon A, Nguyen TH, Mai le Q, Sedyaningsih ER, Harun S, Tumpey TM, Donis RO, Cox NJ, Subbarao K, Katz JM.** 2006. Lack of transmission of H5N1 avian-human reassortant influenza viruses in a ferret model. Proceedings of the National Academy of Sciences of the United States of America **103:**12121-12126.

100. **Hatta M, Halfmann P, Wells K, Kawaoka Y.** 2002. Human influenza a viral genes responsible for the restriction of its replication in duck intestine. Virology **295:**250-255.

101. **Copeland CS, Doms RW, Bolzau EM, Webster RG, Helenius A.** 1986. Assembly of influenza hemagglutinin trimers and its role in intracellular transport. The Journal of cell biology **103:**1179-1191.

102. **Wilson IA, Skehel JJ, Wiley DC.** 1981. Structure of the haemagglutinin membrane glycoprotein of influenza virus at 3 A resolution. Nature **289:**366-373.

103. **Doms RW, Helenius A.** 1986. Quaternary structure of influenza virus hemagglutinin after acid treatment. Journal of virology **60:**833-839.

104. **Boulay F, Doms RW, Wilson I, Helenius A.** 1987. The influenza hemagglutinin precursor as an acid-sensitive probe of the biosynthetic pathway. EMBO J **6:**2643-2650.

105. **Llopis J, McCaffery JM, Miyawaki A, Farquhar MG, Tsien RY.** 1998. Measurement of cytosolic, mitochondrial, and Golgi pH in single living cells with green fluorescent proteins. Proceedings of the National Academy of Sciences of the United States of America **95:**6803-6808.

106. **Takeuchi K, Lamb RA.** 1994. Influenza virus M2 protein ion channel activity stabilizes the native form of fowl plague virus hemagglutinin during intracellular transport. Journal of virology **68:**911-919.

107. **Takeda M, Leser GP, Russell CJ, Lamb RA.** 2003. Influenza virus hemagglutinin concentrates in lipid raft microdomains for efficient viral fusion. Proceedings of the National Academy of Sciences of the United States of America **100:**14610-14617.

108. **Barman S, Adhikary L, Chakrabarti AK, Bernas C, Kawaoka Y, Nayak DP.** 2004. Role of transmembrane domain and cytoplasmic tail amino acid sequences of influenza a virus neuraminidase in raft association and virus budding. Journal of virology **78:**5258-5269.

109. **Rossman JS, Jing X, Leser GP, Balannik V, Pinto LH, Lamb RA.** 2010. Influenza virus m2 ion channel protein is necessary for filamentous virion formation. Journal of virology **84:**5078-5088.

110. **Ali A, Avalos RT, Ponimaskin E, Nayak DP.** 2000. Influenza virus assembly: effect of influenza virus glycoproteins on the membrane association of M1 protein. Journal of virology **74:**8709-8719.

111. **Chen BJ, Leser GP, Jackson D, Lamb RA.** 2008. The influenza virus M2 protein cytoplasmic tail interacts with the M1 protein and influences virus assembly at the site of virus budding. Journal of virology **82:**10059-10070.

112. **Cros JF, Palese P.** 2003. Trafficking of viral genomic RNA into and out of the nucleus: influenza, Thogoto and Borna disease viruses. Virus Res **95:**3-12.

113. **Bui M, Wills EG, Helenius A, Whittaker GR.** 2000. Role of the influenza virus M1 protein in nuclear export of viral ribonucleoproteins. Journal of virology **74:**1781-1786.

114. **Baudin F, Petit I, Weissenhorn W, Ruigrok RW.** 2001. In vitro dissection of the membrane and RNP binding activities of influenza virus M1 protein. Virology **281:**102-108.

115. **Shimizu T, Takizawa N, Watanabe K, Nagata K, Kobayashi N.** 2011. Crucial role of the influenza virus NS2 (NEP) C-terminal domain in M1 binding and nuclear export of vRNP. FEBS Lett **585:**41-46.

116. **O'Neill RE, Talon J, Palese P.** 1998. The influenza virus NEP (NS2 protein) mediates the nuclear export of viral ribonucleoproteins. EMBO J **17:**288-296.

117. **Pleschka S, Wolff T, Ehrhardt C, Hobom G, Planz O, Rapp UR, Ludwig S.** 2001. Influenza virus propagation is impaired by inhibition of the Raf/MEK/ERK signalling cascade. Nat Cell Biol **3:**301-305.

118. **Marjuki H, Alam MI, Ehrhardt C, Wagner R, Planz O, Klenk HD, Ludwig S, Pleschka S.** 2006. Membrane accumulation of influenza A virus hemagglutinin triggers nuclear export of the viral genome via protein kinase Calpha-mediated activation of ERK signaling. The Journal of biological chemistry **281:**16707-16715.

119. **Chen BJ, Leser GP, Morita E, Lamb RA.** 2007. Influenza virus hemagglutinin and neuraminidase, but not the matrix protein, are required for assembly and budding of plasmid-derived virus-like particles. Journal of virology **81:**7111-7123.

120. **Gomez-Puertas P, Albo C, Perez-Pastrana E, Vivo A, Portela A.** 2000. Influenza virus matrix protein is the major driving force in virus budding. Journal of virology **74:**11538-11547.

121. **Wang D, Harmon A, Jin J, Francis DH, Christopher-Hennings J, Nelson E, Montelaro RC, Li F.** 2010. The lack of an inherent membrane targeting signal is responsible for the failure of the matrix (M1) protein of influenza A virus to bud into virus-like particles. Journal of virology **84:**4673-4681.

122. **Rossman JS, Lamb RA.** 2011. Influenza virus assembly and budding. Virology **411:**229-236.

123. **Rossman JS, Jing X, Leser GP, Lamb RA.** 2010. Influenza virus M2 protein mediates ESCRT-independent membrane scission. Cell **142:**902-913.

124. **Bardsley-Elliot A, Noble S.** 1999. Oseltamivir. Drugs **58:**851-860; discussion 861-852.

125. **Liu C, Eichelberger MC, Compans RW, Air GM.** 1995. Influenza type A virus neuraminidase does not play a role in viral entry, replication, assembly, or budding. Journal of virology **69:**1099-1106.

126. **State Department of Agriculture I**, posting date. Biosecurity recommendations for producers. [Online.]

127. **WHO** August 20, 2013 2013, posting date. Summary Recommendations: Prevention and Control of Influenza with vaccines: Recoomendations of the Advisory Committee on Immunization Practices-(ACIP)-United States, 2013-14. [Online.]

128. **WHO.** 2007. A Description of the Process of Seasonal and H5N1 Influenza Vaccine Virus Selection and Development.

129. **Smith DJ, Lapedes AS, de Jong JC, Bestebroer TM, Rimmelzwaan GF, Osterhaus AD, Fouchier RA.** 2004. Mapping the antigenic and genetic evolution of influenza virus. Science **305:**371-376.

130. **Vincent AL, Ma W, Lager KM, Janke BH, Webby RJ, Garcia-Sastre A, Richt JA.** 2007. Efficacy of intranasal administration of a truncated NS1 modified live influenza virus vaccine in swine. Vaccine **25:**7999-8009.

131. **Vincent AL, Lager KM, Janke BH, Gramer MR, Richt JA.** 2008. Failure of protection and enhanced pneumonia with a US H1N2 swine influenza virus in pigs vaccinated with an inactivated classical swine H1N1 vaccine. Veterinary microbiology **126:**310-323.

132. **Loving CL, Lager KM, Vincent AL, Brockmeier SL, Gauger PC, Anderson TK, Kitikoon P, Perez DR, Kehrli ME, Jr.** 2013. Efficacy in pigs of inactivated and live attenuated influenza virus vaccines against infection and transmission of an emerging H3N2 similar to the 2011-2012 H3N2v. Journal of virology **87:**9895-9903.

133. **Kappes MA, Sandbulte MR, Platt R, Wang C, Lager KM, Henningson JN, Lorusso A, Vincent AL, Loving CL, Roth JA, Kehrli ME, Jr.** 2012. Vaccination with NS1-truncated H3N2 swine influenza virus primes T cells and confers cross-protection against an H1N1 heterosubtypic challenge in pigs. Vaccine **30:**280-288.

134. **Solorzano A, Ye J, Perez DR.** 2010. Alternative live-attenuated influenza vaccines based on modifications in the polymerase genes protect against epidemic and pandemic flu. Journal of virology **84:**4587-4596.

135. **Chen GL, Subbarao K.** 2009. Live attenuated vaccines for pandemic influenza. Current topics in microbiology and immunology **333:**109-132.

136. **Ambrose CS, Luke C, Coelingh K.** 2008. Current status of live attenuated influenza vaccine in the United States for seasonal and pandemic influenza. Influenza and other respiratory viruses **2:**193-202.

137. **von Itzstein M, Wu WY, Kok GB, Pegg MS, Dyason JC, Jin B, Van Phan T, Smythe ML, White HF, Oliver SW, et al.** 1993. Rational design of potent sialidase-based inhibitors of influenza virus replication. Nature **363:**418-423.

138. **CDC** 2013, posting date. Influenza Antiviral Drug Resistance. [Online.]

139. **Krystal M, Elliott RM, Benz EW, Jr., Young JF, Palese P.** 1982. Evolution of influenza A and B viruses: conservation of structural features in the hemagglutinin genes. Proceedings of the National Academy of Sciences of the United States of America **79:**4800-4804.

140. **Krammer F, Palese P.** 2013. Influenza virus hemagglutinin stalk-based antibodies and vaccines. Current opinion in virology **3:**521-530.

141. **Krammer F, Hai R, Yondola M, Tan GS, Leyva-Grado VH, Ryder AB, Miller MS, Rose JK, Palese P, Garcia-Sastre A, Albrecht RA.** 2014. Assessment of influenza virus hemagglutinin stalk-based immunity in ferrets. Journal of virology **88:**3432-3442.

142. **Krammer F, Pica N, Hai R, Margine I, Palese P.** 2013. Chimeric hemagglutinin influenza virus vaccine constructs elicit broadly protective stalk-specific antibodies. Journal of virology **87:**6542-6550.

143. **Frace AM, Klimov AI, Rowe T, Black RA, Katz JM.** 1999. Modified M2 proteins produce heterotypic immunity against influenza A virus. Vaccine **17:**2237-2244.

144. **Neirynck S, Deroo T, Saelens X, Vanlandschoot P, Jou WM, Fiers W.** 1999. A universal influenza A vaccine based on the extracellular domain of the M2 protein. Nature medicine **5:**1157-1163.

145. **Fields B, Knipe D, Howley P.** 2006. Fields Virology 2 volume set. {Lippincott Williams & Wilkins}.

146. **Taubenberger JK, Morens DM.** 2006. 1918 Influenza: the mother of all pandemics. Emerging infectious diseases **12:**15-22.

147. **Johnson NP, Mueller J.** 2002. Updating the accounts: global mortality of the 1918-1920 "Spanish" influenza pandemic. Bull Hist Med **76:**105-115.

148. **Reid AH, Fanning TG, Janczewski TA, Lourens RM, Taubenberger JK.** 2004. Novel origin of the 1918 pandemic influenza virus nucleoprotein gene. Journal of virology **78:**12462-12470.

149. **Reid AH, Taubenberger JK, Fanning TG.** 2004. Evidence of an absence: the genetic origins of the 1918 pandemic influenza virus. Nat Rev Microbiol **2:**909-914.

150. **Taubenberger JK, Reid AH, Lourens RM, Wang R, Jin G, Fanning TG.** 2005. Characterization of the 1918 influenza virus polymerase genes. Nature **437:**889-893.

151. **Webster RG, Laver WG.** 1972. The origin of pandemic influenza. Bull World Health Organ **47:**449-452.

152. **Scholtissek C, Rohde W, Von Hoyningen V, Rott R.** 1978. On the origin of the human influenza virus subtypes H2N2 and H3N2. Virology **87:**13-20.

153. **Kawaoka Y, Krauss S, Webster RG.** 1989. Avian-to-human transmission of the PB1 gene of influenza A viruses in the 1957 and 1968 pandemics. Journal of virology **63:**4603-4608.

154. **Palese P, Wang TT.** 2011. Why do influenza virus subtypes die out? A hypothesis. MBio **2**.

155. **Nakajima K, Desselberger U, Palese P.** 1978. Recent human influenza A (H1N1) viruses are closely related genetically to strains isolated in 1950. Nature **274:**334-339.

156. **(CDC) CfDCaP.** 2009. MMWR: Serum Cross-Reactive Antibody Response to a Novel Influenza A (H1N1) Virus After Vaccination with Seasonal Influenza Vaccine, p. 521-556.

157. **Smith GJ, Vijaykrishna D, Bahl J, Lycett SJ, Worobey M, Pybus OG, Ma SK, Cheung CL, Raghwani J, Bhatt S, Peiris JS, Guan Y, Rambaut A.** 2009. Origins and evolutionary genomics of the 2009 swine-origin H1N1 influenza A epidemic. Nature **459:**1122-1125.

158. **Marshall N, Priyamvada L, Ende Z, Steel J, Lowen AC.** 2013. Influenza virus reassortment occurs with high frequency in the absence of segment mismatch. PLoS pathogens **9:**e1003421.

159. **Li C, Hatta M, Nidom CA, Muramoto Y, Watanabe S, Neumann G, Kawaoka Y.** 2010. Reassortment between avian H5N1 and human H3N2 influenza viruses creates hybrid viruses with substantial virulence. Proceedings of the National Academy of Sciences of the United States of America **107:**4687-4692.

160. **Kimble B, Nieto GR, Perez DR.** 2010. Characterization of influenza virus sialic acid receptors in minor poultry species. Virol J **7:**365.

161. **Shinya K, Ebina M, Yamada S, Ono M, Kasai N, Kawaoka Y.** 2006. Avian flu: influenza virus receptors in the human airway. Nature **440:**435-436.

162. **Nelli RK, Kuchipudi SV, White GA, Perez BB, Dunham SP, Chang KC.** 2010. Comparative distribution of human and avian type sialic acid influenza receptors in the pig. BMC Vet Res **6:**4.

163. **Trebbien R, Larsen LE, Viuff BM.** 2011. Distribution of sialic acid receptors and influenza A virus of avian and swine origin in experimentally infected pigs. Virol J **8:**434.

164. **Bancroft CT, Parslow TG.** 2002. Evidence for segment-nonspecific packaging of the influenza a virus genome. Journal of virology **76:**7133-7139.

165. **Hirst GK, Pons MW.** 1973. Mechanism of influenza recombination. II. Virus aggregation and its effect on plaque formation by so-called noninfective virus. Virology **56:**620-631.

166. **Enami M, Sharma G, Benham C, Palese P.** 1991. An influenza virus containing nine different RNA segments. Virology **185:**291-298.

167. **Gao Q, Lowen AC, Wang TT, Palese P.** 2010. A nine-segment influenza a virus carrying subtype H1 and H3 hemagglutinins. Journal of virology **84:**8062-8071.

168. **Donald HB, Isaacs A.** 1954. Counts of influenza virus particles. Journal of general microbiology **10:**457-464.

169. **Smith GL, Hay AJ.** 1982. Replication of the influenza virus genome. Virology **118:**96-108.

170. **Bergmann M, Muster T.** 1995. The relative amount of an influenza A virus segment present in the viral particle is not affected by a reduction in replication of that segment. The Journal of general virology **76 ( Pt 12):**3211-3215.

171. **Odagiri T, Tashiro M.** 1997. Segment-specific noncoding sequences of the influenza virus genome RNA are involved in the specific competition between defective interfering RNA and its progenitor RNA segment at the virion assembly step. Journal of virology **71:**2138-2145.

172. **Liang Y, Hong Y, Parslow TG.** 2005. cis-Acting packaging signals in the influenza virus PB1, PB2, and PA genomic RNA segments. Journal of virology **79:**10348-10355.

173. **Watanabe T, Watanabe S, Noda T, Fujii Y, Kawaoka Y.** 2003. Exploitation of nucleic acid packaging signals to generate a novel influenza virus-based vector stably expressing two foreign genes. Journal of virology **77:**10575-10583.

174. **Fujii K, Fujii Y, Noda T, Muramoto Y, Watanabe T, Takada A, Goto H, Horimoto T, Kawaoka Y.** 2005. Importance of both the coding and the segment-specific noncoding regions of the influenza A virus NS segment for its efficient incorporation into virions. Journal of virology **79:**3766-3774.

175. **Fujii Y, Goto H, Watanabe T, Yoshida T, Kawaoka Y.** 2003. Selective incorporation of influenza virus RNA segments into virions. Proceedings of the National Academy of Sciences of the United States of America **100:**2002-2007.

176. **Ozawa M, Fujii K, Muramoto Y, Yamada S, Yamayoshi S, Takada A, Goto H, Horimoto T, Kawaoka Y.** 2007. Contributions of two nuclear

localization signals of influenza A virus nucleoprotein to viral replication. Journal of virology **81:**30-41.

177. **Ozawa M, Maeda J, Iwatsuki-Horimoto K, Watanabe S, Goto H, Horimoto T, Kawaoka Y.** 2009. Nucleotide sequence requirements at the 5' end of the influenza A virus M RNA segment for efficient virus replication. Journal of virology **83:**3384-3388.

178. **Fournier E, Moules V, Essere B, Paillart JC, Sirbat JD, Isel C, Cavalier A, Rolland JP, Thomas D, Lina B, Marquet R.** 2012. A supramolecular assembly formed by influenza A virus genomic RNA segments. Nucleic acids research **40:**2197-2209.

179. **Noda T, Sugita Y, Aoyama K, Hirase A, Kawakami E, Miyazawa A, Sagara H, Kawaoka Y.** 2012. Three-dimensional analysis of ribonucleoprotein complexes in influenza A virus. Nature communications **3:**639.

180. **Chou YY, Vafabakhsh R, Doganay S, Gao Q, Ha T, Palese P.** 2012. One influenza virus particle packages eight unique viral RNAs as shown by FISH analysis. Proceedings of the National Academy of Sciences of the United States of America **109:**9101-9106.

181. **Gog JR, Afonso Edos S, Dalton RM, Leclercq I, Tiley L, Elton D, von Kirchbach JC, Naffakh N, Escriou N, Digard P.** 2007. Codon conservation in the influenza A virus genome defines RNA packaging signals. Nucleic acids research **35:**1897-1907.

182. **Marsh GA, Rabadan R, Levine AJ, Palese P.** 2008. Highly conserved regions of influenza a virus polymerase gene segments are critical for efficient viral RNA packaging. Journal of virology **82:**2295-2304.

183. **Hutchinson EC, Curran MD, Read EK, Gog JR, Digard P.** 2008. Mutational analysis of cis-acting RNA signals in segment 7 of influenza A virus. Journal of virology **82:**11869-11879.

184. **Marsh GA, Hatami R, Palese P.** 2007. Specific residues of the influenza A virus hemagglutinin viral RNA are important for efficient packaging into budding virions. Journal of virology **81:**9727-9736.

185. **Muramoto Y, Takada A, Fujii K, Noda T, Iwatsuki-Horimoto K, Watanabe S, Horimoto T, Kida H, Kawaoka Y.** 2006. Hierarchy among viral RNA (vRNA) segments in their role in vRNA incorporation into influenza A virions. Journal of virology **80:**2318-2325.

186. **Essere B, Yver M, Gavazzi C, Terrier O, Isel C, Fournier E, Giroux F, Textoris J, Julien T, Socratous C, Rosa-Calatrava M, Lina B, Marquet R, Moules V.** 2013. Critical role of segment-specific packaging signals in

genetic reassortment of influenza A viruses. Proceedings of the National Academy of Sciences of the United States of America **110:**E3840-3848.

187. **Burnet FM, Lind PE.** 1951. A genetic approach to variation in influenza viruses; recombination of characters between the influenza virus A strain NWS and strains of different serological subtypes. Journal of general microbiology **5:**67-82.

188. **Burnet FM, Lind PE.** 1951. A genetic approach to variation in influenza viruses; recombination of characters in influenza virus strains used in mixed infections. Journal of general microbiology **5:**59-66.

189. **Kilbourne ED, Murphy JS.** 1960. Genetic studies of influenza viruses. I. Viral morphology and growth capacity as exchangeable genetic traits. Rapid in ovo adaptation of early passage Asian strain isolates by combination with PR8. The Journal of experimental medicine **111:**387-406.

190. **Maassab HF, Bryant ML.** 1999. The development of live attenuated cold-adapted influenza virus vaccine for humans. Rev Med Virol **9:**237-244.

191. **Robertson JS, Engelhardt OG.** 2010. Developing vaccines to combat pandemic influenza. Viruses **2:**532-546.

192. **Fodor E, Devenish L, Engelhardt OG, Palese P, Brownlee GG, Garcia-Sastre A.** 1999. Rescue of influenza A virus from recombinant DNA. Journal of virology **73:**9679-9682.

193. **Hoffmann E, Neumann G, Kawaoka Y, Hobom G, Webster RG.** 2000. A DNA transfection system for generation of influenza A virus from eight plasmids. Proceedings of the National Academy of Sciences of the United States of America **97:**6108-6113.

194. **Neumann G, Watanabe T, Ito H, Watanabe S, Goto H, Gao P, Hughes M, Perez DR, Donis R, Hoffmann E, Hobom G, Kawaoka Y.** 1999. Generation of influenza A viruses entirely from cloned cDNAs. Proceedings of the National Academy of Sciences of the United States of America **96:**9345-9350.

195. **Chen LM, Davis CT, Zhou H, Cox NJ, Donis RO.** 2008. Genetic compatibility and virulence of reassortants derived from contemporary avian H5N1 and human H3N2 influenza A viruses. PLoS pathogens **4:**e1000072.

196. **Wan H, Sorrell EM, Song H, Hossain MJ, Ramirez-Nieto G, Monne I, Stevens J, Cattoli G, Capua I, Chen LM, Donis RO, Busch J, Paulson JC, Brockwell C, Webby R, Blanco J, Al-Natour MQ, Perez DR.** 2008. Replication and transmission of H9N2 influenza viruses in ferrets: evaluation of pandemic potential. PLoS One **3:**e2923.

197. **Kimble JB, Angel M, Wan H, Sutton TC, Finch C, Perez DR.** 2013. Alternative reassortment events leading to transmissible H9N1 influenza viruses in the ferret model. Journal of virology.

198. **Schrauwen EJ, Herfst S, Chutinimitkul S, Bestebroer TM, Rimmelzwaan GF, Osterhaus AD, Kuiken T, Fouchier RA.** 2011. Possible increased pathogenicity of pandemic (H1N1) 2009 influenza virus upon reassortment. Emerging infectious diseases **17:**200-208.

199. **WHO.** 2011. H5N1 avian influenza: Timeline of major events. *In* WHO (ed.).

200. **Guan Y, Shortridge KF, Krauss S, Webster RG.** 1999. Molecular characterization of H9N2 influenza viruses: were they the donors of the "internal" genes of H5N1 viruses in Hong Kong? Proceedings of the National Academy of Sciences of the United States of America **96:**9363-9367.

201. **WHO.** 2011. Cumulative number of confirmed human cases for avian influenza A(H5N1) reported to WHO, 2003-2013. *In* WHO (ed.).

202. **Ducatez MF, Cai Z, Peiris M, Guan Y, Ye Z, Wan XF, Webby RJ.** 2011. Extent of antigenic cross-reactivity among highly pathogenic H5N1 influenza viruses. Journal of clinical microbiology **49:**3531-3536.

203. **Butt KM, Smith GJ, Chen H, Zhang LJ, Leung YH, Xu KM, Lim W, Webster RG, Yuen KY, Peiris JS, Guan Y.** 2005. Human infection with an avian H9N2 influenza A virus in Hong Kong in 2003. Journal of clinical microbiology **43:**5760-5767.

204. **Guo Y, Li J, Cheng X.** 1999. [Discovery of men infected by avian influenza A (H9N2) virus]. Zhonghua shi yan he lin chuang bing du xue za zhi = Zhonghua shiyan he linchuang bingduxue zazhi = Chinese journal of experimental and clinical virology **13:**105-108.

205. **Lin YP, Shaw M, Gregory V, Cameron K, Lim W, Klimov A, Subbarao K, Guan Y, Krauss S, Shortridge K, Webster R, Cox N, Hay A.** 2000. Avian-to-human transmission of H9N2 subtype influenza A viruses: relationship between H9N2 and H5N1 human isolates. Proceedings of the National Academy of Sciences of the United States of America **97:**9654-9658.

206. **Kimble JB, Sorrell E, Shao H, Martin PL, Perez DR.** 2011. Compatibility of H9N2 avian influenza surface genes and 2009 pandemic H1N1 internal genes for transmission in the ferret model. Proceedings of the National Academy of Sciences of the United States of America **108:**12084-12088.

207. **Kageyama T, Fujisaki S, Takashita E, Xu H, Yamada S, Uchida Y, Neumann G, Saito T, Kawaoka Y, Tashiro M.** 2013. Genetic analysis of novel avian A(H7N9) influenza viruses isolated from patients in China,

February to April 2013. Euro surveillance : bulletin Europeen sur les maladies transmissibles = European communicable disease bulletin **18:**20453.

208. **Lam TT, Wang J, Shen Y, Zhou B, Duan L, Cheung CL, Ma C, Lycett SJ, Leung CY, Chen X, Li L, Hong W, Chai Y, Zhou L, Liang H, Ou Z, Liu Y, Farooqui A, Kelvin DJ, Poon LL, Smith DK, Pybus OG, Leung GM, Shu Y, Webster RG, Webby RJ, Peiris JS, Rambaut A, Zhu H, Guan Y.** 2013. The genesis and source of the H7N9 influenza viruses causing human infections in China. Nature **502:**241-244.

209. **WHO.** 2013. Cumulative number of confirmed cases of avian influenza A(H7N9) reported to WHO, by month, 2013. *In* WHO (ed.).

210. **Fouchier RA, Schneeberger PM, Rozendaal FW, Broekman JM, Kemink SA, Munster V, Kuiken T, Rimmelzwaan GF, Schutten M, Van Doornum GJ, Koch G, Bosman A, Koopmans M, Osterhaus AD.** 2004. Avian influenza A virus (H7N7) associated with human conjunctivitis and a fatal case of acute respiratory distress syndrome. Proceedings of the National Academy of Sciences of the United States of America **101:**1356-1361.

211. **Koopmans M, Wilbrink B, Conyn M, Natrop G, van der Nat H, Vennema H, Meijer A, van Steenbergen J, Fouchier R, Osterhaus A, Bosman A.** 2004. Transmission of H7N7 avian influenza A virus to human beings during a large outbreak in commercial poultry farms in the Netherlands. Lancet **363:**587-593.

212. **Tweed SA, Skowronski DM, David ST, Larder A, Petric M, Lees W, Li Y, Katz J, Krajden M, Tellier R, Halpert C, Hirst M, Astell C, Lawrence D, Mak A.** 2004. Human illness from avian influenza H7N3, British Columbia. Emerging infectious diseases **10:**2196-2199.

213. **REED LJ, MUENCH H.** 1938. A SIMPLE METHOD OF ESTIMATING FIFTY PER CENT ENDPOINTS. American Journal of Epidemiology **27:**493-497.

214. **Apte A, Singh S.** 2007. AlleleID: a pathogen detection and identification system. Methods Mol Biol **402:**329-346.

215. **Kitikoon P, Vincent AL, Gauger PC, Schlink SN, Bayles DO, Gramer MR, Darnell D, Webby RJ, Lager KM, Swenson SL, Klimov A.** 2012. Pathogenicity and transmission in pigs of the novel A(H3N2)v influenza virus isolated from humans and characterization of swine H3N2 viruses isolated in 2010-2011. Journal of virology **86:**6804-6814.

216. **Pearce MB, Jayaraman A, Pappas C, Belser JA, Zeng H, Gustin KM, Maines TR, Sun X, Raman R, Cox NJ, Sasisekharan R, Katz JM, Tumpey TM.** 2012. Pathogenesis and transmission of swine origin

A(H3N2)v influenza viruses in ferrets. Proceedings of the National Academy of Sciences of the United States of America **109:**3944-3949.

217. **Ducatez MF, Hause B, Stigger-Rosser E, Darnell D, Corzo C, Juleen K, Simonson R, Brockwell-Staats C, Rubrum A, Wang D, Webb A, Crumpton JC, Lowe J, Gramer M, Webby RJ.** 2011. Multiple reassortment between pandemic (H1N1) 2009 and endemic influenza viruses in pigs, United States. Emerging infectious diseases **17:**1624-1629.

218. **Liu Q, Ma J, Liu H, Qi W, Anderson J, Henry SC, Hesse RA, Richt JA, Ma W.** 2012. Emergence of novel reassortant H3N2 swine influenza viruses with the 2009 pandemic H1N1 genes in the United States. Archives of virology **157:**555-562.

219. **Zhu H, Zhou B, Fan X, Lam TT, Wang J, Chen A, Chen X, Chen H, Webster RG, Webby R, Peiris JS, Smith DK, Guan Y.** 2011. Novel reassortment of Eurasian avian-like and pandemic/2009 influenza viruses in swine: infectious potential for humans. Journal of virology **85:**10432-10439.

220. **Lakdawala SS, Lamirande EW, Suguitan AL, Jr., Wang W, Santos CP, Vogel L, Matsuoka Y, Lindsley WG, Jin H, Subbarao K.** 2011. Eurasian-origin gene segments contribute to the transmissibility, aerosol release, and morphology of the 2009 pandemic H1N1 influenza virus. PLoS pathogens **7:**e1002443.

221. **Ma W, Liu Q, Bawa B, Qiao C, Qi W, Shen H, Chen Y, Ma J, Li X, Webby RJ, Garcia-Sastre A, Richt JA.** 2012. The neuraminidase and matrix genes of the 2009 pandemic influenza H1N1 virus cooperate functionally to facilitate efficient replication and transmissibility in pigs. The Journal of general virology **93:**1261-1268.

222. **Angel M, Kimble JB, Pena L, Wan H, Perez DR.** 2013. In vivo selection of H1N2 influenza virus reassortants in the ferret model. Journal of virology **87:**3277-3283.

223. **Hoffmann E, Stech J, Guan Y, Webster RG, Perez DR.** 2001. Universal primer set for the full-length amplification of all influenza A viruses. Archives of virology **146:**2275-2289.

224. **Lambre CR, Terzidis H, Greffard A, Webster RG.** 1991. An enzyme-linked lectin assay for sialidase. Clinica chimica acta; international journal of clinical chemistry **198:**183-193.

225. **Grantham ML, Stewart SM, Lalime EN, Pekosz A.** 2010. Tyrosines in the influenza A virus M2 protein cytoplasmic tail are critical for production of infectious virus particles. Journal of virology **84:**8765-8776.

226. **Hall GS, Little DP.** 2007. Relative quantitation of virus population size in mixed genotype infections using sequencing chromatograms. Journal of virological methods **146:**22-28.

227. **Nelson MI, Vincent AL, Kitikoon P, Holmes EC, Gramer MR.** 2012. Evolution of novel reassortant A/H3N2 influenza viruses in North American swine and humans, 2009-2011. Journal of virology **86:**8872-8878.

228. **Mould JA, Paterson RG, Takeda M, Ohigashi Y, Venkataraman P, Lamb RA, Pinto LH.** 2003. Influenza B virus BM2 protein has ion channel activity that conducts protons across membranes. Developmental cell **5:**175-184.

229. **Henkel JR, Weisz OA.** 1998. Influenza virus M2 protein slows traffic along the secretory pathway. pH perturbation of acidified compartments affects early Golgi transport steps. The Journal of biological chemistry **273:**6518-6524.

230. **Sakaguchi T, Leser GP, Lamb RA.** 1996. The ion channel activity of the influenza virus M2 protein affects transport through the Golgi apparatus. The Journal of cell biology **133:**733-747.

231. **Campbell PJ, Danzy S, Kyriakis CS, Deymier MJ, Lowen AC, Steel J.** 2014. The m segment of the 2009 pandemic influenza virus confers increased neuraminidase activity, filamentous morphology, and efficient contact transmissibility to a/puerto rico/8/1934-based reassortant viruses. Journal of virology **88:**3802-3814.

232. **Pielak RM, Chou JJ.** 2010. Flu channel drug resistance: a tale of two sites. Protein & cell **1:**246-258.

233. **Thaa B, Tielesch C, Moller L, Schmitt AO, Wolff T, Bannert N, Herrmann A, Veit M.** 2012. Growth of influenza A virus is not impeded by simultaneous removal of the cholesterol-binding and acylation sites in the M2 protein. The Journal of general virology **93:**282-292.

234. **Li H, Papadopoulos V.** 1998. Peripheral-type benzodiazepine receptor function in cholesterol transport. Identification of a putative cholesterol recognition/interaction amino acid sequence and consensus pattern. Endocrinology **139:**4991-4997.

235. **Iwatsuki-Horimoto K, Horimoto T, Noda T, Kiso M, Maeda J, Watanabe S, Muramoto Y, Fujii K, Kawaoka Y.** 2006. The cytoplasmic tail of the influenza A virus M2 protein plays a role in viral assembly. Journal of virology **80:**5233-5240.

236. **Shope RE.** 1931. Swine Influenza : Iii. Filtration Experiments and Etiology. The Journal of experimental medicine **54:**373-385.

237. **Zhou NN, Senne DA, Landgraf JS, Swenson SL, Erickson G, Rossow K, Liu L, Yoon K, Krauss S, Webster RG.** 1999. Genetic reassortment of avian, swine, and human influenza A viruses in American pigs. Journal of virology **73:**8851-8856.

238. **de Wit E, Spronken MI, Vervaet G, Rimmelzwaan GF, Osterhaus AD, Fouchier RA.** 2007. A reverse-genetics system for Influenza A virus using T7 RNA polymerase. The Journal of general virology **88:**1281-1287.

239. **Grummt I, Roth E, Paule MR.** 1982. Ribosomal RNA transcription in vitro is species specific. Nature **296:**173-174.

240. **Moncorge O, Long JS, Cauldwell AV, Zhou H, Lycett SJ, Barclay WS.** 2013. Investigation of influenza virus polymerase activity in pig cells. Journal of virology **87:**384-394.

241. **Ling X, Arnheim N.** 1994. Cloning and identification of the pig ribosomal gene promoter. Gene **150:**375-379.

242. **Triant DA, Whitehead A.** 2009. Simultaneous Extraction of High-Quality RNA and DNA from Small Tissue Samples. Journal of Heredity **100:**246-250.

243. **Pena L, Vincent AL, Ye J, Ciacci-Zanella JR, Angel M, Lorusso A, Gauger PC, Janke BH, Loving CL, Perez DR.** 2011. Modifications in the polymerase genes of a swine-like triple-reassortant influenza virus to generate live attenuated vaccines against 2009 pandemic H1N1 viruses. Journal of virology **85:**456-469.

244. **Hoffmann E, Webster RG.** 2000. Unidirectional RNA polymerase I-polymerase II transcription system for the generation of influenza A virus from eight plasmids. The Journal of general virology **81:**2843-2847.

245. **Condreay JP, Witherspoon SM, Clay WC, Kost TA.** 1999. Transient and stable gene expression in mammalian cells transduced with a recombinant baculovirus vector. Proceedings of the National Academy of Sciences of the United States of America **96:**127-132.

246. **Volkman LE, Goldsmith PA.** 1983. In Vitro Survey of Autographa californica Nuclear Polyhedrosis Virus Interaction with Nontarget Vertebrate Host Cells. Applied and environmental microbiology **45:**1085-1093.

247. **Nemeroff ME, Barabino SM, Li Y, Keller W, Krug RM.** 1998. Influenza virus NS1 protein interacts with the cellular 30 kDa subunit of CPSF and inhibits 3'end formation of cellular pre-mRNAs. Molecular cell **1:**991-1000.

248. **Luckow VA, Lee SC, Barry GF, Olins PO.** 1993. Efficient generation of infectious recombinant baculoviruses by site-specific transposon-mediated

insertion of foreign genes into a baculovirus genome propagated in Escherichia coli. Journal of virology **67:**4566-4579.

249. **Robertson JS, Nicolson C, Harvey R, Johnson R, Major D, Guilfoyle K, Roseby S, Newman R, Collin R, Wallis C, Engelhardt OG, Wood JM, Le J, Manojkumar R, Pokorny BA, Silverman J, Devis R, Bucher D, Verity E, Agius C, Camuglia S, Ong C, Rockman S, Curtis A, Schoofs P, Zoueva O, Xie H, Li X, Lin Z, Ye Z, Chen LM, O'Neill E, Balish A, Lipatov AS, Guo Z, Isakova I, Davis CT, Rivailler P, Gustin KM, Belser JA, Maines TR, Tumpey TM, Xu X, Katz JM, Klimov A, Cox NJ, Donis RO.** 2011. The development of vaccine viruses against pandemic A(H1N1) influenza. Vaccine **29:**1836-1843.

250. **Zhang X, Kong W, Ashraf S, Curtiss R, 3rd.** 2009. A one-plasmid system to generate influenza virus in cultured chicken cells for potential use in influenza vaccine. Journal of virology **83:**9296-9303.

251. **Shizuya H, Birren B, Kim UJ, Mancino V, Slepak T, Tachiiri Y, Simon M.** 1992. Cloning and stable maintenance of 300-kilobase-pair fragments of human DNA in Escherichia coli using an F-factor-based vector. Proceedings of the National Academy of Sciences of the United States of America **89:**8794-8797.